COPOLYMER CONSTRUCT TO ATTENUATE MECHANOTRANSDUCTION AND ENHANCE LUNG CAPILLARY BARRIER FUNCTION

by

Kristina Marie Giantsos

A dissertation submitted to the faculty of
The University of Utah
in partial fulfillment of the requirements for the degree of

Doctor of Philosophy

Department of Pharmaceutics and Pharmaceutical Chemistry

The University of Utah

May 2011

The University of Utah Graduate School

STATEMENT OF DISSERTATION APPROVAL

The dissertation of **Kristina Marie Giantsos**

has been approved by the following supervisory committee members:

Randal O. Dull	, Chair	**9/2/2010** Date Approved
Grzegorz Bulaj	, Member	**9/2/2010** Date Approved
Jindrich Kopecek	, Member	**9/2/2010** Date Approved
Pavla Kopeckova	, Member	**9/2/2010** Date Approved
Steven Kern	, Member	**9/2/2010** Date Approved

and by **David Grainger**, Chair of the Department of **Pharmaceutics and Pharmaceutical Chemistry**

and by Charles A. Wight, Dean of The Graduate School.

ABSTRACT

Acute lung injury and adult respiratory distress syndrome are characterized by pathological efflux of serum proteins and fluid from capillaries to interstitial tissues and represents a significant complication in the clinical setting with no mitigating therapy. The scope of this research is to lay the foundation for a polymer-based therapy, delivered to inflamed vascular endothelium, that strengthens the capillary barrier. The research spans the use of two polymer prototypes. The first polymer prototype, a tetramethylammonium chloride copolymer with a poly-*N*-(2-hydroxypropyl)methacrylamide (P-HPMA) backbone that binds to endothelium via ionic interactions, is used to show the efficacy of copolymer delivery to highly permeable endothelium. The second polymer prototype retains the HPMA backbone but exchanges cationic side chains for a peptide that targets E-selectin, an endothelial protein that is upregulated during inflammation and mediates leukocyte tethering and rolling. In this work, we are able to show a significant reduction in solute and solvent flux across endothelial monolayers under cytokine-mediated or mechanical stress in the presence of copolymers. We determined that the attenuation of barrier permeability was due to the polymer's inhibition of cell signaling mechanism(s) and not only a result of an increased physical barrier. The administration of copolymers attenuates capillary permeability in an *ex vivo* lung model to demonstrate the viability of

targeted copolymer delivery to vascular endothelium as a treatment for vascular permeability and acute lung injury.

Dedicated to my grandfather,

E.A. Hallford,

for your unwavering belief that I can do anything.

TABLE OF CONTENTS

LIST OF ABBREVIATIONS

AIBN	2,2-azobisisobutryonitrile
ALI	acute lung injury
ANOVA	analysis of variance
ARDS	acute respiratory distress syndrome
BAEC	bovine aortic endothelial cell
BLMVEC	bovine microvascular endothelial cell
BSA	bovine serum albumin
CO_2	carbon dioxide
DIPEA	diisopropylethylamine
DMEM	Dulbecco's modified eagle medium
DMF	dimethylformamide
EDT	ethane dithiol
eNOS	nitric oxide synthase
EPB	E-selectin-PEG-biotin
ESBP	E-selectin binding peptide
FBS	fetal bovine serum
FPLC	fast protein liquid chromatography
GAG(s)	glycosaminoglycan(s)
HEPES	4-(2-hydroxyethyl)piperazine-1-ethanesulfonic acid
HPLC	high performance liquid chromatography
HPMA	*N*-(2-hydroxypropyl)methacrylamide
IACUC	Institutional Animal Care and Use Committee
J_v	volumetric flow rate
K_{fc}	capillary filtration coefficient
L_p	hydraulic conductivity
LDH	lactate dehydrogenase
MII	media II
MA-AP	*N*-(3-aminopropyl)methacrylamide
MA-FITC	5-3-(methacryloylaminoropyl)thioureidyl fluorescein
MALDI-TOF	matrix assisted laser desorption ionization – time of flight
MA-TMA Cl	methacrylamidopropyltrimethylammonium chloride
MEM	minimal essential medium
MPA	mercaptopropanoic acid
L-NAME	N_ω-nitro-L-arginine methyl ester hydrochloride
NO	nitric oxide
NPB	NHS-PEG4-biotin

P_C	capillary pressure
P_{DA}	diffusive permeability coefficient
P_{DO}	double-occlusion pressure
P_{LA}	left atrial pressure
P_{PA}	pulmonary artery pressure
PBS	phosphate buffered saline
PEG	polyethylene glycol
PEO	polyethylene oxide
PGI_2	prostacyclin
PIP	peak inspiratory pressure
PRF MII	phenol red-free media II
RLMVEC	rat lung microvascular endothelial cell
ROS	reactive oxygen species
SCRM	peptide scrambled sequence
SEC	size exclusion chromatography
SMCC	sulfosuccinimidyl 4-[*N*-maleimidomethyl]cyclohexane-1-carboxylate
TCEP	Tris-(2-carboxyethyl) phosphine hydrochloride
TMAC	tetramethyl ammonium chloride
TMR-BSA	tetramethylrhodamine-conjugated BSA

ACKNOWLEDGMENTS

I thank Dr. Randal Dull for his mentorship, both in my undergraduate and graduate studies, and for his many examples of positivism, integrity, and ingenuity, as well as financial support and generosity. I also thank Dr. Pavla Kopeckova for her invaluable polymer chemistry expertise and generosity with her time and resources. My gratitude goes to my committee, Dr. Jindrich Kopecek, Dr. Steven Kern, and Dr. Grzegorz Bulaj, for their genuine support of this project along with constructive criticism and advice, and to Dr. Herron for his wealth of patience and knowledge. Thanks also go to Veronica Lopez-Quintero and Dr. John Tarbell at CUNY for their work on shear experiments in Chapter 3. I thank Dr. Chris Reilly and Diane Lanza for their discussions and input on molecular biology assays. I extend sincere thanks to Mark Cluff for technical assistance with isolated perfused mouse lung studies, Monika Sima for assistance in polymer synthesis and Scott McJames for assistance with the L_p experiment. I also acknowledge and appreciate the general help and friendliness of the Kopecek lab members. I also acknowledge Katie Job's support and invaluable assistance and conversations along the way. I extend thanks to Dr. Chris Rodesch and Keith Carney in the Fluorescence Microscopy Core Facility and Dr. Chad Nelson and Dr. Krishna Parsawar in the Mass Spectrometry and

Proteomics Core Facility. I extend humble thanks for the priceless support and encouragement of my husband and friends and family. Funding for this project was received in part through NIH grant #59306690 and I would like to extend sincere thanks to Dr. Dull and the Stanley Foundation for their generous contributions.

CHAPTER 1

INTRODUCTION TO VASCULAR PERMEABILITY AND A POLYMER BASED THERAPY

Acute lung injury (*1*) and its extreme disease state, adult respiratory distress syndrome (ARDS), continue to represent a major source of morbidity and mortality in the clinical setting. ALI/ARDS can arise from a variety of medical complications such as ischemia/reperfusion injury, mechanical stress resulting from ventilator-induced injury, pneumonia, sepsis, blunt chest trauma, cardiopulmonary bypass surgery, and organ transplant. ALI/ARDS is characterized by severe oxygenation impairment accompanied by a pathological efflux of fluid and serum proteins from the capillaries into interstitial tissues along with the release of cytokines and inflammatory mediators that, over time, have a deleterious effect on the microvascular capillary environment. A current treatment for ALI/ARDS does not exist beyond ventilator strategies. The ultimate goal of this research is the development of a clinically viable treatment for pulmonary edema that improves the vascular capillary barrier function and patient outcome.

1.1 Capillary physiology

The endothelial glycocalyx is a multifunctional layer of entangled glycoproteins, glycolipids, and glycosaminoglycans that coats the surface of vascular endothelial cells and cell junctions. It is approximately 2-3 μm in thickness (*2*) and acts as both an active and passive barrier that regulates adsorption and extravasation of serum proteins and actively participates in signal transduction to temper vascular tone (*3*). Both of these functions are altered in the presence of acute inflammation (*4, 5*).

Passively, the glycocalyx is composed of a dense matrix of membrane-bound and intercalated macromolecules. It has a net negative charge due to its extensive concentration of bound anionic moieties such as sialic acids, carboxyl groups and sulfated carbohydrates. This polyanionic nature facilitates association with cationic plasma proteins, enzymes, growth factors, amino acids, and water; therefore, the glycocalyx can behave as a selective permeability barrier for macromolecules based on size and charge (*3*).

The active role of the glycocalyx involves key glycosaminoglycans such as heparan sulfate (*6*), hyaluronan (HA), and chondroitin sulfate (CS). These glycans are linear heteropolysaccharides that are identified by distinct disaccharide unit repeats. Heparan sulfate is the most extensively studied GAG (*2, 7, 8*) and is prominently featured on the endothelial surface, comprising roughly 50% of the total GAG content (*9*). Heparan sulfate is an oligosaccharide found on syndecan, a transmembrane proteoglycan, as well as on membrane-associated glypicans and perlecans (*10*) and has highly sulfated domains

interspersed in regions of moderate and low sulfation. The biosynthesis of heparan sulfate is highly controlled to create a specific fine structure and it is hypothesized that the sulfation pattern on heparan sulfate carbohydrate chains may function as receptors for specific ligands. Transmembrane syndecans contact the cytoskeleton through α-actinin and are capable of signal transduction through protein kinase C. Syndecans are also implicated in actomyosin contraction through RhoA and Rho kinases. These characteristics alone implicate heparan sulfates and syndecan as mechanical sensors (*11*).

Hyaluronan (HA) is a secreted GAG that remains on the cell surface and intercalates into the glycocalyx while CS is found on syndecan as well, although typically closer to the cell membrane (*10*). Degradation of HA results in heightened macromolecular permeability of the glycocalyx (*5*) and its rheological properties have been implicated in its role as a mechanosensor (*12*). Enzymatic degradation of hyaulronan attenuates flow-mediated nitric oxide production but does not prevent against agonist-induced NO production via acetylcholine administration, indicating that HA is part of the mechanosensing apparatus on the endothelial surface (*13*). The role of CS in the glycocalyx has yet to be definitively elucidated.

1.2 Mechanotransduction

The mechanism by which extracellular forces are translated into signal(s) that are relayed to junctional proteins to allow efflux of fluid and proteins from the capillaries has been extensively studied (*3, 14, 15*) yet is poorly understood. A conceptual model of how fluid flow elicits a cellular response describes the GAG

components of the glycocalyx as drag sensors that transmit force from capillary blood flow to core surface proteins. The signal is propagated to the plasma membrane or the actin cytoskeleton (*3*). Capillary endothelial cells are subjected to two types of stress vectors: a stress perpendicular to the vessel wall attributed to blood pressure and a stress parallel to the vessel wall due to hemodynamic shear as blood flows along the capillary. In the case of hemodynamic shear, the model predicts that fluid shear stress is transmitted to the membrane-associated or transmembrane protein components of the glycocalyx, which deliver the force to the cell (*3*). This model has been corroborated in the studies conducted by Weinbaum et al. (*16*) in which core proteins of the glycocalyx are modeled as sufficiently rigid to resist bending in the presence of shear and to transmit force-mediated perturbations to the actin cortical skeleton via transmembrane domains. Cumulative GAG-mediated displacements of individual actin filaments in the cortical web are on the order of 10 nm for typical fluid shear, which are hypothesized to be a factor in signal transduction (*6*).

The relationship between the glycocalyx and mechanotransduction has been probed primarily through experiments in which components of the glycocalyx are enzymatically degraded and function is reassessed. Florian et al. used heparanase III to degrade heparan sulfate chains on endothelial cells and reported complete inhibition of increases in nitric oxide production in response to fluid shear stress (*7*). In their seminal paper, Pahakis et al. (*8*) removed heparan sulfate, chondroitin sulfate, hyaluronan, and sialic acid, independently, and measured nitric oxide output from endothelial monolayers under the influence of

shear stress. The increased production of nitric oxide in response to shear stress was attenuated by the removal of heparan sulfate, sialic acid, and hyaluronan, but not chondroitin sulfate. This directly implicates specific GAGs as signal transducers. It was also shown that none of the enzymes used had an inhibitory effect on the shear-induced production of prostacyclin (PGI_2), which suggests multiple mechanisms for mechanotransduction (*8*).

The relationship between forces exerted on the glycocalyx and actin cytoskeleton rearrangement was shown when magnetic beads, covalently bound with RGD sequence-bearing peptides, were allowed to bind to the glycocalyx. The application of a strong external magnetic field resulted in an applied torque to the beads and the resistance to bead rotation was taken as an indication of cell stiffness. Disruption of the microfilament lattice with cytochalasin D and the disruption of microtubules with nocodaxole fully inhibited the stiffening response (*14*). In experiments that visualize the spatial displacement of key cell junction proteins using confocal microscopy, shear stress has been shown to rearrange F-actin, vinculin, paxillin, and the tight junction protein ZO-1 (*15*). These findings are a few in a large body of work that implicates mechanical perturbations to the glycocalyx in signal transduction and cell junction integrity.

1.3 Polymer-based therapy

The research contained in this dissertation outlines the development of a water-soluble biomimetic polymer delivered to the vascular endothelium to dampen the mechanical perturbations experienced by the glycocalyx and, thereby, turn off mechanotransduction pathway(s). Mounting evidence suggests

that the benefit of glycocalyx stiffening may mitigate capillary permeability; therefore, an HPMA-based polymer was constructed as a glycocalyx-intercalating agent.

Poly-*N*-(2-hydroxypropyl) methacrylamide (HPMA) is a water soluble, flexible polymer backbone that is capable of conjugation to a variety of targeting moieties via reactive side chains. Kopecek et al. first reported the design and synthesis of polymers of HPMA in 1973 (*17*) and the favorable hydrodynamic properties of P-HPMA were described in 1974 (*18*). [P- denotes a poly-HPMA backbone in the nomenclature used throughout this text.] Since then, HPMA has been used to target anticancer drugs to a wide variety of tumors including prostate (*19*), bone (*20, 21*), ovarian (*22*), renal (*23*), colon (*24, 25*), and T- and B-cell lymphomas (*26*) as well as to the gastrointestinal wall (*27*) and the tumor endothelium itself (*28*). In 1999, the doxorubicin-HPMA copolymer PK1 was the first HPMA-based copolymer drug conjugate to enter clinical trials as a chemotherapeutic agent (*29*). Copolymers may target to tumor sites directly using targeting agents such as antibodies (*30, 31*), lectins (*27*), or peptides (*19, 32*) or copolymers may deliver drug conjugates by passive absorption through highly permeable tumor neovasculature (*22, 33*) this phenomenon is known as the enhanced permeability and retention effect, or EPR (*34*). The advantage of drug conjugation to hydrophilic macromolecules is that this reduces the nonspecific systemic toxicity of the drug (*35, 36*) as well as increases the systemic half-life of the drug provided that polymer conjugates are larger than the glomerular filtration cutoff of approximately 14 Å (*37*).

In addition to drug targeting and delivery, HPMA scaffolds have been used extensively to conjugate cationic residues for the purpose of gene and siRNA delivery. Both uses take advantage of the net negative charge of the cell membrane (*38*) to associate copolymers to the cell surface and thereby trigger endocytotic pathways to deliver cargo into the cell. Seymour et al. have used copolymers of HPMA and trimethylammonium chloride to condense DNA for the purposes of nonviral gene delivery (*39, 40*) as well as using a trimethylammonium chloride copolymer as a coating on viral gene therapy vectors to mask the vector from immune recognition (*41*). Tertiary amine-HPMA copolymers containing folate conjugates have been used to deliver siRNAs to tumor cells (*42*). HPMA copolymers bearing triphenylphosphonium cationic groups have also been shown to have cell internalization properties (*43*).

HPMA has been used extensively as a copolymer backbone in part due to low inherent cytotoxicity (*44-46*), blood compatibility (*44*), and stability at physiological pH (*47*). Immunological studies have shown that P-HPMA does not increase antibody concentration *in vivo* and any immune response occurring in the presence of HPMA copolymers is attributed to the side chain (*48*). Multiple studies have shown a correlation between the intensity of the immune response and the molecular weight of the copolymer (*45, 46*), the composition of its side chains (*45*), the concentration of the copolymer (*45*) and valence of the conjugate when the side chains are known haptens (*46*). Dintzis et al. (*46*) compared multiple polymer backbones of varying molecular weights and hapten loading. Immunogenicity was relatively independent of the chemical makeup of the

polymer backbone and was directly related to the molar mass of the copolymer and the hapten valence. All of the copolymers induced an immune response at some hapten loading ratio and molecular weight. Conversely, these same copolymers were shown to be nonimmunogenic at different hapten ratios and molecular weights (*46*).

In this research, we use HPMA-trimethylammonium chloride copolymers as a proof-in-concept tool to describe how associations with HPMA can attenuate mechanotransduction; however, we acknowledge the inherent problems with using cationic copolymers as a systemic treatment. Firstly, cationic copolymers are used in gene delivery for their excellent access to intercellular compartments due to triggering endocytosis. Liu et al. (*49*) examined the relationship between polymer side chain charge and cellular internalization and ultimate polymer localization. The study determined that strongly basic side chains, in this case 20 mol% methacryloyloxyethyl trimethylammonium chloride, associated with the cell membrane within minutes and were endocytosed via dynamin-dependent pathways. Strongly acidic side chains were endocytosed primary through fluid phase endocytosis. Weakly basic copolymers (2-(*N,N*-dimethylamino)ethyl methacrylate) were endocytosed in a similar manner at a faster rate than were negatively charged copolymers of the same charge density. The disparity between the rate of uptake of positively- and negatively charged copolymers widened as concentration increased, suggesting a concentration- and charge-dependent mechanism for cell association and endocytosis. Rates and pathways of endocytosis were found to be independent of the HPMA backbone

itself, in accordance with previous conclusions that P-HPMA is relatively inactive at the cellular level (*49*).

Secondly, cationic copolymers possess no specific targeting agent and therefore may associate with any negatively charged cell or serum proteins to form aggregates. Significant aggregation of albumin in whole serum has been shown in the presence of poly-L-lysine (pLL). The zeta potential of pLL/DNA complexes decreased sharply from 48 mV for untreated complexes to -16 mV in serum (*50*), indicating albumin association and potential physical trapping in microvessels. Cationic copolymers have also been shown to demonstrate significant systemic toxicity and the relationship between structure and systemic activity has been reviewed extensively (*51, 52*).

In this research, the first polymer prototype was designed to associate with the negatively charged glycocalyx via quaternary ammonium side chains conjugated to the HPMA backbone. We chose quaternary ammonium side chains for their reduced cytotoxicity when compared to primary amine copolymers. Reschel et al. (*53*) studied transfection activity of primary and tertiary amino polyanions and quaternary ammonium polyanions and concluded that polymers containing primary amino groups demonstrated significantly higher gene transfection properties than did quaternary ammonium polycations. They concluded that since successful transfection depends on both endocytosis and endosomal release, primary amino polyanions may be better able to disrupt endosomal compartment membranes by association with surface phosphate groups (*53*). This correlates to the reduced cytotoxicity seen in endothelial cells

exposed to quaternary ammonium-HPMA copolymers compared to primary amino-HPMA copolymers (*54*).

Cationic copolymers were not intended as a permanent solution to accomplish P-HPMA binding to endothelial glycocalyx. However, these copolymers were the logical first step in the development of a polymeric construct that could interact with the cell surface yet potentially minimize cellular uptake by associating loosely through ionic contact. As the delivery of HPMA-based copolymer became a clearly viable avenue for mechanotransduction research, it became necessary to develop a targeting strategy that allows delivery of HPMA to the glycocalyx but elicits minimal to no adverse physiological response.

1.4 E-selectin

The cell surface protein E-selectin has been targeted in a variety of settings where the visualization of or delivery to sites of inflamed endothelium is desirable, such as tumor targeting (*6, 32*), siRNA delivery (*55, 56*), brain inflammation (*57*), arthritis (*58*), and anti-inflammatory drug delivery (*59*). E-selectin is chosen for targeting in inflammatory diseases and cancer by virtue of its upregulation in the presence of inflammation and extended residence time on activated endothelium. The *de novo* biosynthesis of E-selectin peaks within 2-6 hours of inflammatory insult and is mediated by cytokines such as TNF-α, lipopolysaccharides (LPS), and interleukin 1β (IL-1β). Basal levels of E-selectin return within 10-24 hours as the receptor is slowly internalized to lysosomes for degradation (*60*).

E-selectin is primarily found on activated endothelium, whereas P-selectin is found on both platelets and activated endothelium and L-selectin is found only on leukocytes. E-selectin differs from P-selectin in that P-selectin is stored in Weibel-Palade bodies and are upregulated on the cell surface within minutes of thrombin or oxygen radical exposure and is released within 30 minutes from surface membranes following exposure. These selectins all have a common structural organization composed of the lectin domain at the N-terminus, an EGF-domain, a domain whose length is dictated by whether the selectin is E, P, or L, a transmembrane domain, and a short cytoplasmic C-terminal domain (*61*). The lectin binding domain is 60% homologous across all selectin subtypes (*62*).

The specificity of E-selectin for sialyl lewis x was demonstrated by Lowe et al. in Chinese hamster ovary (CHO) cells (*63*) and concurrently by Walz et al. (*64*) who examined the ability for E-selectin binding to white blood cells. An E-selectin—IgG1 chimera was covalently attached to plastic dishes and incubated with granulocytes and myeloid cells. These cells bound to the E-selectin-coated plastic if they were positive for CD15 expression (3-fucosyl-N-acetyl lactosamine) whereas dishes coated with a CD8 fusion protein showed negligible affinity for all cells tested. Incubation with neuraminidase abolished the effect, thus demonstrating the necessity for fucose presence in E-selectin binding. Incubation of the plastic dishes with the sialyl lewis x-determinant CSLEX1 also completely inhibited adhesion of myeloid cells to E-selectin (*64*).

Elucidation of carbohydrate ligands for E-selectin was followed by the discovery of peptide ligands for E-selectin. Martens et al. (*65*) used a phage

display to elucidate several sequences that bound to E-selectin with high affinity (IC_{50} values were between 4.0 and 910 nm). The sequences all conserved tryptophan and methionine residues and were determined to bind E-selectin independent of Ca^{2+}, which suggested an allosteric binding site distinct from that of sialyl lewis x (*65*). Shamay et al. (*32*) later used the peptide sequence from this study with the highest affinity for E-selectin to target an HPMA-doxorubicin copolymer to immobilized E-selectin and later human immortalized vascular endothelial cells (IVECs) in flow cytometry assays. Conjugating the peptide to the copolymer further lowered the binding affinity of peptides to 6 nm by the multivalent effect. These peptide copolymers were shown to localize to lysosomes within 15 hours (*32*), in agreement with studies that found E-selectin-bound antibodies localized to lysosomes after 4 hours postcytokine exposure (*66*).

Beyond its novel targeting capacity, E-selectin also serves as a receptor for leukocyte endothelial binding. Bernardes-Silva et al. demonstrated a significant reduction in neutrophil recruitment to rat brains that were first injected with IL-1β then antibodies to E- and P-selectin (*67*). The ability to block neutrophil recruitment may be exploited in acute lung injury repair as oligosaccharides have been conjugated with sialyl lewis x, the endogenous ligand to E-selectin, with the intent of blocking leukocyte interactions. A modest reduction in capillary permeability was seen in rat models when injected with these sialyl lewis x-oligosaccharide conjugates (*59*). In a related study, similar sialyl lewis x-bearing oligosaccharides demonstrated cardioprotective properties when administered to

feline models of myocardial ischemia/reperfusion injury (*60*). Taken together, these experiments demonstrate the benefit of blocking endothelial selectins from leukocyte binding. The potential to sterically block leukocyte binding while dampening mechanotransduction with a polymer construct would be highly beneficial multifaceted approach to treat vascular permeability and acute lung injury.

1.5 Specific aims

The specific aims outlined in this dissertation are designed to lay the foundation for future research into the mechanism(s) involved in mechanotransduction and a clinically relevant treatment for pulmonary edema and acute lung inflammation. Specifically, these aims are as follows:

1. Aim 1. Develop a polymer construct that demonstrates limited toxicity, effective binding to the endothelial glycocalyx, and efficacy in reducing fluid and solute flux across endothelial monolayers subjected to chemical and mechanical stress. *We hypothesize that positively charged copolymers can bind to the negatively charged glycocalyx and that the use of a poly-HPMA backbone will minimize toxicity and reinforce the endothelial barrier.*
2. Aim 2. Characterize the mechanism by which polymer administration reduces barrier permeability and to determine whether this mechanism falls under the category of passive or active barrier function. The release of nitric oxide (NO) from mechanically-stressed endothelial monolayers is indicative of the activation of cell signaling pathways.

We hypothesize that the quantification of NO production of endothelial cells under mechanical stress in the presence or absence of copolymer can determine the capacity of copolymer administration to reduce the active barrier dysfunction.

3. Aim 3. Translate the *in vitro* polymer findings to an *ex vivo* whole organ model. *We hypothesize that the capacity of copolymer administration to reduce the capillary filtration coefficient, the indicator of acute pulmonary edema accumulation in pericapillary tissues, can be best demonstrated in the presence of all components of pulmonary physiology, e.g., a whole lung model.*
4. Aim 4. Optimize the polymer construct to minimize pleiotropic effects as may arise from *in vivo* administration of a cationic copolymer. *We hypothesize that cationic moieties can be replaced with E-selectin binding ligands that can be used to target polymers directly to areas of acute inflammation.*

The first specific aim is accomplished in Chapters 2 and 3. A copolymer is developed that reduces both solute and protein flux through endothelial monolayers under cytokine- and pressure-mediated barrier distress. This copolymer is shown to bind to endothelium and exhibits minimal cytotoxicity as compared to other prototypes.

The second and third specific aims are addressed in Chapter 3. Chapter 3 was published as a companion piece to Chapter 2, wherein both chapters exhaust *in vitro* and *ex vivo* studies required to demonstrate the utility of the

design of HPMA copolymer delivery to inflamed endothelium. Chapter 3 addresses the characterization of the mechanism of action of polymer administration along with molecular weight requirements for *ex vivo* functional studies.

Chapter 4 includes preliminary studies using a second polymer prototype that relies on receptor targeting for endothelial delivery as opposed to ionic contacts. This second polymer prototype is intended to begin the optimization process for an intravenously delivered therapy. Chapters 2 and 3 demonstrate the potential for HPMA delivery to strengthen the capillary barrier function and Chapter 4 comprises preliminary research to target P(HPMA) to areas of vascular inflammation.

Chapter 5 is a discussion of the conclusions of this dissertation and presents the whole picture of the research herein along with suggestions for future work.

CHAPTER 2

AN ENDOTHELIUM-ASSOCIATED CATIONIC COPOLYMER TO ENHANCE BARRIER FUNCTION OF LUNG CAPILLARY MONOLAYERS*

2.1 Abstract

Biomimetic polymers are hypothesized herein to enhance passive barrier function by reducing the porosity of the endothelial glycocalyx and attenuate mechanotransduction by restricting the motion of the glycoproteins implicated in signal transduction. To this end, cationic copolymers containing methacrylamidopropyl trimethylammonium chloride [P(TMA)Cl] have been developed as an infusible therapy to target the lung capillary glycocalyx in order to mechanically enhance the capillary barrier and turn off pressure-induced mechanotransduction. Copolymers were tested for functional efficacy by measuring both albumin permeability (P_{DA}) and hydraulic conductivity (L_p) across cultured endothelial monolayers. P(TMA)Cl significantly decreased P_{DA} in normal

*This chapter is adapted from Giantsos et al. *Biomaterials* **30:**5885-91 (2009) with permission from the journal.

and inflamed cells and attenuated pressure-induced increases in L_p. Decreases in L_p across endothelial monolayers in the presence of P(TMA)Cl are evidence of a dampening of mechanotransduction-induced barrier dysfunction. This chapter outlines preliminary experiments in the development and optimization of biomimetic polymers that associate with lung endothelium to be used as a therapy to enhance endothelial barrier function and thereby attenuate a major component of vascular inflammation.

2.2 Introduction

The endothelial glycocalyx serves as an interface between blood flow and the endothelial cell surface and acts as both a passive barrier between serum components and pericapillary tissues and active involvement in the stress-induced changes to the integrity of the endothelial junction, including release of endothelium-derived relaxation factors (*68*) such as nitric oxide (*9, 69*) and prostacyclin (*9*), and increases in hydraulic conductivity under increased pressure (*70*). The mechanism by which cells sense extracellular changes in their environment is largely unknown but it is likely a synergistic between the perturbation of mechanosensors at the cell surface and distortions experienced by the cell that are communicated to the actin cytoskeleton (*71*).

The actin cytoskeleton is a dynamic network of filaments and microtubules in constant motion. Under conditions of shear stress the displacement of the cytoskeleton significantly increases at the luminal surface of the cell (*72*) where extracellular domains of transmembrane protein components of the glycocalyx are found. The role of the glycocalyx in the translation of shear stress and

hydrostatic pressure to physiological manifestations has been investigated (*8, 9, 70*). Shear stress increases the production of reactive oxygen species (ROS) in endothelial cells (*73*) and enzymatic removal of key constituents of the glycocalyx, such as heparan sulfate, hyaluronan, and sialic acid, abolishes the increase of ROS (*9*). Increasing the hydrostatic pressure across endothelial cells exponentially increases the hydraulic conductivity of fluid through the monolayer; removal of heparan sulfate, a major component of the transmembrane proteoglycan syndecan, abolishes the increase in hydraulic conductivity (*10*). Taken together, these data suggest that components of the glycocalyx are able to sense changes in their environment and translate these changes into signals that dictate capillary endothelial function.

In order to dampen the signaling arising from perturbations of the glycocalyx that precipitates changes in the microvasculature, water-soluble copolymers are intercalated into the glycocalyx to stiffen the matrix with the aim to dampen mechanotransduction. Cationic copolymers are able to form ionic attachments to the glycocalyx, whose net negative charge is attributed to the high degree of sulfation and carboxyl moieties that reside on its component proteoglycans and glycosaminoglycans (GAGs).

Cationic copolymers are used ubiquitously in nonviral gene delivery as a vehicle in which DNA is packaged through charge-charge interactions and taken up into cells (*41, 47, 53*). The approach taken here is to use cationic HPMA copolymers to interact with the negatively charged endothelial glycocalyx with minimal cellular response.

The ultimate goal for copolymers targeted to the microvasculature is for use in the clinical setting as a treatment for pulmonary edema that occurs during cases of acute lung injury or acute respiratory distress syndrome. In this study, we address three fundamental aspects of any therapy: safety, targeting capacity, and efficacy. We demonstrate the safety of P(HPMA) copolymers by noting the reduction of lactate dehydrogenase (LDH) release in the presence of quaternary ammonium functional groups as opposed to copolymers containing primary amine side chains. We demonstrate polymer attachment to the glycocalyx by incubating fluorescently labeled copolymers with endothelial monolayers and showing high retention of fluorescent signal after extensive wash steps. Lastly, the efficacy of copolymers is demonstrated in their ability to attenuate both albumin diffusion and hydraulic conductivity across endothelial monolayers.

2.3 Materials and methods

2.3.1 Copolymer synthesis/characterization

Polymers are synthesized by radical polymerization of *N*-(2-hydroxypropyl)methacrylamide (HPMA) and *N*-(3-aminopropyl)methacrylamide (MA-AP) or methacrylamidopropyltrimethylammonium chloride (MA-TMA Cl) monomers in two feed ratios using methanol as the solvent with 2,2-azobisisobutryonitrile (AIBN) as the initiator. The concentration of comonomers in the polymerization mixture was 12.5 wt% and the AIBN concentration was 0.6 wt%. For fluorescence studies, 1 mol% 5-3-(methacryloylaminoropyl)thioureidyl fluorescein (MA-FITC) was added to the polymerization mixture. Radical polymerization was allowed to proceed under nitrogen atmosphere at 55°C for 24

hours. Molecular weight and molecular distribution were determined by size exclusion chromatography using an AKTA FPLC equipped with UV and RI detectors and a Superose 6 column in tetramethylammonium chloride (TMAC) buffer (0.25 M CH_3COONa, 0.5 M NaCl, 0.03 M TMAC, pH 6.0). The quaternary ammonium content was determined by the titration of the chloride counterion using $AgNO_3$ (*74*) and fluorescein as the indicator. The primary amine content was determined by ninhydrin assay (*75*). Both assays were performed in triplicate and are presented in Table 2.1 as mean ± standard deviation.

2.3.2 Cytotoxicity

The release of lactate dehydrogenase (LDH) was evaluated using a commercially available bioassay kit (BioVision, Mountain View, CA). A cell suspension (1.5 x 10^4 cells/well) of bovine lung microvascular endothelial cells (BLMVEC) was added to a microtiter plate and incubated at 37°C for 30 minutes with increasing concentrations of 40P(TMA)Cl or 40P(AP). Postincubation, cells were centrifuged at 250 x *g* and the supernatant was added to the reaction solution containing a tetrazolium salt that is cleaved to colored formazan in the presence of LDH. After reacting at room temperature for 30 minutes, absorbance was evaluated on a GENious 96-well plate reader (Tecan, Durham, NC) at 492 nm. The cytotoxicity is calculated according to equation 2.1.

$$Cytotoxicity(\%) = \frac{(sample - C_L)}{(C_H - C_L)} \times 100 \qquad (2.1)$$

Table 2.1.

Copolymer characterization data.

No.	Name	Structure of side chain	Feed composition (mol%)	Polymer composition (mol %)	Molecular weight[c] (kDa) (PDI)	% Yield
1	40P(AP)	$-NH(CH_2)_3-NH_2$	40	35[a]	ND	66%
2	80P(AP)	$-NH(CH_2)_3-NH_2$	80	70[a]	ND	81%
3	40P(TMA)Cl	$-NH(CH_2)_3N(CH_3)_3^+Cl^-$	40	46[b]	53.8 (1.8)	72%
4	80P(TMA)Cl	$-NH(CH_2)_3N(CH_3)_3^+Cl^-$	80	70[b]	65.6 (2.1)	79%

Notation used in Table 2.1: ND: not determined. [a]Determined by ninhydrin test. [b]Determined by titration with $AgNO_3$. [c]Determined by size exclusion chromatography. Fluorescent copolymers were polymerized with 1 mol% MA-FITC in feed composition and content of FITC was determined by UV spectroscopy using a molar extinction coefficient of 80,000 $M^{-1}cm^{-1}$.

C_L represents low control cells receiving no treatment and C_H represents high control cells receiving 1% Triton X-100. Statistics are calculated using n = 3 replicates per group.

2.3.3 Copolymer/cell interactions

BLMVEC were subcultured on glass coverslips pretreated with 0.4% gelatin for 1 hour and 100 µg/mL fibronectin for 1 hour and cultured to confluence. Cells were rinsed with PBS (pH 7.4) then incubated for 30 minutes at 37ºC with 40P(FITC)TMA Cl at a concentration of 1 mg/mL in phenol red-free DMEM supplemented with 1% BSA, 25 mM HEPES at pH 7.4. Cells were subsequently washed in PBS and fixed for 10 minutes in 2% paraformaldehyde at room temperature. Monolayers were rinsed in PBS then incubated at room temperature with 0.1% Triton X-100 to permeabilize cell membranes. Phalloidin conjugated with AlexaFluor 660 (Invitrogen) was dissolved in methanol (6.6 µM), diluted to 0.165 µM in PBS, and 200 µL was added to each glass-mounted cell monolayer. Incubation time was 40 minutes at 37ºC then cells were washed in PBS and mounted onto slides using ProLong Gold Antifade reagent to mitigate photobleaching of the far-red dye. Slides were imaged on an Olympus FV1000-xy confocal microscope at 40x magnification in 0.1 µm sections at excitation wavelength of 663 and emission wavelength of 690 in channel 1 and ex/em 494/521 in channel 2. Sections were rendered in 3D using Volocity software (PerkinElmer, Waltham MA).

2.3.4 Albumin diffusion

BLMVEC were subcultured on Costar Transwell polycarbonate membranes with a 0.4 μm pore size and a growth area of 1.12 cm^2 at a density of 2.5 x 10^5 cells/cm^2. Before seeding, the filters were treated with bovine gelatin and fibronectin and experiments were performed 7-10 days after plating. On the day of the experiment, warm test media, which is composed of HEPES (25 mM), penicillin/streptomycin (0.01%), and bovine serum albumin (BSA, 1%) in MCDB-131 (11.6 g/L) at pH 7.4, hereby denoted as Media II or MII, is added to a custom block chamber designed to hold Transwell chambers. Cell media containing 1% tetramethylrhodamine-conjugated BSA (TMR-BSA) in place of bovine serum albumin is added to the abluminal chamber of the Transwell directly onto BLMVEC monolayers, with or without polymer solution, to create a final volume of 0.5 mL and TMR-BSA concentration of 0.5 mg/mL. The abluminal chamber is sampled once per hour, replacing media, and signal from the TMR-BSA is detected on a microplate reader at ex/em 541/572 nm. The permeability diffusion coefficient is derived using equation 2.2.

$$P_{DA} = \frac{\Delta C \times A_{vol}}{A \times t \times L_{conc}} \tag{2.2}$$

P_{DA} is the diffusive permeability coefficient in cm/s, ΔC is the change in tracer concentration in the abluminal chamber, A_{vol} is the abluminal chamber volume in mL, A is the monolayer surface area (cm^2), t is time in seconds, and L_{conc} is the luminal concentration of tracer in mg/mL. Post-experimentation, cells are fixed in

formalin and stained with Ladd Multiple Stain to ensure confluent and intact monolayers. The experiment was performed in triplicate.

2.3.5 Hydraulic conductivity measurements

Snapwell filters housing confluent monolayers of BLMVEC were inserted into custom permeability chambers, which were custom built from two solid polycarbonate cylinders. The bottom half contains a small pressure-equilibrated reservoir (abluminal) that houses a Snapwell filter and seals with a rubber O-ring. The top half of the chamber contains a concavity that provides a 1 mL reservoir above the filters; it seals against the top rim of the Snapwell with a second O-ring. Two spring-loaded latches on the outside of the chamber lock the two halves of the cylinder together to form a watertight housing for the cells and their supports. The top of the permeability chamber has two stopcock-controlled ports for inflow and outflow of tissue culture media. A combination camera stand and glass capillary tube holder is custom built as one tightly fitted structure and machined from heavy aluminum. This design allows the camera to be calibrated only once for multiple uses of the equipment. The camera is a Sony RS-170 monochromatic video camera and programming of the video tracking and analysis software was done using LabVIEW (National Instruments, Austin, TX). The pressure manifold is composed of repurposed disposable polystyrene serological pipettes connected to a 5-stopcock manifold. Silastic tubing connects the inflow port of the permeability chamber with the pressure manifold. The portion of the silastic tubing that runs beneath the camera and houses the air bubble is fitted with an 18 cm length of clear borosilicate capillary

tubing with an internal diameter of 1.9913 mm ± 0.0004.

A schematic for the experiment process is given in Figure 2.1. During an L_p experiment, cell monolayers were placed in the chambers with MII and allowed to equilibrate for 1 hour under a hydrostatic pressure of 1 cm H_2O. After 1 hour, the pressure was increased to 10 cm H_2O. Following another hour, either a 1 mg/mL solution of 40P(TMA)Cl, P(HPMA), or MII only, denoted as control, was applied to the chamber housing BLMVEC monolayers. After 30 minutes, cells treated with polymer were washed with MII and monitored for another hour. Water pressure was increased by 5 cm H_2O every hour and L_p data were constitutively collected every 5 seconds. Postexperiment, Snapwell chambers were fixed in formalin and stained with Ladd Multiple Stain to ensure confluence. All monolayers included in data analysis were confirmed to be 100% confluent at the end of each experiment. Each experimental group is the product of 5-7 replicates.

2.3.6 Statistics

Data are expressed as means ± standard deviation with differences between groups assessed using nonparametric Dunn's test to show differences between three or more groups with unequal variances or paired t-tests when evaluating data between pressure increases. Graphics were generated in Kaleidagraph (Synergy Software, Reading, PA) and significance is concluded if $P < 0.05$.

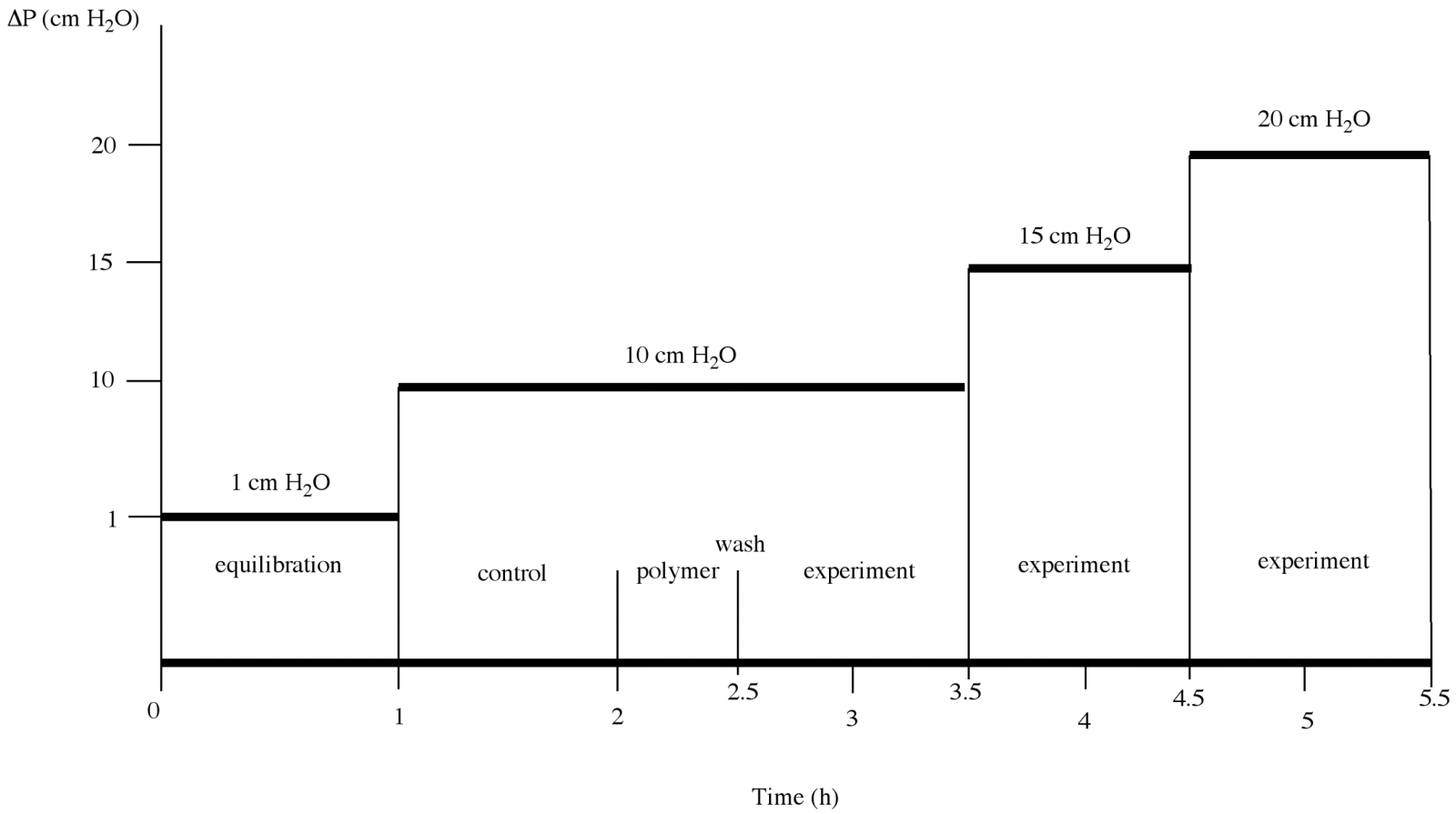

Figure 2.1. Outline for polymer application and pressure increases during an L_p experiment as a factor of time.

2.4 Results

2.4.1 Copolymer synthesis/characterization

Copolymers of HPMA and primary amine or quaternary ammonium cationic groups were synthesized for side-by-side comparison (Figure 2.2). For either copolymers of HPMA and trimethylammonium chloride (TMA Cl) or primary amine side chains (AP), two charge densities were obtained, either approximately 40 or 80 mol% cation composition (Table 2.1). Precise assessment of the final copolymer content of cationic residues results in values 5-10% lower than the feed ratios, in accordance with expectation and probability of polymerization. The molecular weights and polydispersity indices were similar for 40P(TMA)Cl and 80P(TMA)Cl and were obtained only for quaternary ammonium copolymers since these copolymers were the primary focus of binding and functional studies.

2.4.2 Cytotoxicity

The cytotoxicity of copolymers was evaluated by monitoring the release of LDH from cultured microvascular endothelial cells. LDH release was minimal in groups treated with P(HPMA) or P(TMA)Cl; only at the highest concentration of polymer and highest mol% of TMA [80P(TMA)Cl at 10 mg/mL] does the cytotoxicity exceed 10% (Figure 2.3 A). At the same concentration and composition percent, primary amine comonomers elicit 5- to 6-fold increases in LDH release (Figure 2.3 B). Marked cytotoxicity occurs in the presence of copolymers containing a high percentage of primary amines, but at 40 mol% both

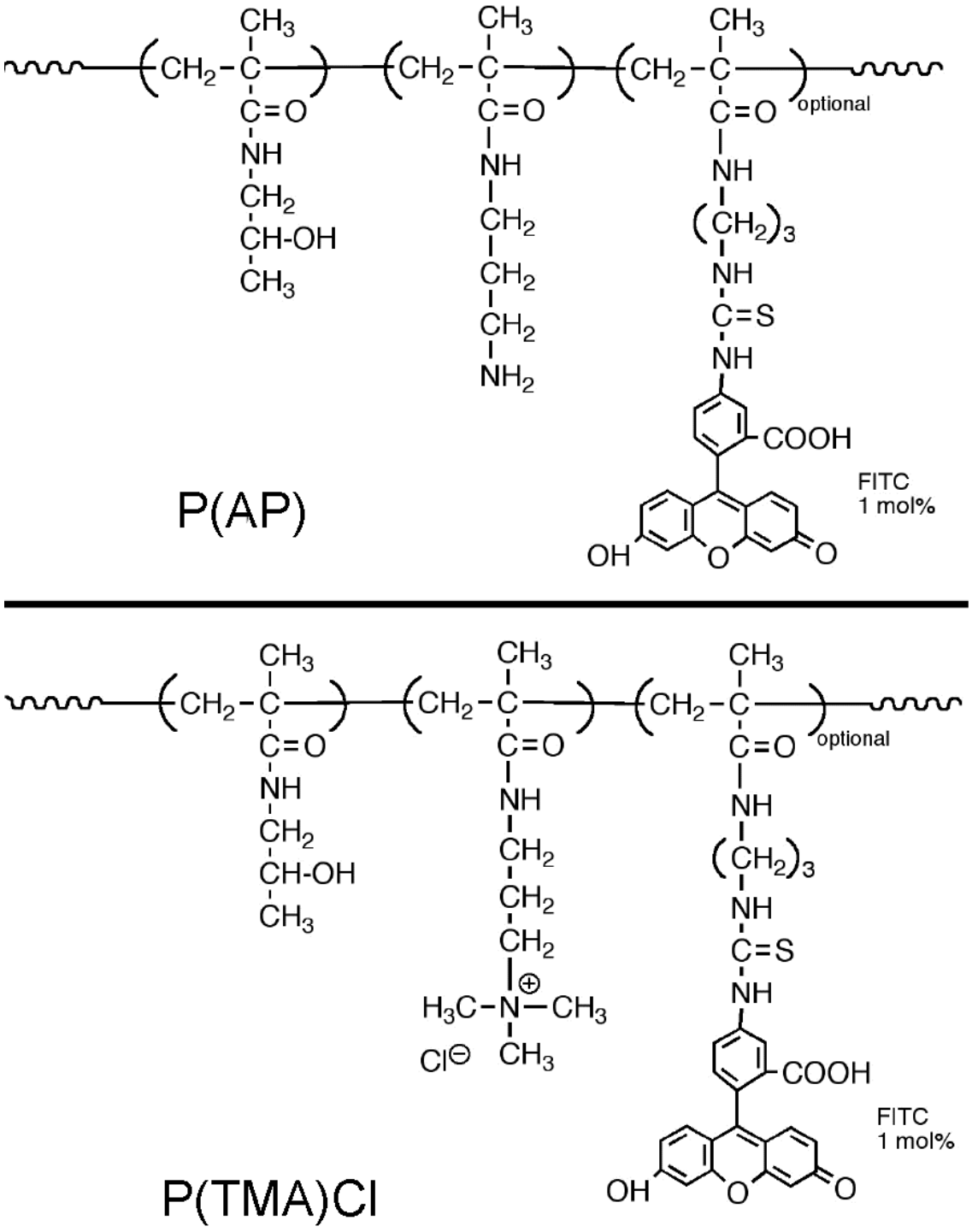

Figure 2.2. Polymer structures of (A) P(AP) and (B) P(TMA)Cl

cationic polymers behave similarly. Copolymers possessing quaternary ammonium groups exhibit significantly less cytotoxicity than copolymers composed of primary amine groups at higher feed compositions and are therefore chosen for further studies.

2.4.3 Copolymer-cell interactions

We show that positively charged copolymers can interact with the endothelial glycocalyx (Figures 2.4 A and 2.4 B). Fluorescently labeled 40P(FITC)TMA Cl is shown as the green layer on the top of the cells and the actin cytoskeleton is shown in red in the lower half of the image. A clear line is

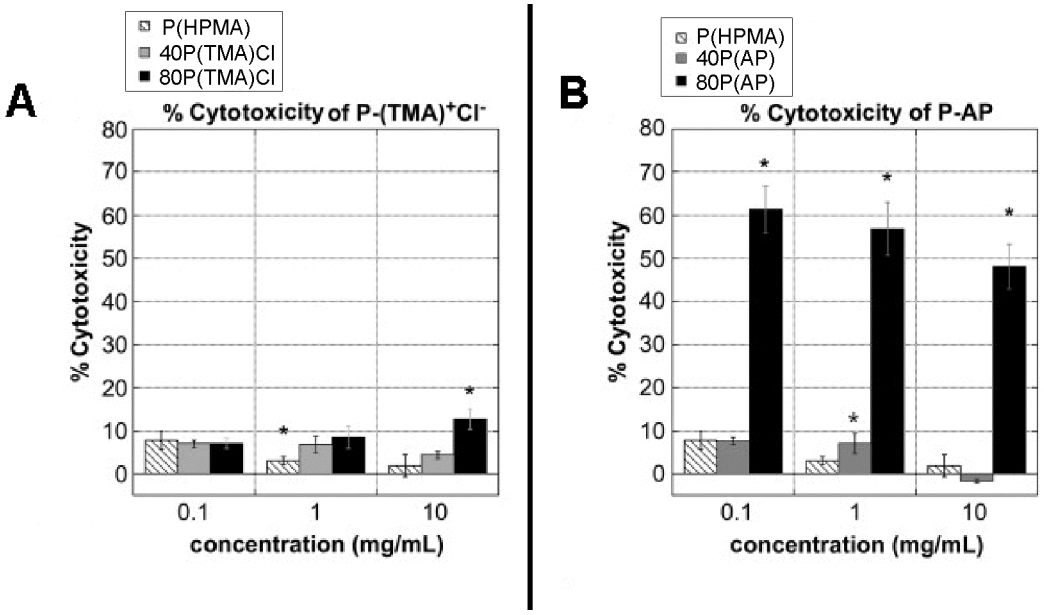

Figure 2.3. Cytotoxicity of copolymers as ascertained through LDH release for (A) P(TMA)Cl and (B) P(AP) of increasing concentrations. Copolymers containing primary amines showed significant cytotoxicity at higher mol% composition and higher concentrations whereas the cytotoxicity of quaternary ammonium copolymers exceeded 10% only at maximal charge mol% composition and concentration. * $P < 0.05$, Independent t-test, N = 4-5.

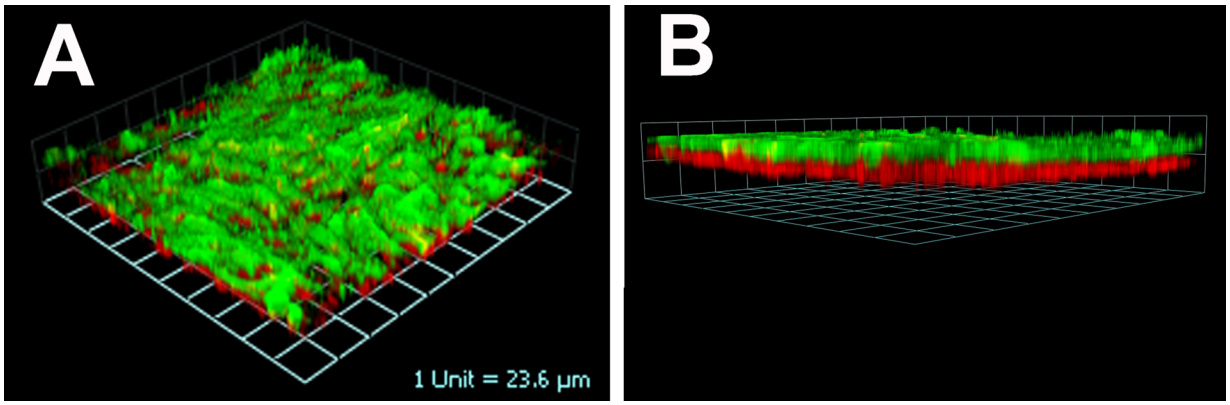

Figure 2.4. Confocal images of surface-bound 40P(FITC)TMA Cl (*46*) and actin cytoskeleton (red) as seen at (A) 45° and (B) 90° to the z axis. Figure incorporates approximately 75 cells imaged at 40x magnification. 40P(FITC)TMA Cl covers the monolayer after vigorous rinsing steps and actin staining demarcates the cell membrane from the cytoplasmic compartment.

visible between the extracellular polymer and the internal actin cytoskeleton (Figure 2.4 B) demonstrating that the polymer is able to interact with the glycocalyx at the cell surface.

2.4.4 Albumin diffusion

Endothelial monolayers treated with 5 and 10 mg/mL concentrations of 40P(TMA)Cl demonstrated a significant reduction in the permeability coefficient compared to control monolayers receiving no treatment (Figure 2.5 A). When P(HPMA) was used in place of 40P(TMA)Cl, no statistical difference was seen among any of the groups (Figure 2.5 B).

To test the potential of polymers to decrease P_{DA} under inflammatory conditions, endothelial monolayers were exposed to the inflammatory agonist bradykinin (1 µM) during experimentation. The addition of bradykinin to cells increased the albumin permeability coefficient by nearly 2-fold after 1 hour (Figure 2.6). After one subsequent hour of monolayer exposure to

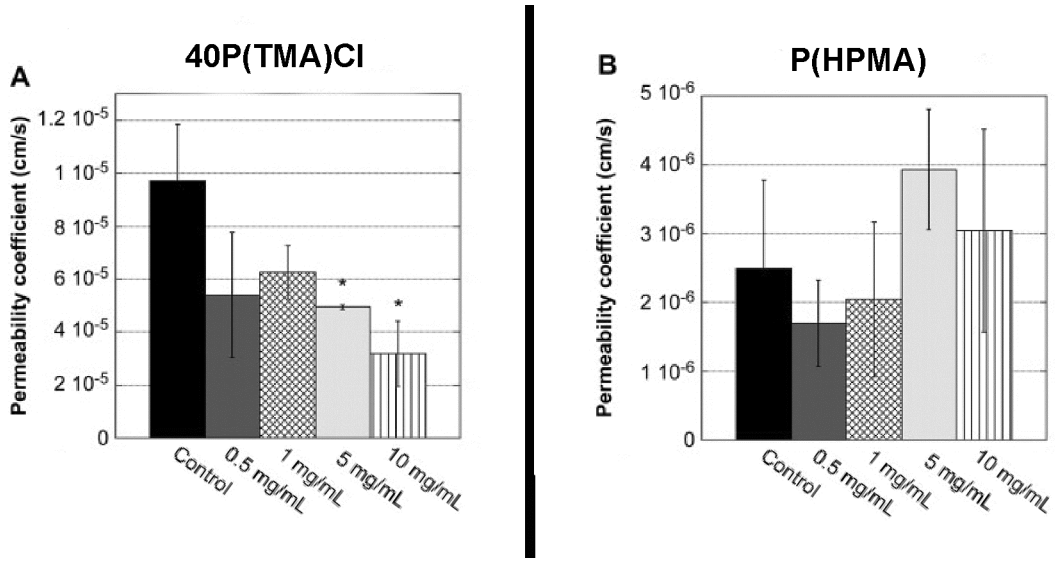

Figure 2.5 Permeability coefficients of albumin diffusion across confluent BLMVEC in the presence of (A) 40P(TMA)Cl or (B) P(HPMA). 40P(TMA)Cl reduces P_{DA} in a concentration-dependent manner consistent with quantitative binding to the glycocalyx and enhancement of passive barrier function. P(HPMA) was unable to significantly reduce P_{DA} with respect to control at any concentration. *P < 0.05; Nonparametric Dunn's test, N=3.

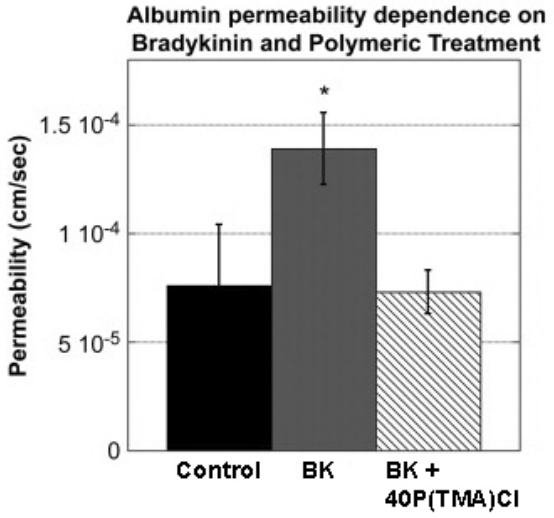

Figure 2.6 Albumin diffusion coefficients of cell monolayers treated with cytokine and/or 40P(TMA)Cl. Addition of bradykinin (BK, grey bar) to monolayers increases permeability coefficient. Concurrent addition of 40P(TMA)Cl (shaded bar) abolishes the bradykinin-induced increase in P_{DA} compared to control diffusion coefficients (black bar). *P < 0.05; Nonparametric Dunn's test, N=3

bradykinin and 40P(TMA)Cl, the permeability coefficient was reduced to that of control cells receiving neither polymer nor bradykinin.

2.4.5 Hydraulic conductivity of endothelial monolayers

Copolymer solutions were applied to cell monolayers prior to L_p experimentation. A schematic for the experiment protocol is given in Figure 2.1. L_p values were normalized to the average of the L_p values acquired during the last 5 minutes of the 10 cm H_2O pressure interval in order to facilitate comparison between experiments. Peak normalized L_p values are the average of the L_p values acquired during the last 5 minutes of a given interval. Figure 2.7 compares cells receiving no polymer treatment to those receiving 40P(TMA)Cl and P(HPMA) at a concentration of 1 mg/mL. Treatment with 40P(TMA)Cl decreased L_p by 76% compared to controls after cells had been subjected to pressures of 20 cm H_2O. Increasing the polymer concentration by ten fold further reduced L_p by 20% but when compared to controls, percent L_p reduction was 76% and 81% for concentrations of 1 mg/mL and 10 mg/mL, respectively (data not shown). These figures show compelling evidence for the ability of polymers to enhance the function of the glycocalyx by reducing hydraulic conductivity across endothelial monolayers.

2.5 Discussion

The ultimate goal for copolymers targeted to the microvasculature is for use in the clinical setting as a treatment for pulmonary edema. This study addresses three fundamental aspects of any therapy: safety, targeting capacity,

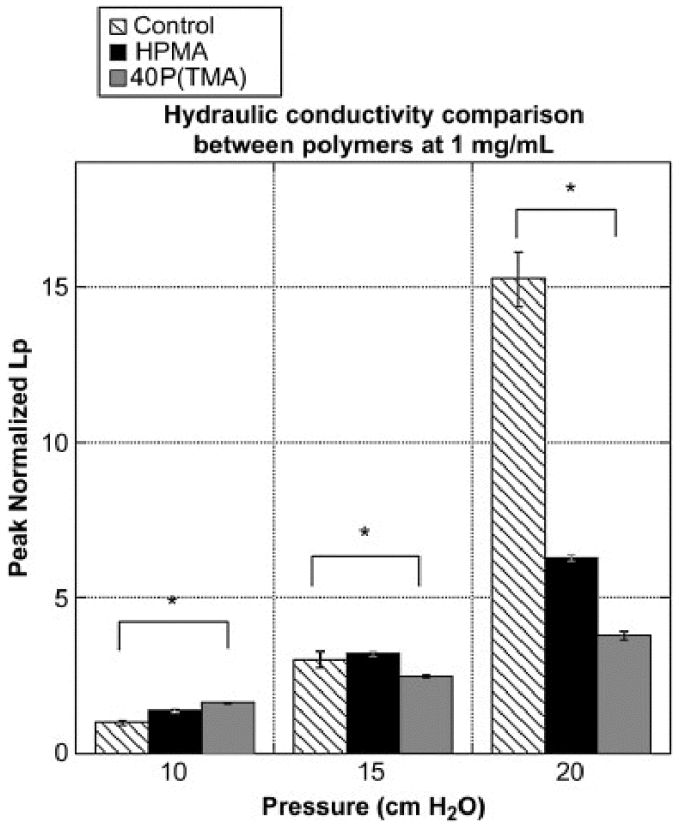

Figure 2.7. Hydraulic conductivity measurements taken from control cells (stripe) and cells treated with P(HPMA) (black) or 40P(TMA)Cl (shaded). 40P(TMA)Cl significantly reduced peak normalized Lp at 20 cm H_2O pressure. *$P < 0.05$; Dunn's nonparametric test, N = 5-7.

and efficacy. The safety of HPMA-based copolymers is demonstrated by noting the reduction of LDH release in the presence of quaternary ammonium functional groups as opposed to copolymers containing primary amine side chains. Confocal experiments demonstrate the capacity for cationic copolymers to form strong associations with the glycocalyx. Lastly, the efficacy of copolymers is demonstrated in their ability to attenuate both albumin diffusion and hydraulic conductivity across endothelial monolayers.

Cationic copolymers were synthesized to contain increasing molar ratios of primary amine and quaternary ammonium conjugates in order to maximize

binding to the glycocalyx while minimizing cell uptake. Initial cytotoxicity experiments suggested that primary amine copolymers and 80P(TMA)Cl would elicit an undesirable cellular response so the characterization of molecular weights and averages of copolymers was restricted to the copolymers to be used in further studies, namely 20P(TMA)Cl and 40P(TMA)Cl. Cellular response was measured using an LDH release assay; lactate dehydrogenase is released from cells prior to apoptosis and is therefore a standard marker for cell death. Consistent with previous studies quantifying transfection efficiency for gene delivery purposes (*53*), we also saw that copolymers composed of primary amines elicited a greater cellular response than did those composed of quaternary ammonium. It has been shown in studies that evaluate cationic copolymers for gene delivery that copolymers that carry quaternary ammonium charges tend to elicit less cytotoxicity and have a lower transfection activity than copolymers composed of primary amines in cellular systems (*53*). As P(HPMA) itself elicits negligible immunogenic response (*44, 45*), it would be expected that copolymers with greater cationic charge density should elicit the greater cytotoxicity response in serum-free media.

The capacity of 40P(TMA)Cl to bind to the negatively charged glycocalyx was demonstrated using confocal microscopy. Fluorescently labeled 40P(FITC)TMA Cl was incubated with confluent endothelial monolayers and washed extensively from the cell surface before imaging. Copolymer is visualized in green and the actin cytoskeleton in red. The staining pattern of the copolymer is consistent with reports of heterogeneity of the glycocalyx across the

capillary (*76*). The staining of submembrane actin served to distinguish the cytoplasmic compartment from the cell surface. A clear line of delineation between the cell surface and cytoplasm is visible, suggesting that the polymer remains on the exterior of the cell.

In functional assays, the diffusion of labeled albumin across confluent monolayers is a model for protein extravasation through the endothelial barrier and serves as a measure of barrier integrity. When 40P(TMA)Cl was added to monolayers, the permeability coefficient decreased with increasing polymer concentration and reached significant levels of difference at concentrations of 5 and 10 mg/mL. No such trend was seen with P(HPMA). Since there is no pressure upon the cell monolayer to force copolymer into the glycocalyx, P(HPMA) has no effect on P_{DA} thus it is clear that ionic contacts are necessary to bring the copolymer into contact with the cell surface to reduce protein flux from the apical to basal sides of the cell monolayers.

To test the efficacy of cationic copolymer on enhancing barrier function in the course of inflammatory states, the inflammatory agonist bradykinin was added to cell chambers and P_{DA} increased dramatically after 1 hour. Concurrent addition of 40P(TMA)Cl to monolayers subjected to bradykinin treatment reduced P_{DA} to levels similar to those of controls. This is likely due to the ability of 40P(TMA)Cl to intercalate into the glycocalyx and block serum proteins from moving from one side of the barrier to the other, thus enhancing the passive function of the glycocalyx.

Previous work has shown the influence of hydrostatic pressure on the flux of fluid from the capillary lumen to the surrounding tissue (*7, 70*). The intercalation of polymer into the glycocalyx is hypothesized to reduce mechanotransduction that occurs when glycoproteins on the cell surface experience perturbations due to hemodynamic forces. Biomimetic copolymer administration is hypothesized to dampen signaling to the actin cytoskeleton, which contacts transmembrane glycoproteins, focal adhesions and adherens junctions, all of which regulate fluid flux across the capillary (*71*). Dull et al. have shown previously that pressure increases across endothelial monolayers increase fluid flux from the luminal side of the monolayer to the basolateral side and that removal of key components of the glycocalyx abolishes the pressure-induced increase in hydraulic conductivity (*70*), thus providing evidence that the glycocalyx plays an active role in mechanotransduction. 40P(TMA)Cl was removed from the permeability chambers in L_p experiments after an incubation period in order to mimic the effect of an infusion and subsequent washout period of copolymer delivered to the microvascular capillary lumen. There was a significant decrease in hydraulic conductivity between control cells and those treated with solutions of 40P(TMA)Cl. P(HPMA) alone was also able to reduce hydraulic conductivity when compared to controls, which can be attributed to incomplete polymer removal from cell monolayers as polymers in a static system under pressure will be able to associate with the glycocalyx via van der Waals and dipole-dipole interactions. The decrease in hydraulic conductivity suggests polymeric intercalation into the glycocalyx, which can either enhance the passive

role of the glycocalyx, potentially by creating a thicker barrier for fluid to pass through, and attenuate the active role of mechanotransduction by theoretically limiting the motion of cell surface glycoproteins.

2.6 Conclusion

The safety, applicability and efficacy of a water-soluble biomimetic polymer with potential as a clinical therapy for patients with acute lung injury are shown in this work. Moreover, there is compelling evidence that deformations in the endothelial glycocalyx are a major factor in mechanotransduction and that the administration of a material capable of limiting such deformations is relevant. The clinical implications for a simple yet elegant therapy to counteract the life-threatening effects of pulmonary edema are significant and further development of this approach is encouraged by the data presented thus far.

CHAPTER 3

MECHANISM AND *EX VIVO* STUDIES OF COPOLYMER DELIVERY TO VASCULAR ENDOTHELIUM UNDER MECHANICAL STRESS[‡]

3.1 Abstract

Therapeutic compound(s) capable of attenuating changes in vascular barrier function would represent a significant advance in critical care of pulmonary edema and the associated increases in vascular permeability that continue to represent a significant problem in the clinic. We have previously reported the development of HPMA-based copolymers, targeted to endothelial glycocalyx that are able to enhance barrier function. In this work, we report the refinement of copolymer design and extend our physiological studies to demonstrate that the polymers: 1) reduce both shear- stress and pressure-mediated increase in hydraulic conductivity, 2) reduce nitric oxide production in response to elevated hydrostatic pressure and, 3) reduce the capillary filtration coefficient (K_{fc}) in an isolated perfused mouse lung model. These copolymers

---

[‡]The shear-induced hydraulic conductivity measurements (section 3.3.3) were performed by Veronica Lopez-Quintero, a graduate student at the City College of CUNY under the advisement of Dr. John Tarbell, a close collaborator with Dr. Dull. The polymers used in the experiment were my design and the resulting

represent an important tool for use in mechanotransduction research and a novel strategy for developing clinically useful copolymers for the treatment of vascular permeability.

3.2 Introduction

It has been long appreciated that endothelial cells are able to sense mechanical forces imparted by flowing blood and respond accordingly. The glycocalyx is exposed to shear stress as blood flow distorts surface proteoglycans parallel to the capillary wall and increased pressure exerted perpendicularly drives flow and shear stress through inter-endothelial junctions containing glycocalyx (*77*); these forces can, in excess, have a deleterious effect on the integrity of the capillary barrier.

Nitric oxide (NO) is produced in response to shear through calcium dependent and calcium independent pathways. Within seconds after onset of shear, transient increases in intracellular calcium activate nitric oxide synthase (eNOS) to produce NO (*78*). The calcium-independent activation of eNOS by laminar shear is a result of phosphorylation of the enzyme (*79*). Low levels of constitutively expressed NO are responsible for vascular homeostasis in normal tissues whereas increased levels of NO are capable of reaction with endogenous superoxide to form the powerful oxidant peroxynitrite and thereby instigate barrier

---

figures and data analysis, along with the remainder of the polymer syntheses and experiments in this chapter, are my own. This chapter is adapted from Giantsos-Adams et al. *Biomaterials* **32:**288-94 (2011) with permission from the journal.

dysfunction via deleterious pathways involving reactive oxygen species (*80*). Likewise, it has been shown that the removal of specific components of the glycocalyx inhibits this response (*8*), implicating the endothelial glycocalyx as a mechanosensor.

The endothelial glycocalyx carries a net negative charge due to sulfate and carboxyl groups and sialic acids found on proteoglycans that decorate the cell surface and cell junctions. *In vitro* studies have shown that the administration of a positively charged copolymer that interacts with the negatively charged glycocalyx is able to enhance the passive barrier function of the glycocalyx and dampen the role of the active barrier regulation component, namely mechanotransduction (*54*). In this work, the net negative charge of the endothelial cell surface is exploited to deliver a water-soluble cationic copolymer that interacts with the glycocalyx in order to enhance the physical barrier and reduce mechanical perturbations to the glycocalyx and thereby attenuate mechanotransduction.

The goal of these copolymers, clinically, is to lay the foundation for the development of a treatment for acute lung injury associated with inflammation and altered pulmonary vascular pressures, and to be used in the laboratory as a tool toward a better understanding of mechanotransduction pathways. Some work has been done in the realm of therapeutic polymers delivered to lung endothelium to treat acute lung injury (*81*) or as a free radical scavenger (*82*), however, to date the effort is preliminary and the mechanism is largely unexplored. This work explores the relationship between mechanotransduction

and polymer molecular weight and charge distribution in order to begin to optimize future endeavors in the realm of polymer delivery to enhance barrier function. Here, we show that cationic copolymers possessing low charge density are able to reduce shear- and pressure-mediated barrier dysfunction, reduce the formation of nitric oxide and reduce the filtration coefficient in an intact lung model.

3.3 Materials and methods

3.3.1 Polymer synthesis/characterization

Polymers are synthesized by radical polymerization of HPMA and MA-TMA Cl monomers in varying feed compositions using methanol as the solvent and AIBN as initiator. The concentration of comonomers in polymerization mixture was 12.5 wt% and the AIBN concentration was 0.6 wt% or 0.2 wt% for 20P(TMA)Cl or 10P(TMA)Cl, respectively. Radical polymerization was allowed to proceed under nitrogen atmosphere at 55°C for 24 hours. Molecular weight and molecular distribution were determined using AKTA FPLC (GE Healthcare, Piscataway, NJ) equipped with UV and RI detectors using a Superose 6 column in tetramethylammonium chloride (TMAC) buffer (0.25 M CH_3COONa, 0.5 M NaCl, 0.03 M TMAC, pH 6.0). A Superose 6 preparative column under the same conditions was used in conjunction with this system for polymer fractionation. Quaternary ammonium content was determined by titration of chloride counterion using 0.01M $AgNO_3$ (*74*). Titrations were performed in triplicate with a custom 1 mL buret (Wilmad Glass) and values are presented as mean and standard deviation.

3.3.2 Cell Culture

Bovine aortic endothelial cells (BAEC) and rat lung microvascular endothelial cells (RLMVEC) were purchased from Vec Technologies (Rensselaer, NY) and grown in T-75 flasks with 10% FBS in complete medium, purchased from Vec Technologies, at 37°C in 5% CO_2. Upon reaching confluence (3-4 days) the cells were split for continuing maintenance of the cell line. BAEC were plated at a density of 1.25 x 10^5 cells/cm^2 on polycarbonate Transwells previously coated with 1% fibronectin. RLMVEC were plated on 1% fibronectin and 0.05% gelatin or 10% FBS-MEM for Snapwells or Transwells, respectively, and incubated in 5% CO_2 at 37°C. The shear-permeability experiments were run 4-6 days after plating and pressure-permeability experiments were run on days 9 and 10 after plating. Cells were used from passages 4 to 7.

3.3.3 Shear-induced hydraulic conductivity (L_p)

Prior to L_p measurements, BAEC were cultured on Transwell membrane supports (12 mm diameter, 0.4 μm pore size) and grown to confluence. On the day of the experiment, monolayers were incubated with either 20P(TMA)Cl (70.2 kD, PD 1.8), 20P(TMA)-F3 (135 kD, 1.1 PD), or 20P(TMA)-F5 (24 kD, PD 1.2) at a concentration of 1 mg/mL in 1% BSA for 30 minutes at 37°C and then were rinsed twice with experimental media (MEM supplemented with 1% BSA) and placed in the transport apparatus to determine shear-induced hydraulic conductivity as previously described (*83*). The measurement of fluid flow across the endothelial monolayer was performed inside a Plexiglas box maintained at

37°C. The seeded filters were placed inside a chamber to form a luminal (top) compartment and an abluminal (bottom) compartment separated only by the BAEC monolayer. The abluminal compartment was connected to a reservoir via Tygon and borosilicate glass tubing. The vertical displacement of the reservoir with respect to the liquid covering the cells applied a hydrostatic pressure differential across the monolayer. At 10 cm H_2O differential pressure, the volumetric flow rate (J_v) was measured by tracking the position of an air bubble that was placed into the calibrated borosilicate glass tube. The hydraulic conductivity was calculated from equation 3.1.

$$Lp = \frac{Jv/A}{\Delta P} \tag{3.1}$$

A represents the area of the BAEC monolayer and ΔP is the pressure differential across the monolayer. During each experiment, one untreated endothelial monolayer was tested as control while a copolymer solution was applied to a separate monolayer and both experiments were run concurrently. After 60 minutes of applied pressure differential, a baseline L_p was established for each respective monolayer and a defined shear stress was applied to each endothelial monolayer. L_p values were collected for 4 hours. Shear was applied to the surface using a rotating disk separated by a distance h (500 μm) from the monolayer surface. The rotating disk generated a fluid shear stress distribution on the monolayer surface defined by equation 3.2.

$$\tau = \frac{\mu \omega r}{h} \quad (3.2)$$

The variable μ represents the viscosity of the media, ω is the rotational speed, and r is the radial distance from the center of the disk. The parameters were adjusted in order to achieve a maximum steady shear stress of 20 dyn/cm^2 at the edge of the disk. The average shear stress over the entire filter area is 2/3 of the maximum. The luminal compartment and the reservoir were supplied with 5% CO_2 throughout the experiment to maintain the media at pH 7.4.

3.3.4 Pressure-induced hydraulic conductivity

The system used to measure the volumetric flux rate (J_v) and hydraulic conductivity (L_p) has been described previously (*84*) and also thoroughly in section 2.3.5. RLMVEC monolayers were allowed to equilibrate for 1 hour under a hydrostatic pressure of 1 cm H_2O in PRF-MII (phenol red-free DMEM with 25 mM HEPES, 1% BSA, and 0.01% penicillin/streptomycin at pH 7.4). For experiments involving L-NAME (Nω-nitro-L-arginine methyl ester hydrochloride), cells were incubated at 37ºC for 1 hour prior to experiment with 10 μM L-NAME and the NO blocker was present in media for the duration of the experiment. For polymer-treated experimental groups, after the 1 hour equilibration period, a solution of 20P(TMA)Cl (1 mg/mL) in PRF MII was added to the luminal cell chamber and the pressure was increased to 10 cm H_2O. After 30 minutes, polymer was washed from cells with a 6-fold volume of PRF MII and the experiment was allowed to proceed under 10 cm H_2O pressure for another half hour. The water pressure was subsequently increased by 10 cm H_2O every

hour; L_p data were constitutively collected every 5 seconds. At the end of the experiment, Snapwells were removed from permeability chambers and monolayers were fixed in formalin and stained with Ladd Multiple Stain (Ladd Research, Williston, VT) to confirm monolayer integrity. An aliquot (500 µL) of the media above the cells was collected, centrifuged and frozen for NO analysis.

3.3.5 Nitric oxide detection

The nitric oxide content was evaluated using an NO Quantification Kit (Active Motif, Carlsbad, CA). Nitrates in the sample were reduced to nitrites using nitrate reductase and the Greiss reaction was utilized to colorimetrically quantify the products of NO in the supernatant samples. Assays were performed in triplicate and evaluated using a microplate reader (Tecan, Mannedorf, Switzerland) at absorbance wavelength 540 nm with reference wavelength 612 nm.

3.3.6 *Ex vivo* lung preparation

All animal experiments were approved by the University of Utah's Institutional Animal Care and Use Committee (IACUC) and are in accordance with the Guide for the Care and Use of Laboratory Animals (National Research Council). C57/BL6 mice (20-25 grams) were anesthetized with ketamine/xylazine (80/10 mg/kg), a tracheotomy was performed and they were mechanically ventilated with a pressure-controlled ventilator (Kent Scientific, Torrington, CT). Respiratory rate was 50/minute, and peak inspiratory pressure (*23*) was 7-10 cm H_2O. The chest and pericardial sac were sequentially opened

and ligatures were placed around the aorta and pulmonary artery. Heparin (200 U) was injected into the pulmonary artery and allowed to circulate for 2 minutes. The mouse was exsanguinated via a left ventriculostomy and the left atrium was cannulated via the left ventriculostomy. The pulmonary artery was cannulated via the right ventricle and lungs were perfused with Krebs-Ringers-bicarbonate solution (Sigma Chemical, St. Louis, MO) containing 3% bovine serum albumin (BSA; Fraction V, Proliant, Ankeny, IA). Pulmonary artery (P_{PA}) and left atrial pressures (*85*) were measured continuously via in-line pressure transducers (P-75, Harvard Apparatus, Natick, MA) connected to an A/D board. Solenoids (20PSI, 12V DC, Cole Parmer, Mount Vernon, IL) were placed in-line on both the arterial and venous tubing and could be closed simultaneously for measuring double occlusion pressures (P_{DO}). An in-line ultrasonic flow probe (Transonic, Ithaca, NY) was placed in the pulmonary artery cannula and flow data was recorded in real-time. Lungs were suspended from a force transducer (Radnoti, Minrovia, CA) and lung weight was zeroed; lung weight, vascular pressures and flow were recorded using a custom-written program (Labview, National Instruments, Austin, TX). An experiment scheme is presented in Figure 3.1.

3.3.7 Calculation of K_{fc}

Lungs were perfused at 2 ml/min, left atrial pressure = 2 cm H_2O during a 20 minute isogravimetric period. To measure K_{fc}, P_{LA} was increased to 7 cm H_2O for 20 minutes and the slope of weight gain/time during 18-20 minutes was used to derive K_{fc} according to equation 3.3.

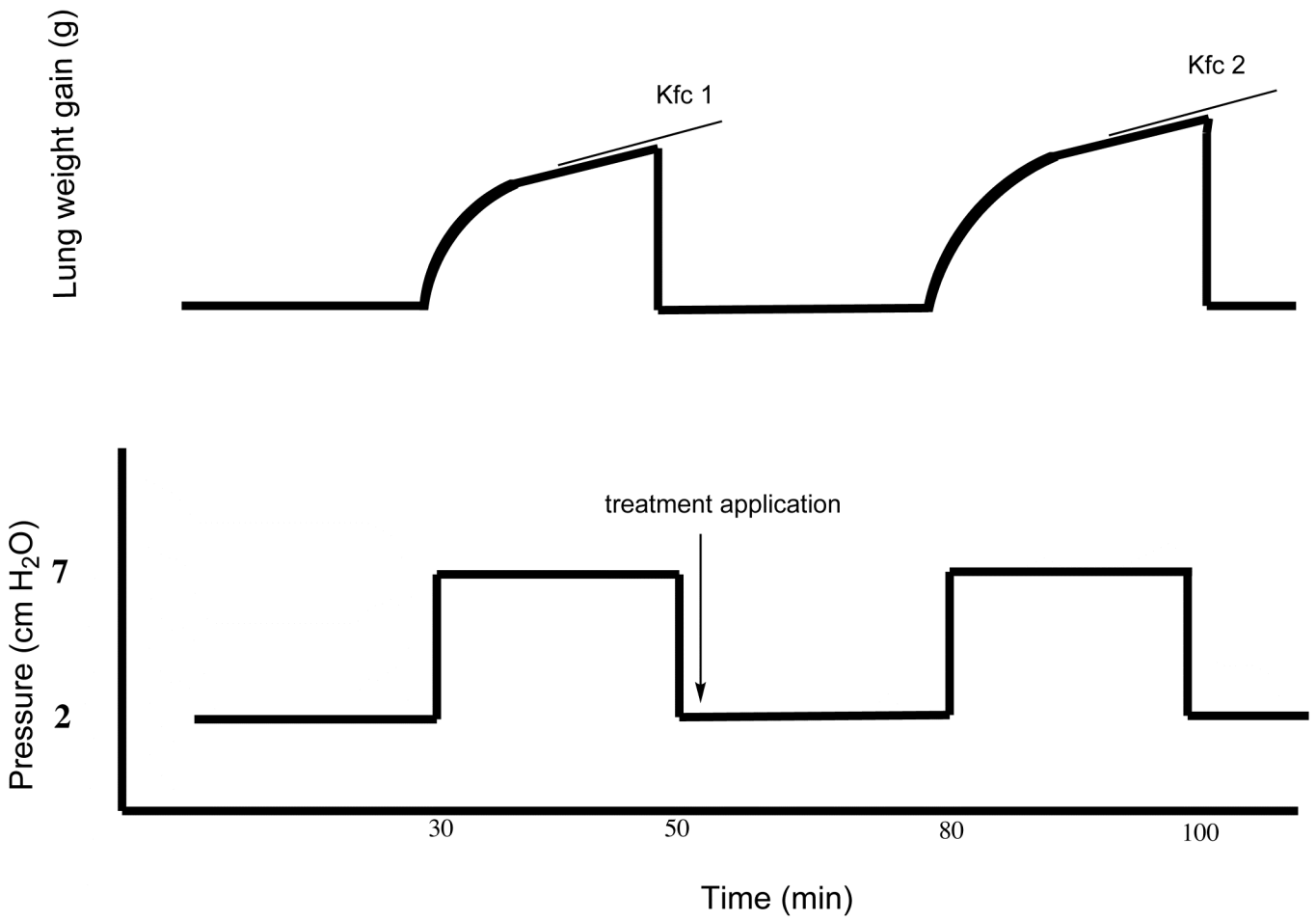

Figure 3.1. Schematic of an isolated perfused lung experiment. Pressure (bottom plot) is the independent variable and lung weight gain (top plot) is the dependent variable.

$$K_{fc} = \frac{\frac{\Delta wt}{t}}{P_c} \quad (3.3)$$

The relationship $\Delta wt/t$ is the slope of the line depicting weight gain over time and P_c is the capillary pressure calculated according to equation 3.4.

$$P_c = P_{PA} + \frac{P_{LA}}{2} \quad (3.4)$$

Units are in mL/min/cm H_2O, P_{PA} represents pulmonary artery pressure and P_{LA} represents left atrial pressure. This value was normalized to 100 grams of predicted lung weight. After the 20 minute increase in P_{LA}, the pressure is reduced to 2.0 cm H_2O for 20 minutes and the polymer was perfused into the lungs via the pulmonary artery catheter at a rate of 1 mg/mL/min. P_{LA} was then increased to 7 cm H_2O and K_{fc} was measured from 18-20 minutes. The ratio of $K_{fc}2/K_{fc}1$ was used to assess the effect of polymers on whole lung permeability.

3.3.8 Statistical analysis

L_p values are presented as mean ± standard deviation. A P-value less than 0.05 is considered significant. Statistics were performed with ANOVA and Tukey's post hoc comparison where appropriate. All other statistical tests are specified in the figure caption.

3.4 Results

3.4.1 Copolymer synthesis and characterization

Copolymers of HPMA and MA-TMA Cl were synthesized in two feed ratios to create polymers of either 10 or 20 mol% quaternary ammonium content. Table 3.1 gives the nomenclature and characterization data for each copolymer used

Table 3.1

Copolymer characterization data

Name	Feed composition (mol %)	Polymer composition [mol % (SD)]	Molecular weight [kDa (PDI)]	Charges per macromolecule
20P(TMA)Cl	20	19.9 (1.4)	70.2 (1.8)*	95
20P(TMA)Cl-F3	20	19.9 (1.4)	135 (1.1)	182
20P(TMA)Cl-F5	20	19.9 (1.4)	24 (1.2)	32
10P(TMA)Cl-F2	10	10.7 (0.7)	90 (1.2)	65
PEO	---	---	82 (1.1)	--

Polymer nomenclature and characterization data. Approximate percent composition of TMA Cl is denoted as the number, in percent, before TMA Cl and fractionated polymers have either F2, F3 or F5 following the name. * Indicates non-fractionated copolymer.

and Figure 3.2 shows the molecular structure for TMA-HPMA copolymers. The unfractionated molecular weight of 10P(TMA)Cl (Mw 135 kD, 1.9 PD) was higher than that of 20P(TMA)Cl (70.2 kD, PD 1.8) because of the lower AIBN concentration in the polymerization reaction mixture. 10P(TMA)Cl and a portion of 20P(TMA)Cl were fractionated. The molecular weight profile for unfractionated 20P(TMA)Cl and fractionated 20P(TMA)Cl-F3 and 20P(TMA)Cl-F5 are given in Figures 3.3, 3.4, and 3.5, respectively. Fractionation resulted in narrow molecular weight distributions. The exact concentration of quaternary ammonium charges per mole of polymer was found to be within 1% of the theoretical value. These values were then used to calculate the charges per macromolecule of polymer to indicate respective relative charge densities.

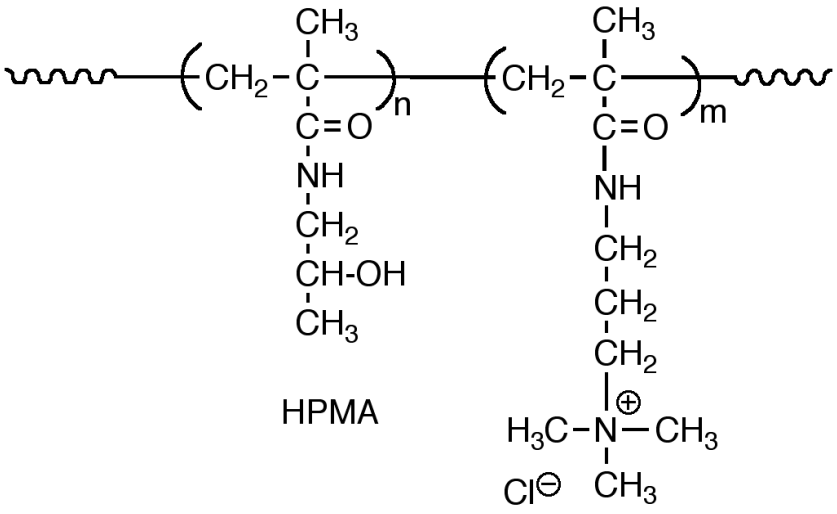

Figure 3.2. Structure of a P(TMA)Cl copolymer. All copolymers used in this study possess this basic structure. Alterations are made in percent composition of TMA Cl and molecular weight.

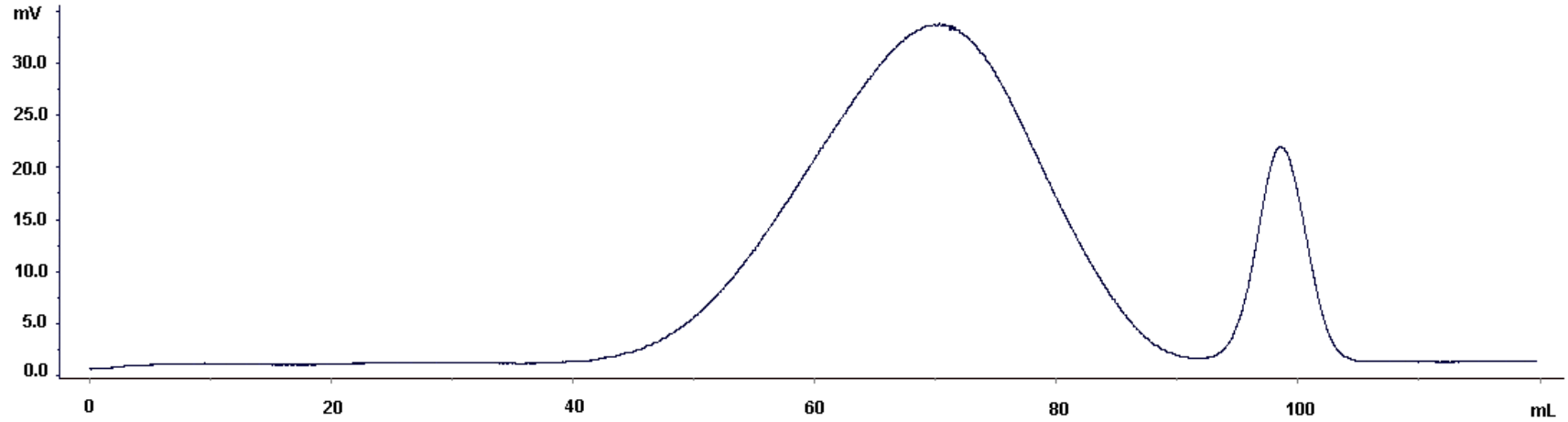

Figure 3.3. Molecular weight profile for unfractionated 20P(TMA)Cl copolymer. Profiles are generated using AKTA software and a Superose 6 column in tetramethylammonium chloride (TMAC) buffer (0.25 M CH_3COONa, 0.5 M NaCl, 0.03 M TMAC, pH 6.0). Molecular weight 70.2 kDa, PDI 1.8.

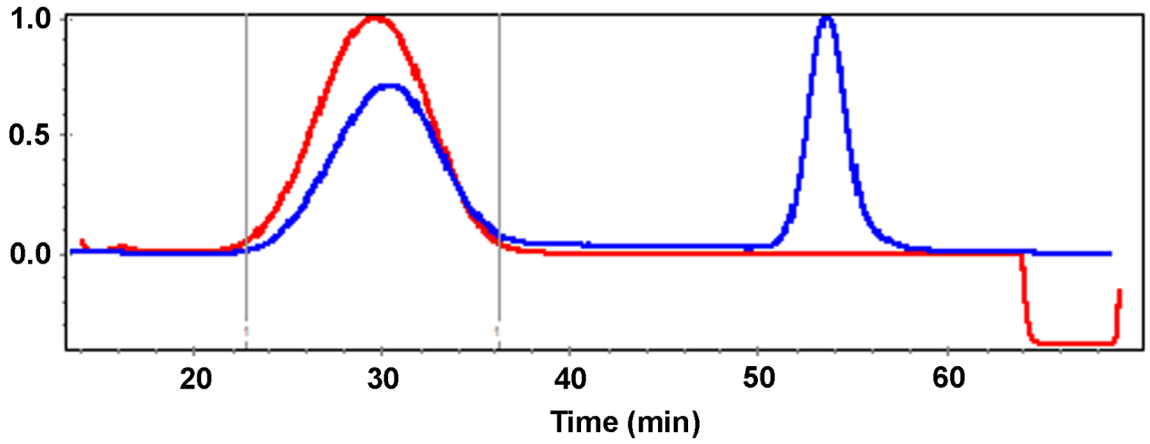

Peak 1	
Peak limits (min)	22.862 - 36.192
dn/dc (mL/g)	0.170
Polydispersity	
Mw/Mn	1.072(0.2%)
Mz/Mn	1.157(0.4%)
Molar mass moments (g/mol)	
Mn	1.260e+5(0.1%)
Mp	1.258e+5(0.1%)
Mv	n/a
Mw	1.351e+5(0.2%)
Mz	1.458e+5(0.4%)

Figure 3.4. Size exclusion profile and characterization data for 20P(TMA)Cl-F3. The blue trace is refractive index (RI) and the red trace is light scattering (LS) data. Profiles are generated using AKTA instrumentation, ASTRA MiniDawn software, and a Superose 6 column in tetramethylammonium chloride (TMAC) buffer (0.25 M CH_3COONa, 0.5 M NaCl, 0.03 M TMAC, pH 6.0).

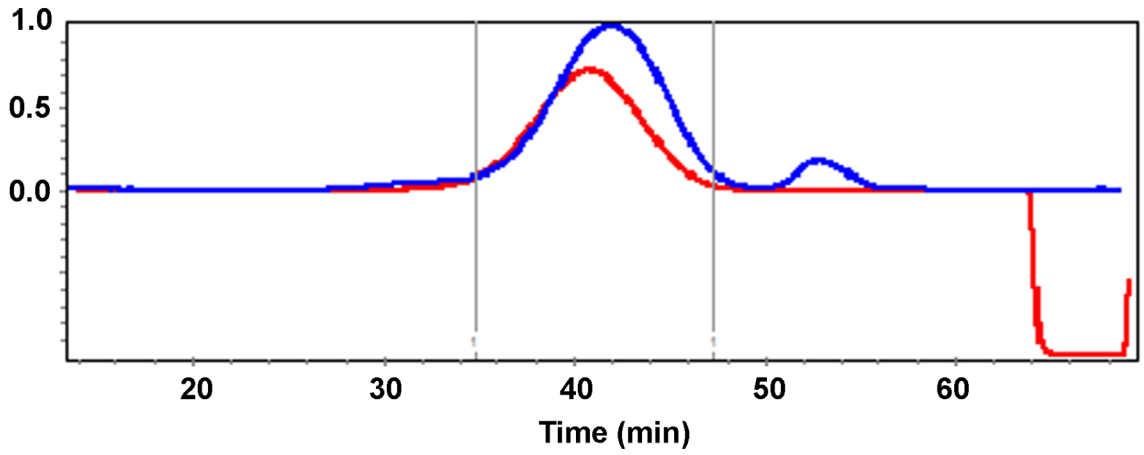

Peak 1	
Peak limits (min)	34.796 - 47.301
dn/dc (mL/g)	0.170
Polydispersity	
Mw/Mn	1.151(0.6%)
Mz/Mn	1.294(0.9%)
Molar mass moments (g/mol)	
Mn	2.089e+4(0.5%)
Mp	2.271e+4(0.4%)
Mv	n/a
Mw	2.403e+4(0.3%)
Mz	2.702e+4(0.7%)

Figure 3.5. Size exclusion profile and characterization data for 20P(TMA)Cl-F5. The blue trace is refractive index (RI) and the red trace is light scattering (LS) data. Profiles are generated using AKTA instrumentation, ASTRA MiniDawn software, and a Superose 6 column in tetramethylammonium chloride (TMAC) buffer (0.25 M CH_3COONa, 0.5 M NaCl, 0.03 M TMAC, pH 6.0).

3.4.2 Shear induced hydraulic conductivity

When BAEC monolayers were compared to controls receiving no polymer solution that were run side-by-side with polymer groups, all monolayers treated with 20P(TMA)Cl had significantly decreased hydraulic conductivity responses to shear. In Figure 3.6, this is represented as the data points collected in the last 5 minutes of every hour of the experiment. The first hour is excluded as this is an equilibration period and polymer solution was not added until after the first 60 minutes. In order to test whether the molecular weight of the polymer would have an effect on the degree to which the polymer reduced the cellular response to shear, a polydisperse polymer (20P(TMA)Cl, Figure 3.6 A), and both a high- and low-molecular weight fraction of a polymer with similar charge density (20P(TMA)Cl-F3, Figure 3.6 B and 20P(TMA)Cl-F5, Figure 3.6 C, respectively) were tested. All variations of the polymer significantly reduced shear-induced hydraulic conductivity. The polymer data were normalized to represent percent decrease from respective control L_p data (Figure 3.7) according to equation 3.5.

$$M = \frac{[control(t)] - [polymer(t)]}{[control(t)] - 1} \tag{3.5}$$

Control(t) is the value of the normalized J_v/A response without polymer at time t, and polymer(t) is the value of the normalized J_v/A response in the presence of polymer at time t and 1 represents the baseline value that is obtained in the absence of shear stress. As defined, the higher the value of M, the greater suppression of mechanotransduction since greater differences between control(t) and polymer(t) will result in a larger value for M. Monolayers treated with

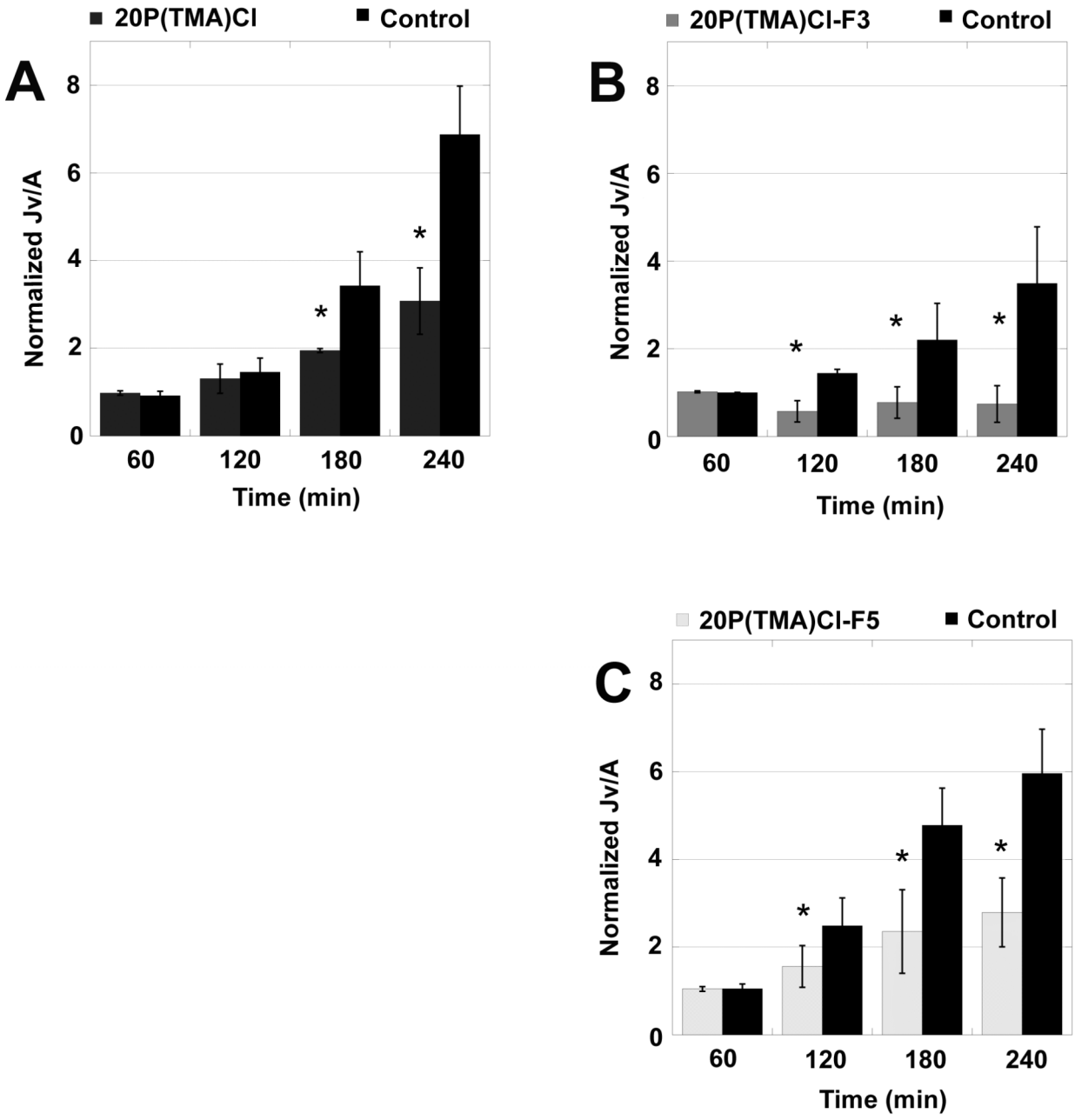

Figure 3.6. Normalized L_p values of control and polymer-treated monolayers. BAEC monolayers were incubated for 30 minutes with 1 mg/mL of A) 20P(TMA)Cl (dark grey bars), B) 20P(TMA)Cl-F3 (medium grey bars), or C) 20P(TMA)Cl-F5 (light grey bars). All monolayers pre-incubated with polymer display a 50-75% decrease in L_p response to shear compared to control monolayers. * $P < 0.05$ ANOVA, N = 3.

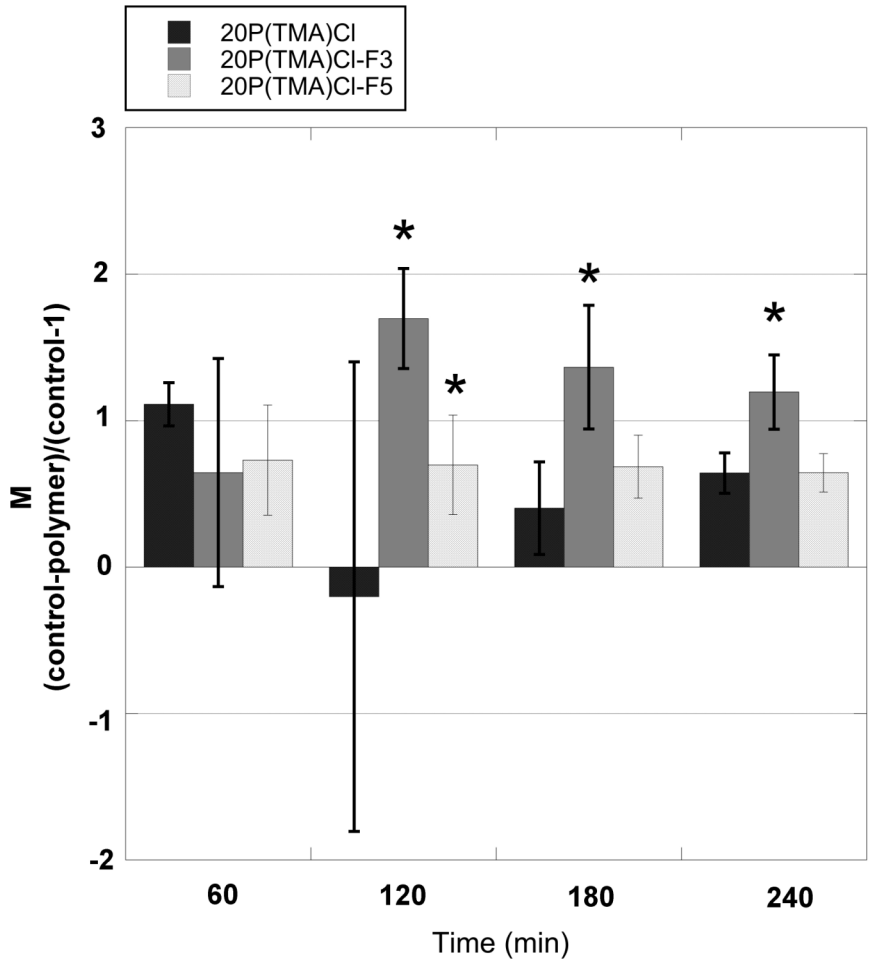

Figure 3.7. Shear-induced hydraulic conductivity of monolayers treated with 20P(TMA)Cl (dark grey bars), 20P(TMA)-F3 (medium grey bars), or 20P(TMA)-F5 (light grey bars) and normalized to their respective controls. Normalized values for 20P(TMA)Cl-F3 are significantly higher than for other groups indicating a greater reduction in shear-mediated hydraulic conductivity with high molecular weight copolymers. * $P < 0.05$ difference from 20P(TMA)Cl. # $P < 0.05$ difference from all groups. N = 3.

20P(TMA)Cl-F3 demonstrate a significantly higher value for M than do monolayers preincubated with either 20P(TMA)Cl or 20P(TMA)Cl-F5. We are able to show with these data that cationic copolymer incubation protects the endothelium against shear-induced increases in hydraulic conductivity and that this protective effect augmented in the presence of a narrowly distributed high molecular weight copolymer.

3.4.3 Pressure-induced hydraulic conductivity

Previously, we reported a decrease in pressure-induced hydraulic conductivity using 40P(TMA)Cl, a cationic copolymer composed of approximately 40 mol% positive charges per macromolecule (*54*). Figure 3.8 A shows that a further reduction of the charge density to approximately 20 mol% significantly lowers the pressure-induced hydraulic conductivity of cell monolayers in response to 30 cm H_2O fluid pressure. The administration of L-NAME, an inhibitor of nitric oxide synthase (NOS), is also able to significantly reduce the hydraulic conductivity from control cells receiving no treatment. We found no significant difference between cell monolayers treated with L-NAME and monolayers transiently incubated with a 1 mg/mL dose of 20P(TMA)Cl. It is shown here that the administration of a copolymer that interacts with the endothelial glycocalyx reduces the fluid conductance of the cell monolayer in response to hydrostatic pressure to a similar degree as monolayers whose mechanotransductive signal pathway is attenuated intercellularly.

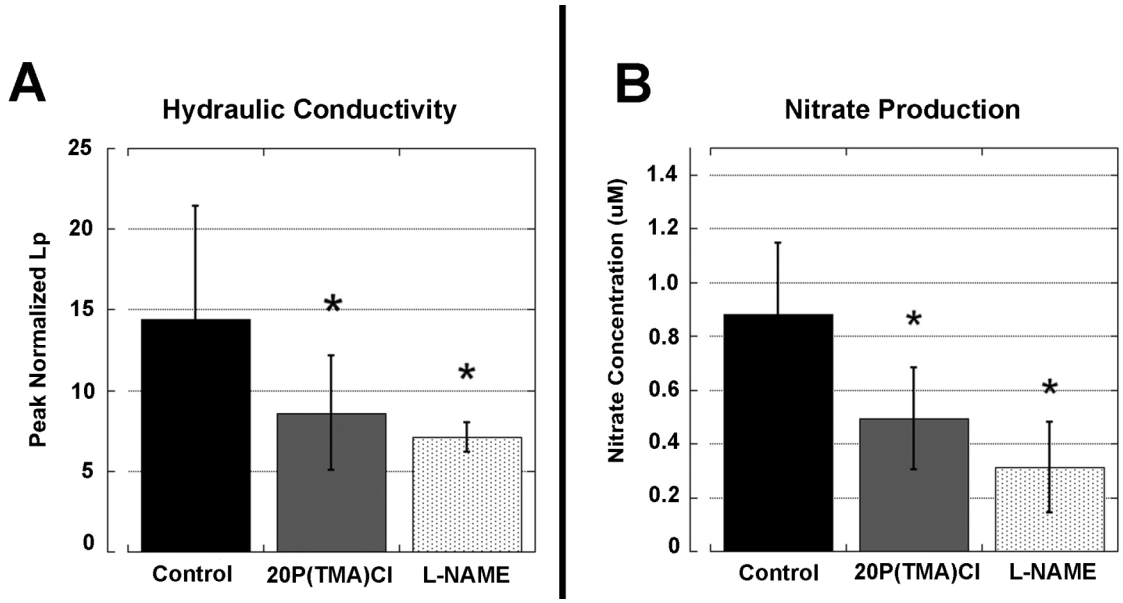

Figure 3.8. Peak normalized L_p values and nitrate concentration in cell media above tested monolayers. A) Peak normalized pressure-induced hydraulic conductivity values obtained after 30 minutes of 30 cm H_2O pressure. Addition of 20P(TMA)Cl and L-NAME, respectively, significantly decreased the pressure-induced increase in hydraulic conductivity through monolayers. No statistical difference exists between polymer treated and nitric oxide inhibited monolayers. * $P \leq 0.05$, ANOVA/Tukey's post hoc. N = 8 per group. B) Nitrate concentration of media above monolayers exposed to pressure of 30 cm H_2O for 60 minutes. Incubation with polymer significantly reduces the nitric oxide concentration to that of cells incubated with the NO inhibitor L-NAME indicating an intracellular mechanism for barrier dysfunction attenuation. *$P < 0.01$, N = 8 per group.

3.4.4 Nitric oxide production in response to hydrostatic pressure

To determine whether the barrier-enhancing effect of polymer administration was a consequence of a simple physical barrier enhancement or whether polymer administration altered mechanotransduction pathways, the media directly above cell monolayers that were exposed to high pressures in hydraulic conductivity experiments (outlined in section 3.4.3) was sampled and assayed for nitrite content. Because nitric oxide is unstable in aqueous media

and rapidly produces both nitrate and nitrite as end products, the supernatant was incubated with nitrate reductase and the resulting nitrite was assayed according to Greiss reaction protocol. The concentration of nitric oxide products in cell supernatant is reported in Figure 3.8 B. The administration of either L-NAME (10 μM) or 20P(TMA)Cl (1 mg/mL) copolymer significantly reduced the nitric oxide production of cell monolayers when compared to control. There was no significant difference between groups treated with either L-NAME or copolymer, therefore, one may conclude that 20P(TMA)Cl attenuates nitric oxide production via an intercellular mechanism and that the polymer-assisted attenuation of mechanotransduction is not solely the enhancement of a physical barrier alone.

3.4.5 Isolated perfused lung preparation

To test the therapeutic benefit of copolymers in a whole-organ system, we exposed isolated perfused mouse lungs to increased left atrial pressures and a subsequent infusion of polymer solutions, either 10P(TMA)Cl or PEO (Figure 3.9) of comparable molecular weights and polydispersities (90 kD, PD 1.2 and 82 kD, PD 1.1, respectively). Commercially available, narrowly polydisperse PEO was included in the study as an uncharged control polymer for comparison to HPMA copolymers with quaternary ammonium charges. The ratio of $K_{fc}2$ to $K_{fc}1$ is significantly decreased in the presence of both 10P(TMA)Cl and PEO, indicating a role for copolymer administration to distressed vascular endothelium and showing that this effect is independent of cationic residues.

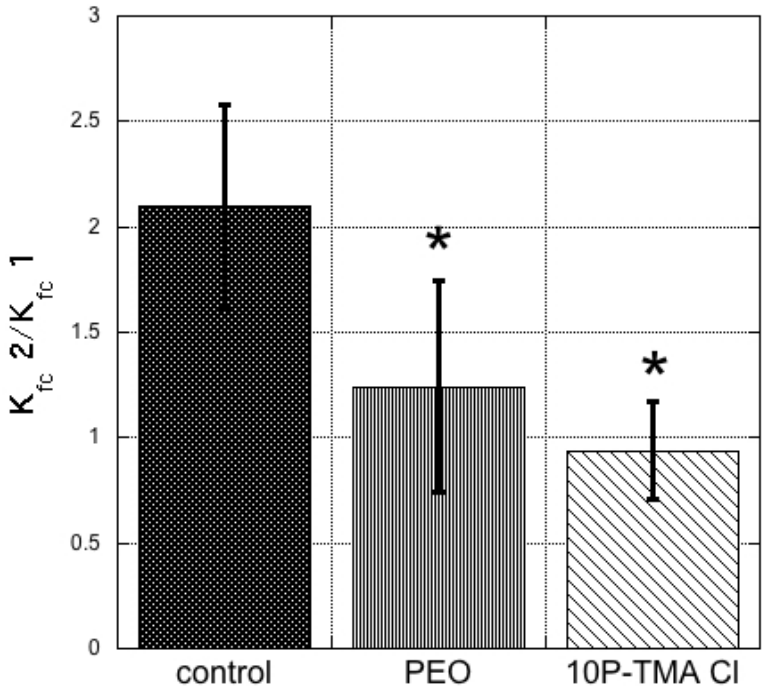

Figure 3.9. Mouse whole lung capillary filtration coefficient (K_{fc}) for lungs perfused with buffer alone (control, black bar), 1% PEO (grey bar), or 1% 10P(TMA)Cl (hatched bar). A significant reduction in K_{fc} occurs when lungs are perfused with either PEO or 10P(TMA)Cl with a lower mean K_{fc} observed in the presence of targeted copolymer.
* $P < 0.05$. ANOVA Dunnett's post hoc test, N = 4 per group.

3.5 Discussion

The development of water-soluble biomimetic copolymers that target the endothelial glycocalyx may be useful both as a tool to characterize mechanotransduction pathway(s) *in vitro* and as a prototype for developing clinical compounds to improve capillary barrier function during vascular inflammation. Cationic copolymers have historically been used as gene delivery platforms and may be composed of primary or tertiary amines or quaternary ammonium groups (*41, 47, 53*). We choose quaternary ammonium structures in order to minimize cellular activation and uptake by eliminating the ability for covalent bond formation, as quaternary ammonium does not possess a lone pair of electrons. We have previously shown the ability of HPMA-TMA Cl copolymers to bind to the endothelial surface and demonstrated an enhancement of barrier function and minimal cytotoxicity (*54*). The lowest mol% of quaternary ammonium in copolymers used in previous studies was 40 mol%; however, in present studies we are able to show the therapeutic benefit of this copolymer with a lower overall charge density (e.g., 10-20 mol% TMA Cl composition). The benefit to lowering charge density is that there is a subsequent increase in cell viability as we have shown in previous LDH-release cytotoxicity assays (*54*) and as has been shown also by Reschel et al. (*53*).

In shear-induced hydraulic conductivity assays, a significant decrease in the shear-induced cell response is seen in cells pretreated with 20P(TMA)Cl (Figure 3.5). All of the L_p experiments display the characteristic “sealing” behavior in which L_p decreases continuously to its baseline value during the first

60 minutes of exposure to the pressure differential. The sealing effect was not affected by any of the polymer treatments since the baseline control and treatment L_p values are not significantly different during the first 60 minutes (data not shown). Three polymers were tested on endothelial monolayers, each polymer composed of the same overall charge density (20 mol%) but differing molecular weights and distributions: 20P(TMA)Cl is a polydisperse copolymer (PD 1.8), 20P(TMA)Cl-F3 is a high molecular weight fraction of 20P(TMA)Cl (135 kD, PD 1.1) and 20P(TMA)Cl-F5 is a low molecular weight fraction (24 kDa, PD 1.2; characterization data is given in Table 3.1). Both fractions have a lower polydispersity than 20P(TMA)Cl. Figures 3.5 A – C show that shear-mediated hydraulic conductivity is significantly reduced in endothelial monolayers treated with each copolymer. In Figure 3.6, the hydraulic conductivity output data for each polymer-treated monolayer were normalized to their respective control monolayers and compared. We show a significantly higher values for M generated from monolayers treated with 20P(TMA)Cl-F3, the 135 kDa copolymer. The molecular weight of linear polymers is often an indicator of the hydrodynamic radius of a macromolecule, whose influence on mechanotransduction has not been well defined. We conclude that larger macromolecules have a greater protective effect against shear-mediated barrier damage.

Previously, we reported a significant decrease in pressure-mediated hydraulic conductivity in the presence of 1 mg/mL 40P(TMA)Cl (*54*), a copolymer with twice the charge density of polymers used in this study. Dull et al. have

previously demonstrated that increases in hydraulic conductivity are coincident with cellular increases in nitric oxide production (*70*) and are therefore indicative of the activation of mechanotransduction pathways. In Figure 3.7 A, the administration of 20P(TMA)Cl to endothelial monolayers significantly reduces pressure-mediated hydraulic conductivity when compared to control monolayers receiving no treatment and that 20P(TMA)Cl significantly reduces peak normalized L_p levels, generated after 30 minutes at 30 cm H_2O pressure, to the same levels as are generated when cells are incubated with the nitric oxide synthase inhibitor, L-NAME. In Figure 3.7 B, we showed that these same cells generated significantly less nitric oxide in the presence of 20P(TMA)Cl than in untreated control cell monolayers when the media above the cells in these experiments was assayed for nitric oxide metabolites. There was no significant difference in NO production detected between groups treated with L-NAME and 20P(TMA)Cl, however, this does not necessarily prove that 20P(TMA)Cl attenuates mechanotransduction through nitric oxide-dependent pathways, only that copolymer administration attenuates mechanotransduction. Power analysis suggests that in order to elucidate a difference among 20P(TMA)Cl and L-NAME treated groups, the sample size would need to increase to 100 to have an 85% chance of seeing a difference between the groups. As a sample size of this magnitude is both cost- and time-prohibitive, an alternative method of experimentation would need to be employed. We do, however, conclusively demonstrate that 20P(TMA)Cl reduces NO production in endothelial monolayers,

thus indicating that copolymers improve endothelial barrier function by inhibiting cell signaling pathway(s) that induce mechanotransduction.

In order to determine polymer behavior in a whole lung model, high molecular weight fractions of 10P(TMA)Cl and polyethylene oxide (PEO) were perfused through an isolated perfused mouse lung model and the whole lung filtration coefficient was measured before and after polymer treatment. Perfusions of mouse lungs with 10P(TMA)Cl significantly decreased $K_{fc}2/K_{fc}1$ and thus reduce the pressure-induced permeability response in comparison to lungs receiving no treatment. We compared 10P(TMA)Cl to PEO, which carries no formal charge and is comparable to the HPMA backbone in water solubility and limited toxicity. Both polymers are high molecular weight, low polydispersity, and are able to significantly reduce the capillary filtration coefficient when compared to controls receiving no polymer perfusion. The protective effect of PEO in endothelial barrier regulation has been shown in transendothelial resistance studies and is reported in literature (*81*). However, in an *in vivo* situation, a targeting moiety is necessary to anchor a therapeutic copolymer to the endothelium for any length of time that extends beyond transient contact.

The second optimization step of 10P(TMA)Cl was to reduce its polydispersity since in previous experiments we observed an increase in pulmonary artery pressure after perfusion with a polydisperse formulation of 40P(TMA)Cl (Mw 54 kD, PD 1.8; data not shown). We hypothesized that the cause of the increase in pulmonary artery pressure was that low molecular weight polymer chains passed through the cell-cell junctions and stimulated

contraction of underlying smooth muscle cells. The conclusion is that increasing molecular weight and reducing polydispersity improves vascular retentions, maintains normal pulmonary artery pressure ($P_{PA}2/P_{PA}1 = 1.1$, data not shown) and is able to reduce $K_{fc}2/K_{fc}1$ in whole lung studies.

3.6 Conclusion

In this study we demonstrate the ability of water-soluble, biomimetic HPMA-based cationic copolymers to attenuate both shear- and pressure-mediated increases in hydraulic conductivity across endothelial monolayers and that higher molecular weight copolymers have greater barrier protection properties. We demonstrate a reduction in nitric oxide production in the presence of hydrostatic pressure in cells pretreated with 20P(TMA)Cl, suggesting a mechanism for the reduction in cellular response that impedes mechanotransduction. Here we lay the ground work for the use of copolymers in research to gain greater understanding of the mechanism involved in endothelial mechanotransduction and show the potential for biomimetic targeted polymers to be used clinically in the treatment of states of enhanced permeability. To this end, we show that 10P(TMA)Cl reduces the capillary filtration coefficient in whole lung model.

CHAPTER 4

E-SELECTIN TARGETED COPOLYMER TO ATTENUATE MECHANOTRANSDUCTION IN INFLAMED ENDOTHELIUM

4.1 Abstract

The efficacy of copolymer delivery to areas of acute vascular inflammation to enhance barrier function has been demonstrated in previous chapters. In this chapter, cationic side chains are replaced with a targeting mechanism on the polymer to optimize delivery of polymer specifically to inflamed endothelium. Previously, we have used trimethylammonium chloride-HPMA copolymers to bind to negatively charged endothelium, however; this approach is for mechanotransduction research purposes only and can not represent a clinically viable therapy. For this purpose, a targeting moiety that binds to E-selectin has been incorporated and is hypothesized to reduce the deleterious effects of acute inflammation by both dampening mechanotransduction and blocking leukocyte adhesion to the capillary wall. In this section, we introduce an HPMA-peptide conjugate that specifically binds to E-selectin and demonstrate its specificity to its target protein.

4.2 Introduction

In Chapters 2 and 3, the benefit of cationic copolymer delivery to inflamed vascular endothelium is demonstrated in both *in vitro* and *ex vivo* models. Cationic copolymers are able to reduce capillary permeability under conditions of pressure- and shear-mediated barrier stress, in the presence of inflammatory cytokines, and in whole mouse lungs subjected to high pressure. In this chapter, we refine the copolymers' targeting capacity to selectively target E-selectin, the receptor protein responsible for leukocyte binding, which is upregulated during acute inflammation. The HPMA backbone is retained for its ability to intercalate into the endothelial glycocalyx to turn off mechanotransduction via cell signaling pathway(s).

The properties of E-selectin are reviewed extensively by Barthel et al. (*60*). Briefly, E-selectin is a 64 kDa protein that is synthesized *de novo* in endothelial cells in response to inflammatory cytokines and is upregulated to the cell surface 2-6 hours after inflammatory insult. It is responsible for the recognition of leukocytes and the mediation of early rolling events that preclude extravasation. E-selectin has also been implicated in the increased permeability of the endothelial barrier via physical interactions with cytoskeletal proteins or changes in the shape of endothelial cells (*60*).

Leukocytes are carriers of sialyl lewis x, a well-documented ligand for E-, L-, and P-selectin (*86-88*). Sialyl lewis x is a tetrasaccharide composed of sialic acid, fucose, galactose, and glucuronic acid. Lowe et al. (*63*) determined that this carbohydrate structure is a ligand for E-selectin by constructing a cell line to

express human α1,3/4 fucosyltransferase, which induced cells to display sialyl lewis x. Transfected cells then bound to E-selectin, thus implicating sialyl lewis x as the ligand (*63*). The enzymatic removal of sialic acid via neuraminidase has been shown to decrease the affinity of E-selectin for the ligand (*89, 90*), thereby demonstrating the necessity of the sialic acid moiety. In designing sialyl lewis x mimics, the positioning of the sialic acid carboxyl is conserved (*91*) along with fucosyl hydroxyl groups (*91, 92*).

The use of sialyl lewis x and its analogs, either free or conjugated to polymers, has been explored for cancer therapy (*1, 32*), *in vivo* imaging of areas of acute inflammation and/or tumor growth (*57, 93*), and anti-inflammatory drug delivery (*86*). The ability of sialyl lewis x to block leukocyte binding to the endothelial surface has been explored as a treatment for vascular permeability as a result of ischemia/reperfusion injury (*94*) since leukocyte adhesion is one of the important early events that leads to pulmonary injury. Mulligan et al. (*59*) explored the deleterious effect of neutrophil activation and contact with the capillary wall and demonstrated the significant protective effect that sialyl lewis x-conjugated oligosaccharide intravenous infusion had against IgG immune complex-induced E-selectin-dependent lung injury (*59*).

A limiting factor in the use of carbohydrates is the time and expense required for synthesis. The use of a peptide analog to sialyl lewis x that targets E-selectin is beneficial in that it can be made to increase bioavailability by extending the *in vivo* half-life of the analog via straightforward modifications, can be made in large quantities and can be easily modified to conjugate a polymer

scaffold. Sialyl lewis x forms weak attachments with E-selectin, in keeping with its function to transiently recruit leukocytes to be tethered more tightly to adhesion molecules. The binding affinity of sialyl lewis x is in the mM range (*95*) where peptide analogs to sialyl lewis x can be designed with increased ligand affinity for E-selectin (*32, 91*). In this work, we present a novel therapy for the treatment of vascular inflammation and demonstrate the ability for a peptide-conjugated polymer to bind to immobilized E-selectin.

4.3 Materials and methods

4.3.1 Copolymer synthesis/characterization

Polymer precursor, composed of primary amine groups and fluorescein, was synthesized by radical solution polymerization of *N*-(2-hydroxypropyl)methacryalamide (HPMA), *N*-(3-aminopropyl)methacrylamide (MA-AP) and 5-3-(methacryloylaminoropyl)thioureidyl fluorescein (MA-FITC, mol ratio 92 : 7 : 1) in methanol. The concentration of comonomers in the polymerization mixture was 12.5 wt% with 0.56 wt% AIBN and 0.04 wt% mercaptopropanoic acid (MPA). Radical polymerization was allowed to proceed in sealed ampoule under nitrogen atmosphere at 50ºC for 24 hours. The polymer was first precipitated into acetone and then purified by dialysis. The yield was 400 mg (62 wt%). The molecular weight (24 kD, 1.6 PD) was determined on a Superose 6 column in PBS using AKTA FPLC (GE Healthcare) equipped with UV, RI and light scattering MiniDawn (Wyatt Inc.) and calculated by ASTRA software (Wyatt, Inc.). The SEC profile of the polymer precursor containing NH_2 is available in Figure 4.1. The polymer contained 0.056 mmol/g fluorescein (0.85

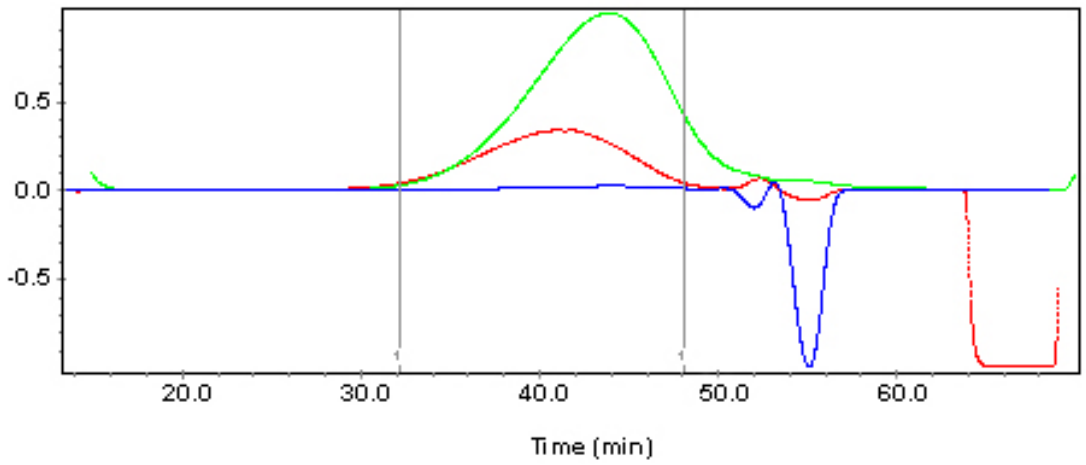

Peak 1	
Peak limits (min)	32.164 - 48.022
dn/dc (mL/g)	0.170
Polydispersity	
Mw/Mn	1.403(2%)
Mz/Mn	1.994(2%)
Molar mass moments (g/mol)	
Mn	1.704e+4(1%)
Mp	1.559e+4(0.6%)
Mv	n/a
Mw	2.390e+4(0.7%)
Mz	3.398e+4(1%)

Figure 4.1. Size exclusion profile and characterization data for the polymer precursor P(FITC)NH_2 before maleimide conjugation. The green trace represents UV data collection, the red line is light scattering data, and the blue line is the refractive index profile. Profiles are generated using AKTA instrumentation, ASTRA MiniDawn software, and a Superose 6 column in acetate buffer (0.25 M CH_3COONa, pH 6.5).

mol%) as determined by UV (borate buffer pH 8.5, molar extinction coefficient 78,000 M^{-1} cm^{-1}) and 0.46 mmol/mg (6.9 mol%) primary amine groups determined by ninhydrin method using amine monomer as the calibration standard.

To incorporate the maleimide groups, the polymer precursor (100 mg, 0.046 mmol NH_2) was reacted with sulfosuccinimidyl 4-[*N*-

maleimidomethyl]cyclohexane-1-carboxylate (SMCC, 27 mg, 0.08 mmol) and diisopropylethylamine (DIPEA, 15 mg, 1.7 mmol) in 1.5 ml dimethylformamide (DMF) for 24 hours. The reaction mixture was precipitated into acetone/Et_2O (3:1) and purified on Sephadex LH-20 column in methanol. The yield was 90 mg (90 wt%). The molecular weight of maleimide-containing polymer (29 kDa, PD 1.6) was determined using Superose 6 column in 0.1 M acetate buffer, pH 6.5, with 30% acetonitrile using P(HPMA) calibration samples (see Figure 4.2 for SEC profile and MiniDawn characterization data). The maleimide content was 0.37 mmol/g (5.6 mol%), which was determined by reacting different concentrations of polymer with an excess of thiol (glutathione) followed by determining the residual SH by Ellman's reagent (*96*). The molar ratio of the highest concentration was Mal : SH : Ellman's = 1 : 3 : 25.

4.3.2 Solid phase peptide synthesis

Amino acids were purchased in their protected forms and used directly for solid phase synthesis without further purification. Peptide sequences ESBP (Ac-CDITWDQLWDLMK-NH_2) and SCRM (Ac-CKMIDWTWLQLDD-NH_2) were synthesized according to solid phase protocol (*97*) on Rink-Amide resin, which yields a C-terminal amine. Sequence and copolymer data are available in Table 4.1. The N-terminus was acetylated using acetic anhydride as a final step. The nascent peptides were dried overnight then cleaved from the resin with a mixture of trifluoroacetic acid (81% v/v), water (11.5% v/v), phenol (5% w/v), and ethanedithiol (EDT, 2.5% v/v) to yield the sequences ESBP and SCRM. The solvent was removed from crude peptide by rotovap and subsequently

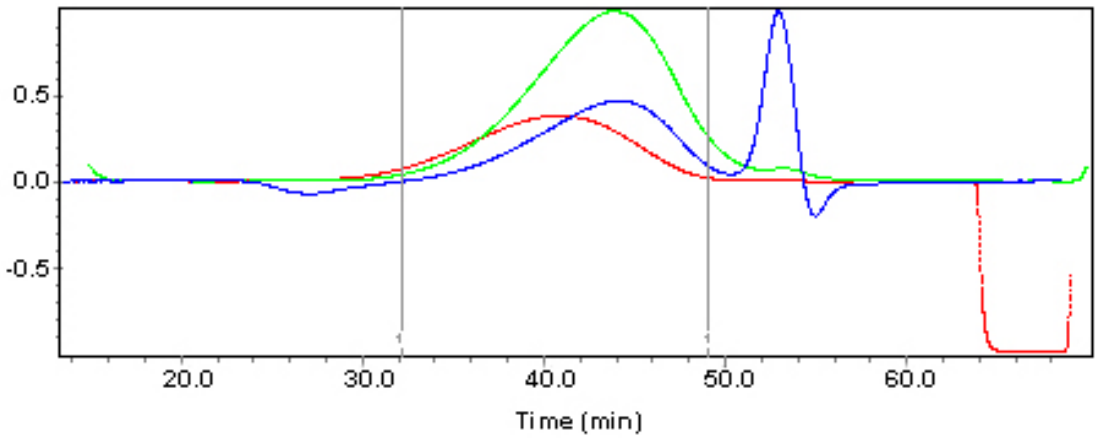

	Peak 1
Peak limits (min)	32.165 - 49.040
dn/dc (mL/g)	0.170
Polydispersity	
Mw/Mn	1.572(2%)
Mz/Mn	3.235(2%)
Molar mass moments (g/mol)	
Mn	1.857e+4(2%)
Mp	1.849e+4(0.3%)
Mv	n/a
Mw	2.919e+4(0.7%)
Mz	6.007e+4(2%)

Figure 4.2. Size exclusion profile and characterization data for the polymer precursor P(FITC)MAL after maleimide conjugation. The green trace represents UV data collection, the red line is light scattering data, and the blue line is the refractive index profile. Profiles are generated using AKTA instrumentation, ASTRA MiniDawn software, and a Superose 6 column in acetate buffer (0.25 M CH_3COONa, pH 6.5).

Table 4.1

Copolymer characterization data

Name	Peptide sequence	Molecular weight, kDa, (PDI)	Peptide content (mmol/g)	FITC content (mmol/g)	Weight %	Mol%
P(FITC)ESBP	Ac-CDITWDQLWDLMK-NH_2	29(1.6)	0.16	0.06	33	3.5
P(FITC)SCRM	Ac-CKMIDWTWLQLDD-NH_2	29(1.6)	0.12	0.06	25	2.3

Polymer nomenclature and characterization data. Ac- denotes acetylation.

precipitated in cold ether. The product was dissolved in water and lyophilized. The molecular weight and purity of each peptide was verified by MALDI-TOF mass spectroscopy (see Figure 4.3 and Figure 4.4 for mass/charge ratio data). Crude peptide was purified by HPLC reverse phase semipreparative C12 column with H_2O/acetonitrile and 0.1% trifluoroacetic acid as mobile phase (Figure 4.5).

4.3.3 Polymer-peptide conjugation

Polymer precursor containing maleimide groups (15 mg, 5.7 μmol maleimide) was dissolved in 75 μl DMF. ESPB or SCRM peptide, containing cysteine (4 mg, 2.3 μmol), were each dissolved in 40 μl DMF and incubated for 15 min with 40 μl Tris-(2-carboxyethyl) phosphine hydrochloride (TCEP, 10 mM in 50 mM HEPES buffer, pH adjusted to 7.0). The peptide solution was added dropwise into polymer solution and stirred for 2 hours at room temperature and overnight at 4ºC. Nonbound peptide was separated from the polymer on PD10 column in PBS buffer. Incorporation of peptide is evaluated by UV spectroscopy using the molar extinction coefficient for tryptophan (5,500 $M^{-1}cm^{-1}$) (*98*). Peptide content was found to be 0.163 mmol/g (3.5 mol%, 34 wt %) for P(FITC)ESBP and 0.121 mmol/g (2.3 mol%, 25 wt%) for P(FITC)SCRM. Data for complete polymer peptide conjugate is available in Table 4.1.

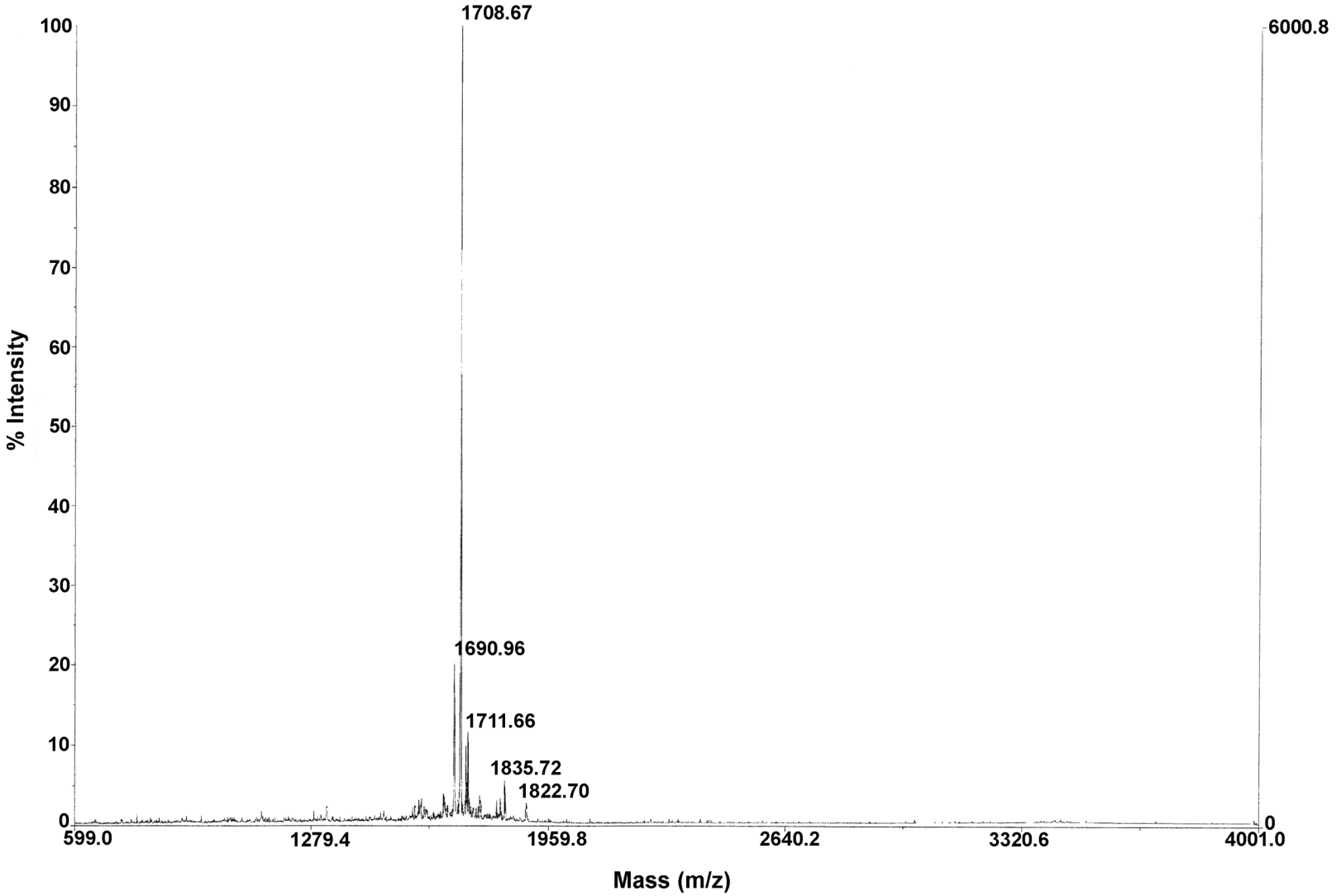

Figure 4.3. Mass spectrum of purified ESBP peptide sequence. The mass peak at 1708 correlates with the projected mass of ESBP. Spectrum was generated by MALDI-TOF technique.

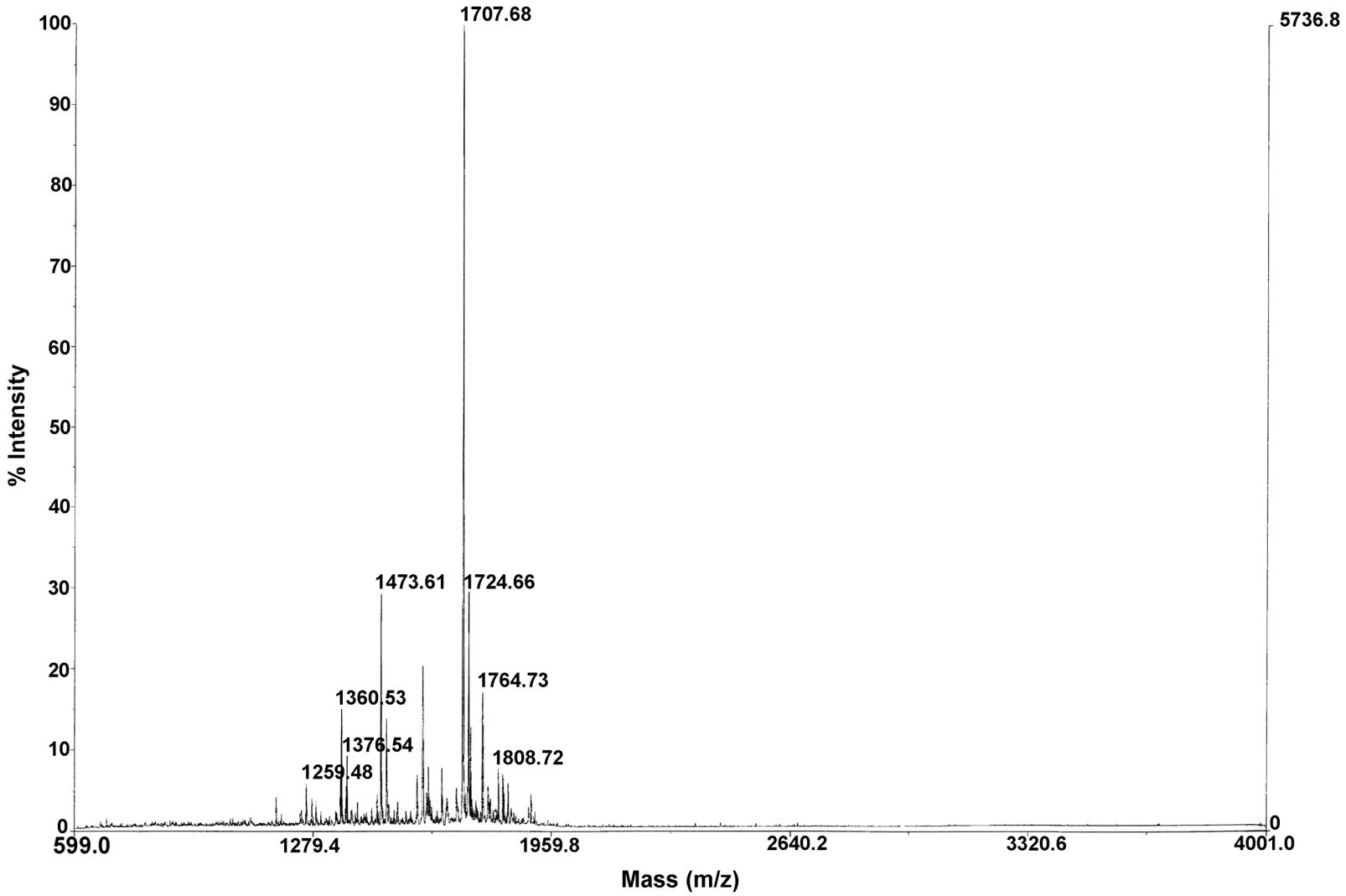

Figure 4.4. Mass spectrum of purified SCRM peptide sequence. The mass peak at 1708 correlates with the projected mass of SCRM. Spectrum was generated by MALDI-TOF technique.

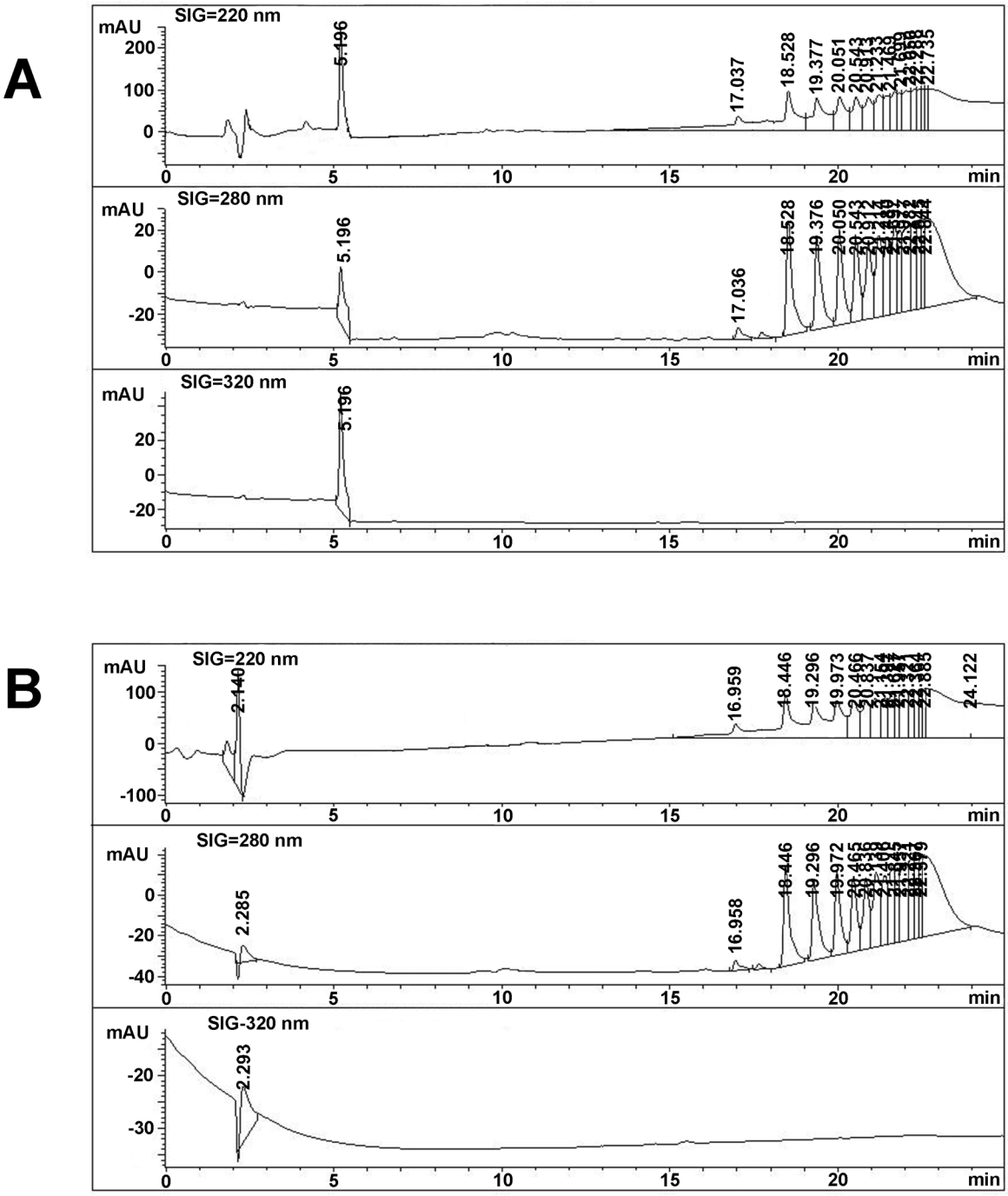

Figure 4.5. Analytical HPLC profiles of A) ESBP conjugated to AF350 and B) buffer only. Signals are, from top to bottom traces, collected at 220, 280, and 320 nm, respectively. Profiles are generated on C6 reverse phase column in water and acetonitrile with 0.01% TFA. In Figure A, the peak at 5.196 minutes is the peptide. Figure B shows that peaks beginning at minute 16 are inherent in buffer and not associated with the peptide.

4.3.4 E-selectin-PEG-biotin

Recombinant human E-selectin (50 µg) was dissolved in cold PBS (0.5 mg/mL) and E-Z Link NHS-PEG4-biotin (NPB, 5.05 µL, 1.7 mM) in cold PBS was added (biotin:E-selectin 10:1). The reaction was allowed to proceed for 4 hours on ice. Unreacted NPB was separated from conjugated E-selectin-PEG-biotin (EPB) by NEP-5 column (Sephadex G25) against PBS. EPB binding to microtiter plates was confirmed using a 20x serial dilution of anti-CD62 E-selectin antibody (0.2-100 µL) in wells containing either immobilized E-selectin or blocking serum only. The primary antibody was washed extensively and incubated with a fluorescein-labeled secondary IgG (DyLight 488, Jackson Immunoresearch). Fluorescence was analyzed immediately using microtiter plate reader (Tecan, Mannedorf, Switzerland) at optimized gain with excitation wavelength 488 nm and emission wavelength 535 nm.

4.3.5 Peptide specificity

NeutrAvidin microtiter plates (Pierce Chemical, lower limit of biotin detection 5 ng/mL) were washed 3 times in wash buffer (25 mM Tris, 150 mM NaCl, pH 7.2, with 0.1% BSA and 0.05% Tween 20) and 10 µg/mL of NPB was added to each well. Plates were incubated for 2 hours at room temperature then overnight at 4ºC. Plates were subsequently washed three times in wash buffer and blocked for 1 hour with a solution of 10% donkey serum in PBS. A serial dilution of P(FITC)ESBP or P(FITC)SCRM was performed in 1% donkey serum and reacted with bound E-selectin for 20 minutes. Polymer solutions are washed three times with wash buffer and wells are filled with PBS supplemented with 1%

donkey serum for analysis. Fluorescence was measured immediately using a microtiter plate reader at excitation wavelength 488 nm and emission wavelength 535 nm.

4.4 Results

4.4.1 Peptide and polymer synthesis and characterization

The polymer P(FITC)ESBP is conjugated to an E-selectin binding peptide sequence (ESBP) that is the targeting peptide designed to interact with E-selectin (E-Selectin Binding Peptide) and SCRM is the peptide sequence composed of the same amino acids but randomized to serve as a non-binding control. Peptides were N-acetylated and C-amidated to confer greater blood stability to peptides.

The polymer precursor was synthesized in two steps. A synthesis scheme is presented in Figure 4.5. In the first step, HPMA, fluorescein, and aminopropyl monomers were polymerized to yield a polymer precursor composed of primary amine groups that function as reactive side chains for maleimide incorporation. The molecular weight was 23 kDa (PD 1.4, Figure 4.1). The amine content of the polymer precursor was determined to be 0.046 mmol/g (6.9 mol%) and 0.056 mmol/g (0.85 mol%) was determined for fluorescein.

In the second step, primary amines incorporated into the precursor were reacted with SMCC to yield maleimide reactive groups. The molecular weight of the polymer precursor was measured by SEC to be 29 kD (PD 1.6, Figure 4.2). A slight increase in molecular weight upon maleimide

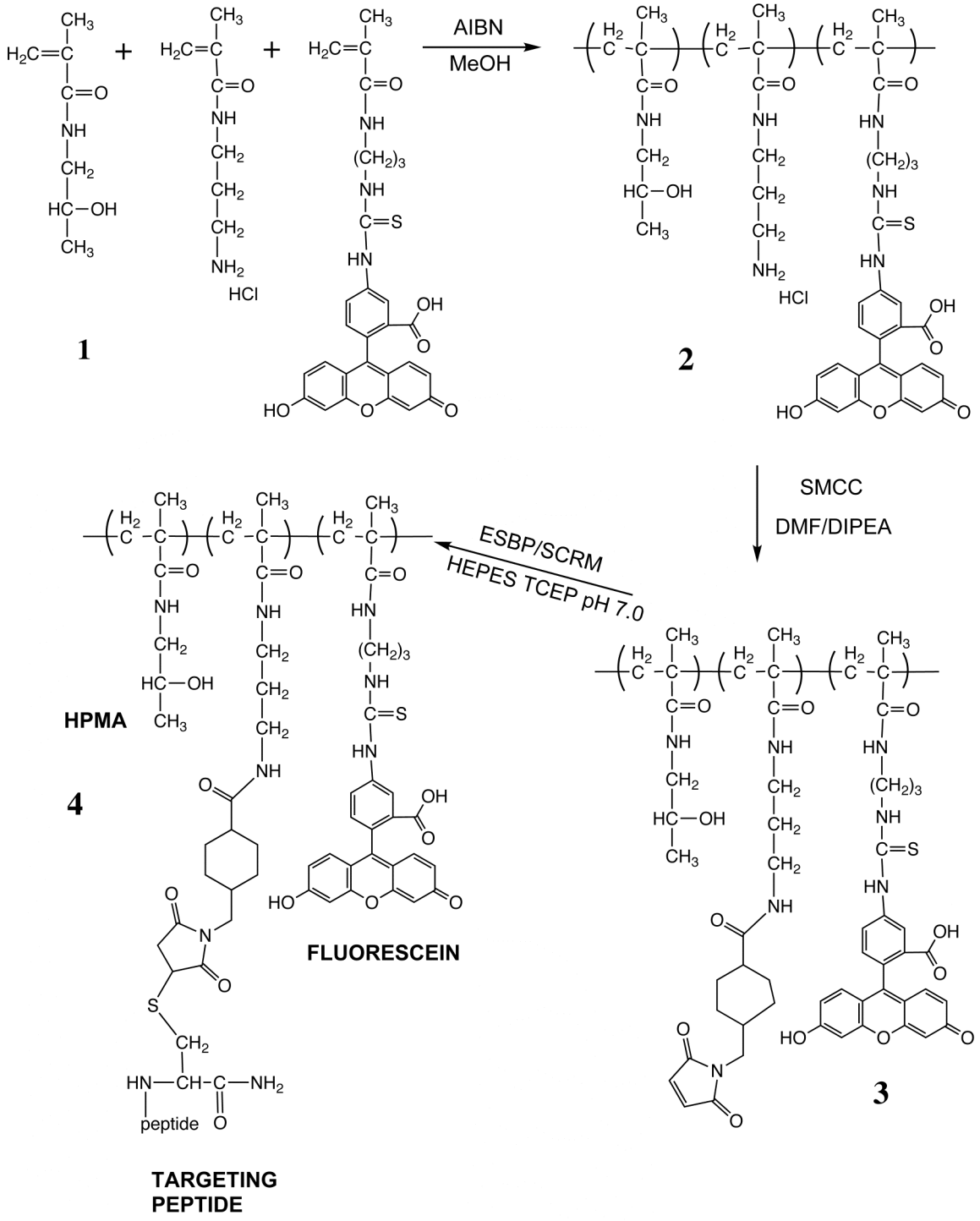

Figure 4.5. Scheme for P(FITC)ESBP or P(FITC)SCRM synthesis

conjugation is common due to disulfide crosslinking. Peptides were conjugated to maleimide-containing side chains on the polymer precursor via the peptide thiol located on the N-terminal cysteine. This approach was taken to minimize allosteric conjugation to the polymer since the cysteine thiol is the only available reactive group to maleimide in the polymer mixture.

4.4.2 Peptide specificity

Peptide specificity for E-selectin was shown using streptavidin-coated plates onto which biotin-labeled E-selectin was immobilized. Protein immobilization was confirmed by the reaction of an anti-E-selectin antibody and an Alexa 488-conjugated secondary antibody fluorescent IgG to immobilized E-selectin (Figure 4.6). Blocking the plates with 10% donkey serum reduced the nonspecific interactions between the polycarbonate microtiter wells and antibodies. Figure 4.6 shows an increase in antibody signal in plates coated with immobilized E-selectin than in plates containing no protein.

To determine the specificity of P(FITC)ESBP for E-selectin, wells containing immobilized E-selectin were blocked then incubated for 20 minutes with either P(FITC)ESBP or P(FITC)SCRM. Polymers were washed extensively from the plates and residual fluorescence was measured (Figure 4.7). To demonstrate that polymers were not binding nonspecifically to wells, polymer was incubated in serum-blocked wells containing no E-selectin (DS/ESBP or DS/SCRM, Figure 4.7). There was a significantly higher increase in polymer signal when P(FITC)ESBP was incubated with E-selectin than from any other group (E-sel/ESBP, Figure 4.7). There was no significant difference among

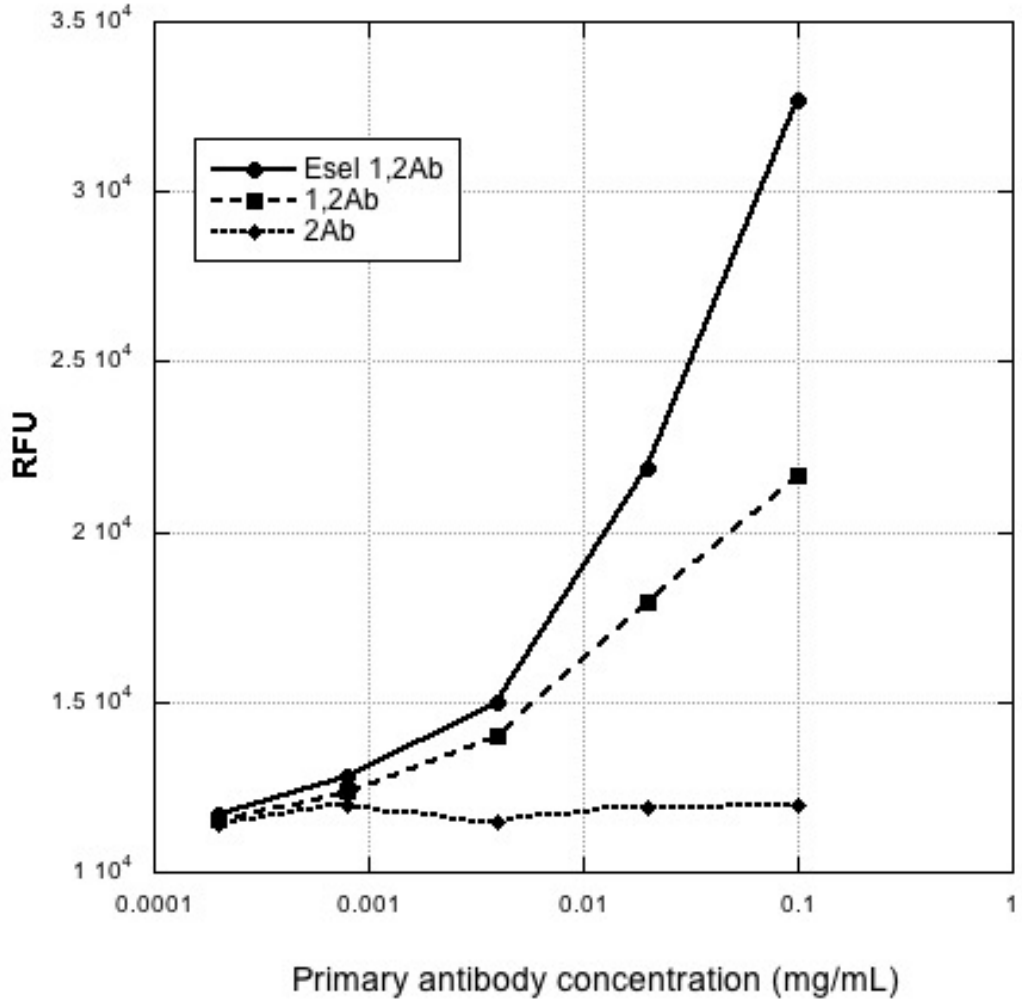

Figure 4.6. Antibody binding to immobilized E-selectin to show that E-selectin was present in wells during experimentation. A serial dilution of anti-E-selectin antibody was incubated with immobilized E-selectin (Esel 1,2Ab; ●) or wells containing only blocking serum (1,2Ab; ■). Secondary antibody only was added to wells containing only blocking serum as a negative control (2Ab; ◆). N=1.

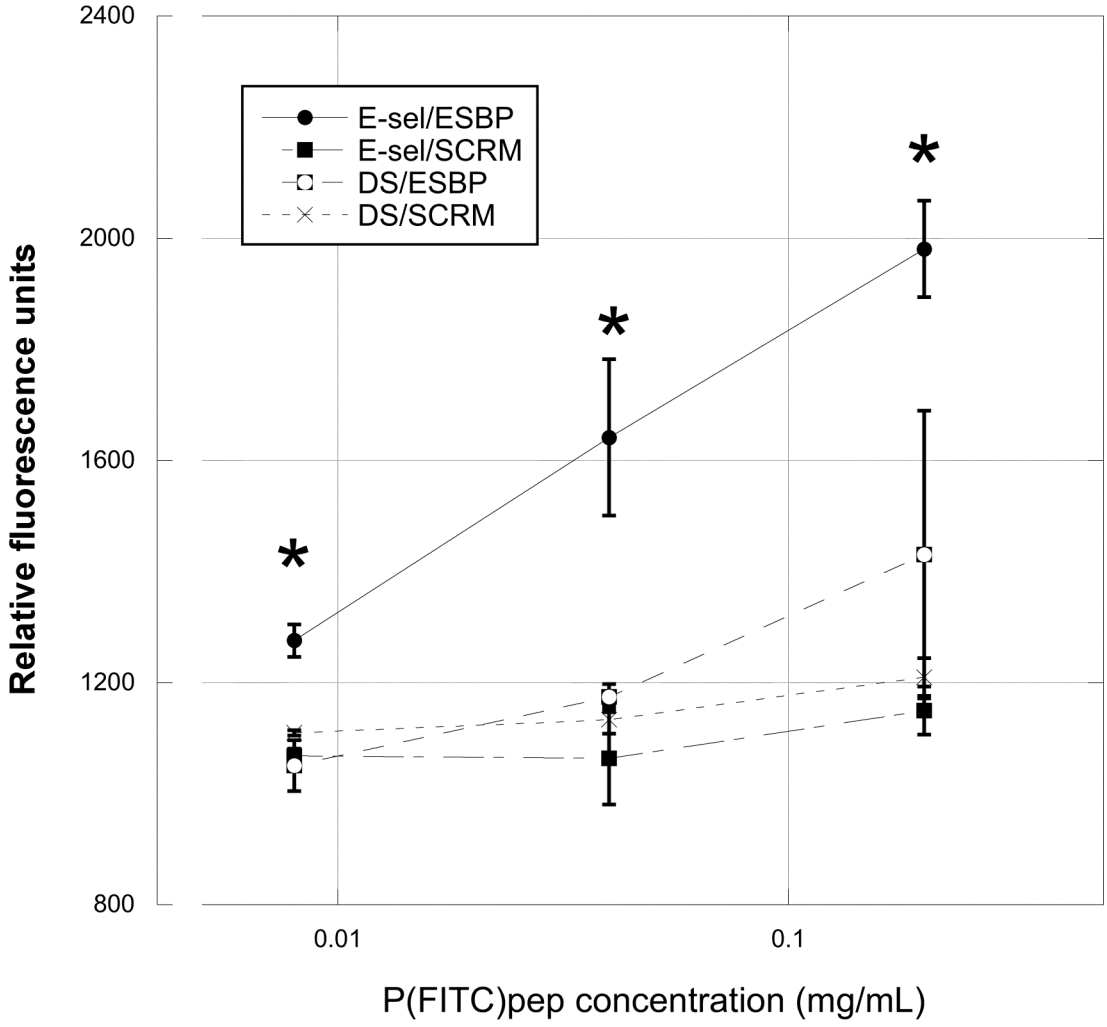

Figure 4.7. Specificity of P(FITC)ESBP for E-selectin. Increasing concentrations of P(FITC)ESBP or P(FITC)SCRM were incubated with immobilized E-selectin to test for copolymer specificity or blocking protein only to test for nonspecific interactions with substrate. The ESBP conjugate (E-sel/ESBP, ●) displayed significantly higher affinity for E-selectin than did copolymer conjugated with the scrambled sequence (E-sel/SCRM, ■). There was no difference between P(FITC)SCRM incubated with either E-selectin or substrate only (DS/SCRM, ×) or P(FITC)ESBP incubated with substrate only (DS/ESBP, ◘). * $P < 0.05$, $N = 3$.

groups when polymer was incubated with blocking serum alone or when P(FITC)SCRM was incubated with E-selectin, thus demonstrating that the ESBP sequence is a ligand for E-selectin and that its polymer conjugate, P(FITC)ESBP, demonstrates specificity when compared to the scrambled sequence conjugate.

4.5 Discussion

The use of sialyl lewis x as a targeting moiety has been explored for a variety of purposes (*32, 60, 86, 93*), however, the trend toward the use of carbohydrate analogs has largely shifted in favor of peptide targeting moieties as peptide synthesis is faster, delivers higher compound yield, and is less cumbersome than carbohydrate synthesis. Herein, we describe a novel use for a copolymer-peptide conjugate that targets E-selectin to attenuate vascular permeability using a multifaceted approach. The ESBP targets E-selectin, which is upregulated on the endothelial cell surface in the presence of acute inflammation. Once the copolymer binds to E-selectin, it can block receptor binding sites, thereby attenuating the leukocyte tethering and rolling pattern. Lastly, the copolymer conjugate is hypothesized to turn off mechanotransduction via glycocalyx-HPMA interactions, which has been shown previously to reduce the cell-signaling cascade that is produced in the presence of mechanical stress.

The E-selectin binding peptide sequence used in these experiments was initially derived from phage display experiments (*65*) and has been used to target anticancer drugs (*32*) and imaging nanoparticles (*6*) to sites of E-selectin upregulation. This lab has shown that HPMA copolymers that bind to inflamed vascular endothelium and interact with the endothelial glycocalyx reduce fluid

and solute flux through capillary endothelial monolayers (*54*) and Beauharnois et al. have demonstrated the ability of sialyl lewis x-bearing oligosaccharides to competitively inhibit ligand binding to P- and L-selectins during hydrodynamic shear stress (*99*). Taken together, we approach the mechanism of strengthening the lung capillary endothelial barrier with a multifaceted system.

Herein, E-selectin binding peptide (ESBP) is conjugated to HPMA via a thioether linkage facilitated by the addition of cysteine at the peptide C-terminus and the incorporation of maleimide reactive groups into the polymer precursor. The specificity of the reaction between maleimide and cysteine is exploited to increase E-selectin binding by ensuring that the entire peptide remains free of steric hindrance that may occur with a less site-directed approach. The peptide was N-acetylated and C-amidated in order to provide additional protection against nonspecific proteases found *in vivo*. There were found to be an average of 8 peptides per macromolecule of P(FITC)ESBP, which should increase the binding capability by multivalency effect (*85*). In competitive binding assays that use sialyl lewis x as the inhibitor, HPMA conjugated to a similar E-selectin binding peptide and has yielded an IC_{50} of 6 nM (*32*). The free peptide is reported to bind with an IC_{50} value of 5 μM (*65*).

The specificity of P(FITC)ESBP was determined by immobilizing E-selectin on streptavidin coated microtiter plates. Surface amines on E-selectin were exploited to bind a succinimidyl ester that was conjugated to a 29 Å PEG spacer that terminated with a biotin reactive group. The addition of the 29 Å PEG spacer was designed to expose E-selectin binding sites that may have otherwise

been buried against the microtiter support wall. The affinity of the peptide conjugate for E-selectin was tested by adding an increasing concentration of P(FITC)ESBP to wells with immobilized protein followed by an extensive wash step. The data show that the fluorescence signal from P(FITC)ESBP increased with increasing polymer concentration in the well and no such increase was seen for either P(FITC)SCRM incubated with E-selectin or wells containing no E-selectin that were incubated with either polymer (Figure 4.3). These controls eliminated the possibility that the copolymer was reacting nonspecifically to either E-selectin or the substrate.

4.6 Conclusion

This chapter details the synthesis and binding specificity of an HPMA copolymer conjugated with a peptide that binds E-selectin. This polymer design lays the foundation for future mechanotransduction research and a potential therapy for ALI/ARDS.

CHAPTER 5

CONCLUSIONS AND FUTURE WORK

5.1 Conclusions

The research contained in this dissertation establishes the mechanistic foundations for developing a polymer-based treatment to attenuate pulmonary edema, a major complication of acute lung injury. We have shown that positively charged copolymers, designed to target the negatively charged endothelial glycocalyx, can enhance the capillary barrier by turning off mechanotransduction. Preliminary experiments, described in Chapter 2, focus on the development of a copolymer that demonstrates safety, endothelial surface binding, and efficacy in reducing the monolayer permeability to fluid and solute flux. To demonstrate safety, we show that copolymers, composed of quaternary ammonium side chains, elicit very little cytotoxicity even at higher concentrations and are, therefore, a better prototype than copolymers with primary amine structures. HPMA was chosen as the comonomer due to its established characteristics as a water-soluble, nonimmunogenic substrate for polymer delivery (*44, 45*). We have demonstrated the ability of positively charged copolymers to attach to the endothelial cell surface using fluorescently labeled polymer and confocal

microscopy. The ability of the polymer to reside on the cell surface with minimal internalization was shown by a clear line of delineation between the polymer on the cell surface and the actin cytoskeleton.

To demonstrate functional efficacy, quaternary ammonium based copolymers were utilized in a variety of *in vitro* assays. In cytokine-mediated endothelial permeability, the addition of 40P(TMA)Cl reduced the flux of albumin through cell monolayers in the presence of the inflammatory mediator, bradykinin. This reduction was taken as evidence that polymer administration can mitigate the passive diffusion of protein across the endothelium, which is a major component of vascular inflammation. Both 20P(TMA)Cl and 40P(TMA)Cl reduced pressure-induced hydraulic conductivity through bovine and rat microvascular endothelial monolayers. This reduction in monolayer permeability paralleled a reduction of nitric oxide released from cells under identical mechanical stress. This we take as evidence that polymeric contacts with the endothelial glycocalyx are able to attenuate mechanotransduction, or the active relay of signal(s) from extracellular mechanical forces to intercellular junctional proteins.

The next focus of experimentation was to optimize copolymers destined for potential pulmonary administration. We made important observations regarding the characteristics that any polymer-based therapy must possess and the mechanism by which polymer administration strengthens the endothelial barrier. For *in vitro* testing we used widely polydisperse copolymers. In whole mouse lung studies, it was discovered that treatment with polydisperse

copolymers significantly increased pulmonary artery pressure, a side effect that would be deleterious in a clinical setting. We hypothesized that the increase in pulmonary artery pressure was a result of one, or both, of two factors: low molecular weight copolymers were diffusing through the endothelial junctions to cause smooth muscle contraction or that the charge density of the polymer had surpassed a threshold and was causing aggregation of media proteins and a subsequent microvascular embolization. Two modifications to the polymer were made: first, low molecular weight polymers were removed by fractionation and the charge density was reduced to 10 mol%. The optimized polymer was administered to mouse lungs and a reduction in the capillary filtration coefficient was observed in the presence of either 10P(TMA)Cl or PEO, our control polymer of comparable geometry, water solubility and molecular weight. We hypothesized that HPMA and PEO backbones used the same mechanism to reduce the capillary filtration coefficient, namely by dampening the mechanical stress experienced by the glycocalyx. Collectively, these experiments validate the ability of a copolymer solution that reduce the flux of fluid and protein into pericapillary tissues in a whole lung model.

Cationic targeting moieties have been used to this point as a proof-of-concept tool to illustrate the efficacy of copolymer contact with the glycocalyx to reduce mechanotransduction. Once polymeric treatment of vascular inflammation showed more promise as a viable therapy, optimization of the targeting moiety was a necessity. Pleiotropic effects remain the primary concern with the introduction of a cationic copolymer *in vivo*. Nonspecific ionic quaternary

ammonium targeting moieties were replaced with a peptide ligand for E-selectin, which is upregulated on endothelial cells 2-6 hours after inflammatory insult. E-selectin has been used in a variety of applications to target inflammation in a range of tissue types (*6, 57, 93*). To this end, the HPMA backbone was retained and maleimide reactive groups were used to conjugate a cysteine-terminal peptide to the polymer precursor. Copolymer bearing E-selectin binding peptide (ESBP), a 13-amino acid peptide sequence (CDITWDQLWDLMK), was tested for specificity on immobilized E-selectin and it was shown that the polymers bind to their target protein. These experiments provide the basis for targeted polymer-based compounds to inflamed endothelium that could be clinically relevant for the treatment for acute pulmonary edema and vascular permeability.

5.2 Future work

There are two primary directions in which this research may be taken: 1) to further investigate the mechanism(s) of mechanotransduction, and 2) optimization of polymers as a viable clinical treatment for ALI/ARDS.

5.2.1 Mechanotransduction research

There is an irrefutable effect of copolymers on mechanotransduction. The mechanism(s) by which perturbations to the endothelial glycocalyx translate to downstream cell signaling and subsequent junctional opening remains unknown. The barrier-enhancing effect of copolymer-glycocalyx interaction has been proven in the presence of hydrostatic pressure and shear stress, the two vectors of mechanical forces on endothelial cells. We have also demonstrated a

significant suppression of nitric oxide formation from monolayers treated with copolymer, which demonstrates that the barrier enhancing effect of copolymer administration takes place at the intercellular level and is not only a physical barrier effect.

The decrease in NO production in the presence of 20P(TMA)Cl is evidence that polymer administration has an effect on the cell signaling pathway(s) that enables mechanotransduction to alter cell-cell junction integrity. For example, the effect of shear stress and hydrostatic pressure on endothelial nitric oxide production is a well-documented phenomenon (*8, 78, 83*), however, the mechanism by which pressure and shear stress is first detected by the cell is largely unknown. A possible approach to mechanism elucidation is visualization and quantification of junctional proteins in the presence of polymer and hydrostatic pressure and/or shear stress. For instance, Thi et al. (*15*) have demonstrated the ability to visualize the intracellular rearrangement of cytoskeletal structural components and junction proteins under fluid shear stress using confocal microscopy. This method of visualization can potentially elucidate the rearrangements of cellular components in the presence of copolymers to determine those that are involved in mechanotransduction signaling.

One significant question that arises from this research is how rigid a polymer needs to be in order to dampen mechanotransduction. In our experiments, the only polymer backbone that was tested was HPMA. P(HPMA) alone, without cationic side chains, was shown to reduce hydraulic conductivity in monolayers under hydrostatic pressure (Figure 2.7) although to a lesser extent

than did 40P(TMA)Cl. The conclusion of this observation is that HPMA intercalating into the glycocalyx, effectively thickening the matrix on the cell surface, dampens mechanotransduction. The addition of PEO appeared to have a barrier strengthening effect in whole mouse lungs as well, although more replicates would be necessary to determine if a difference between HPMA and PEO backbones exists. The use of a variety of linear, neutral, water-soluble polymers of differing flexibilities may give some insight into how the stiffness of the glycocalyx alters mechanotransduction. The persistence length is defined as the distance at which the correlation between the polymer vector and its length is lost and is therefore a measure of rigidity. For example, PEO is known as a very flexible, dynamic polymer with a persistence length of 3.7 Å in water (*100*). It is a linear polymer composed of single bonds; its lack of side chains confers unrestricted motion and its periodic oxygen molecules give it excellent water solubility. P(HPMA) may be predicted to be less flexible than PEO; its persistence length is reported to be 11 nm in aqueous solution (*101*), which may be attributed to the drag that its side chains may induce in polar solvent. A saccharide-based linear polymer such as cellulose may be predicted to have even less flexibility (persistence length 14.5 nm (*102*)), thus allowing for a range of polymer types to be tested in contact with the glycocalyx. The stiffness of the glycocalyx in the presence of polymer may be tested either by using atomic force microscopy (*103*) or magnetic beads in an applied torque (*14*), and the hydraulic conductivity system used in this research is an excellent tool to correlate the stiffness of the glycocalyx with barrier function and integrity.

5.2.2 Clinical use optimization

The original intent for the development of biomimetic polymers that intercalate with the endothelial glycocalyx was to design a clinically applicable treatment to reduce vascular permeability, which occurs in conjunction with acute lung injury. In order to be a viable treatment, some optimization of the polymer backbone and targeting side chains would be necessary.

In vivo, peptides are susceptible to serum-mediated damage such as enzymatic degradation, immunogenicity, and hydrolysis. Enzymatic degradation usually begins at the administration site and may be so extensive that it completely hinders the intact peptide from reaching its target (*104*). Peptide conjugation to a water-soluble polymer increases the systemic half-life by sterically blocking enzymatic degradation (*105-107*), which is an excellent first line of peptide defense but does not render the peptide impervious to plasma protein-mediated attack. A few modifications that may be made to the peptide targeting moiety to add stability are diastereomer substitution or terminal modifications, or the use of a non-peptide analog to sialyl lewis x.

The incorporation of D-amino acids may make peptides more stable *in vivo* as unsuitable protease substrates; however, their use may also render the peptide inefficient receptor agonists. Recently, a peptide composed of 24 amino acid residues was altered by replacing two phenylalanine residues with their D-conformers and the *in vivo* stability was measured. The exchange of only 2 residues extended the blood half-life by 25% (*108*). We hypothesize that this approach may be applied to the E-selectin binding sequence used in Chapter 4.

The particular sequence described in Chapter 4 was derived from a phage display experiment in which many peptides were discovered to bind to E-selectin. Each peptide sequence had four conserved residues (*65*). These common residues, the fourth and eighth tryptophan and penultimate methionine plus the C-terminal carboxyl, correspond to reports on sialyl lewis x analog requirements for binding, namely pi stacking and carboxyl positioning (*109*). Other residues on the peptide are not likely to be involved in receptor binding and therefore would be good candidates for D-amino acid substitution.

An approach taken in this research was to acetylate and amidate the N-terminus and C-terminus of ESBP, respectively. C-terminal amidation serves to protect the peptide from carboxy peptidase activity and acyl peptide derivatives have been shown to increase enzymatic stability in serum-containing media (*110, 111*), however, even modified peptide half-life remains relatively short at 77 minutes (*110*).

The use of non-peptide analogs to sialyl lewis x that bind E-selectin have been extensively explored (*91, 92, 112, 113*) as the main drawbacks to using sialyl lewis x is expense of materials and moderate E-selectin binding affinity. While the chemistry of such analogs tends to be cumbersome, it is often more simple than synthesis of the entire sialyl lewis x tetrasaccharide. An advantage to synthetic compounds is the reduction in systemic protease activity increase, *in vivo* half-life and bioavailability, and higher binding affinity for E-selectin than its native ligand (*112*). While sialyl lewis x binds E-, P-, and L-selectin, the binding

specificity differs between selectins. This aspect may be exploited through engineering to target a particular selectin of interest (*113*).

The advantages to using a polymer backbone such as P(HPMA) are long-lasting circulation in the blood stream, limited toxicity, water solubility and ease of synthesis and conjugation (*44, 45, 114*). High molecular weight nondegradable polymers, however, remain in circulation long after the desired effect has been attained and tend to accumulate in organs (*115*) and cellular organelles (*32, 49*). A solution to this problem is to use an enzymatically degradable polymer backbone with tailored degradation kinetics. Many polymer designs conjugate a drug to a non-degradable polymer backbone by using a pH- or enzymatically degradable linker in order to release the drug at a controlled rate (*116*) and/or specific target area (*117, 118*). This rationale may be exploited to synthesize a polymer of sufficient molecular weight to intercalate into the glycocalyx then be degraded over time as the acute inflammatory period passes. Since our polymer construct is designed for systemic delivery, it should reach the lung vasculature within seconds if administered via the internal jugular vein. A potential synthesis scheme would involve GFLG-di-methacrylamide monomers, obtained through solid phase peptide synthesis, that are polymerized with HPMA monomers and a chain transfer agent to keep the molecular weight of P(HPMA) low. Reversible addition-fragmentation chain transfer (RAFT) polymerization should be used so that upon degradation P(HPMA) exits the system through renal clearance. A polymer containing the GFLG linker has been shown to degrade by 80% after 48 hours in human plasma (*117*), which should be sufficient time to mitigate the

critical aspects of acute vascular inflammation. The degradation rate may increase in the presence of an acute inflammatory response due to increased circulating levels of plasma proteases; the outcome of those studies, along with rheological testing to determine the threshold for crosslinking-mediated hydrogel formation, would dictate the optimal GFLG content.

A final optimization step would be to measure the distribution and pharmacokinetics of polymer adsorption and excretion. A bolus of optimized E-selectin peptide conjugated polymer, labeled with an MRI contrast agent such as Gd^{3+} (*119*), could be administered via jugular vein to a whole mouse model with induced pulmonary inflammation induced by high tidal volume ventilation. Polymer should be allowed to circulate and the mouse would be imaged using MRI to determine the percentage of the bolus that adheres to lung microvasculature. The carotid artery would be cannulated and the outflow should be sampled for fluorescein-conjugated copolymer concentration over time. An ideal delivery method is a bolus injection that maximally absorbs polymer to protect other organs from any undesirable side effect.

REFERENCES

(1) Fukuda, M. N., Ohyama, C., Lowitz, K., Matsuo, O., Pasqualini, R., Ruoslahti, E., and Fukuda, M. (2000) A peptide mimic of E-selectin ligand inhibits sialyl Lewis X-dependent lung colonization of tumor cells. *Cancer Res 60*, 450-6.

(2) Stevens, A. P., Hlady, V., and Dull, R. O. (2007) Fluorescence correlation spectroscopy can probe albumin dynamics inside lung endothelial glycocalyx. *Am J Physiol Lung Cell Mol Physiol 293*, L328-35.

(3) Tarbell, J. M., and Pahakis, M. Y. (2006) Mechanotransduction and the glycocalyx. *J Intern Med 259*, 339-50.

(4) Mulivor, A. W., and Lipowsky, H. H. (2004) Inflammation- and ischemia-induced shedding of venular glycocalyx. *Am J Physiol Heart Circ Physiol 286*, H1672-80.

(5) Henry, C. B., and Duling, B. R. (2000) TNF-alpha increases entry of macromolecules into luminal endothelial cell glycocalyx. *Am J Physiol Heart Circ Physiol 279*, H2815-23.

(6) Funovics, M., Montet, X., Reynolds, F., Weissleder, R., and Josephson, L. (2005) Nanoparticles for the optical imaging of tumor E-selectin. *Neoplasia 7*, 904-11.

(7) Florian, J. A., Kosky, J. R., Ainslie, K., Pang, Z., Dull, R. O., and Tarbell, J. M. (2003) Heparan sulfate proteoglycan is a mechanosensor on endothelial cells. *Circ Res 93*, e136-42.

(8) Pahakis, M. Y., Kosky, J. R., Dull, R. O., and Tarbell, J. M. (2007) The role of endothelial glycocalyx components in mechanotransduction of fluid shear stress. *Biochem Biophys Res Commun 355*, 228-33.

(9) Oohira, A., Wight, T. N., and Bornstein, P. (1983) Sulfated proteoglycans synthesized by vascular endothelial cells in culture. *J Biol Chem 258*, 2014-21.

(10) Taylor, K. R., and Gallo, R. L. (2006) Glycosaminoglycans and their proteoglycans: host-associated molecular patterns for initiation and modulation of inflammation. *FASEB J 20*, 9-22.

(11) Okina, E., Manon-Jensen, T., Whiteford, J. R., and Couchman, J. R. (2009) Syndecan proteoglycan contributions to cytoskeletal organization and contractility. *Scand J Med Sci Sports 19*, 479-89.

(12) Nijenhuis, N., Mizuno, D., Schmidt, C. F., Vink, H., and Spaan, J. A. (2008) Microrheology of hyaluronan solutions: implications for the endothelial glycocalyx. *Biomacromolecules 9*, 2390-8.

(13) Mochizuki, S., Vink, H., Hiramatsu, O., Kajita, T., Shigeto, F., Spaan, J. A., and Kajiya, F. (2003) Role of hyaluronic acid glycosaminoglycans in shear-induced endothelium-derived nitric oxide release. *Am J Physiol Heart Circ Physiol 285*, H722-6.

(14) Wang, N., Butler, J. P., and Ingber, D. E. (1993) Mechanotransduction across the cell surface and through the cytoskeleton. *Science 260*, 1124-7.

(15) Thi, M. M., Tarbell, J. M., Weinbaum, S., and Spray, D. C. (2004) The role of the glycocalyx in reorganization of the actin cytoskeleton under fluid shear stress: a "bumper-car" model. *Proc Natl Acad Sci U S A 101*, 16483-8.

(16) Weinbaum, S., Zhang, X., Han, Y., Vink, H., and Cowin, S. C. (2003) Mechanotransduction and flow across the endothelial glycocalyx. *Proc Natl Acad Sci U S A 100*, 7988-95.

(17) Kopecek, J., and Bazilova, H. (1973) Poly[N-(2-hydroxypropyl) methacrylamide] 1. Radical polymerization and copolymerization. *European Polymer Journal 10*, 405-410.

(18) Kopecek, J., and Bazilova, H. (1974) in *European Polymer Journal*.

(19) Larson, N., Ray, A., Malugin, A., Pike, D. B., and Ghandehari, H. (2010) HPMA Copolymer-Aminohexylgeldanamycin Conjugates Targeting Cell Surface Expressed GRP78 in Prostate Cancer. *Pharm Res*.

(20) Miller, K., Erez, R., Segal, E., Shabat, D., and Satchi-Fainaro, R. (2009) Targeting bone metastases with a bispecific anticancer and antiangiogenic polymer-alendronate-taxane conjugate. *Angew Chem Int Ed Engl 48*, 2949-54.

(21) Pan, H., Sima, M., Kopeckova, P., Wu, K., Gao, S., Liu, J., Wang, D., Miller, S. C., and Kopecek, J. (2008) Biodistribution and pharmacokinetic studies of bone-targeting N-(2-hydroxypropyl)methacrylamide copolymer-alendronate conjugates. *Mol Pharm 5*, 548-58.

(22) Peterson, C. M., Lu, J. M., Sun, Y., Peterson, C. A., Shiah, J. G., Straight, R. C., and Kopecek, J. (1996) Combination chemotherapy and

photodynamic therapy with N-(2-hydroxypropyl) methacrylamide copolymer-bound anticancer drugs inhibit human ovarian carcinoma heterotransplanted in nude mice. *Cancer Res 56*, 3980-5.

(23) Hongrapipat, J., Kopeckova, P., Prakongpan, S., and Kopecek, J. (2008) Enhanced antitumor activity of combinations of free and HPMA copolymer-bound drugs. *Int J Pharm 351*, 259-70.

(24) Gao, S. Q., Lu, Z. R., Kopeckova, P., and Kopecek, J. (2007) Biodistribution and pharmacokinetics of colon-specific HPMA copolymer--9-aminocamptothecin conjugate in mice. *J Control Release 117*, 179-85.

(25) Kopecek, J. (1992) Polymers for colon-specific drug delivery. *Journal of Controlled Release 19*, 121-130.

(26) Sirova, M., Mrkvan, T., Etrych, T., Chytil, P., Rossmann, P., Ibrahimova, M., Kovar, L., Ulbrich, K., and Rihova, B. (2010) Preclinical evaluation of linear HPMA-doxorubicin conjugates with pH-sensitive drug release: efficacy, safety, and immunomodulating activity in murine model. *Pharm Res 27*, 200-8.

(27) Wroblewski, S., Berenson, M., Kopeckova, P., and Kopecek, J. (2000) Biorecognition of HPMA copolymer-lectin conjugates as an indicator of differentiation of cell-surface glycoproteins in development, maturation, and diseases of human and rodent gastrointestinal tissues. *J Biomed Mater Res 51*, 329-42.

(28) Pola, R., Studenovsky, M., Pechar, M., Ulbrich, K., Hovorka, O., Vetvicka, D., and Rihova, B. (2009) HPMA-copolymer conjugates targeted to tumor endothelium using synthetic oligopeptides. *J Drug Target 17*, 763-76.

(29) Vasey, P. A., Kaye, S. B., Morrison, R., Twelves, C., Wilson, P., Duncan, R., Thomson, A. H., Murray, L. S., Hilditch, T. E., Murray, T., Burtles, S., Fraier, D., Frigerio, E., and Cassidy, J. (1999) Phase I clinical and pharmacokinetic study of PK1 [N-(2-hydroxypropyl)methacrylamide copolymer doxorubicin]: first member of a new class of chemotherapeutic agents-drug-polymer conjugates. Cancer Research Campaign Phase I/II Committee. *Clin Cancer Res 5*, 83-94.

(30) Etrych, T., Strohalm, J., Kovar, L., Kabesova, M., Rihova, B., and Ulbrich, K. (2009) HPMA copolymer conjugates with reduced anti-CD20 antibody for cell-specific drug targeting. I. Synthesis and in vitro evaluation of binding efficacy and cytostatic activity. *J Control Release 140*, 18-26.

(31) Johnson, R. N., Kopeckova, P., and Kopecek, J. (2009) Synthesis and evaluation of multivalent branched HPMA copolymer-Fab' conjugates targeted to the B-cell antigen CD20. *Bioconjug Chem 20*, 129-37.

(32) Shamay, Y., Paulin, D., Ashkenasy, G., and David, A. (2009) E-selectin binding peptide-polymer-drug conjugates and their selective cytotoxicity against vascular endothelial cells. *Biomaterials 30*, 6460-8.

(33) Matsumura, Y., and Maeda, H. (1986) A new concept for macromolecular therapeutics in cancer chemotherapy: mechanism of tumoritropic accumulation of proteins and the antitumor agent smancs. *Cancer Res 46*, 6387-92.

(34) Iyer, A. K., Khaled, G., Fang, J., and Maeda, H. (2006) Exploiting the enhanced permeability and retention effect for tumor targeting. *Drug Discov Today 11*, 812-8.

(35) Putnam, D., and Kopecek, J. (1992) Polymer conjugates with anticancer activity. *Advances in Polymer Science 122*, 55-112.

(36) Krinick, N. L., Sun, Y., Joyner, D., Spikes, J. D., Straight, R. C., and Kopecek, J. (1994) A polymeric drug delivery system for the simultaneous delivery of drugs activatable by enzymes and/or light. *J Biomater Sci Polym Ed 5*, 303-24.

(37) Bronzino, J. D. (2000) *The biomedical engineering handbook*, CRC Press.

(38) Yeung, T., Gilbert, G. E., Shi, J., Silvius, J., Kapus, A., and Grinstein, S. (2008) Membrane phosphatidylserine regulates surface charge and protein localization. *Science 319*, 210-3.

(39) Howard, K. A., Dash, P. R., Read, M. L., Ward, K., Tomkins, L. M., Nazarova, O., Ulbrich, K., and Seymour, L. W. (2000) Influence of hydrophilicity of cationic polymers on the biophysical properties of polyelectrolyte complexes formed by self-assembly with DNA. *Biochim Biophys Acta 1475*, 245-55.

(40) Oupicky, D., Konak, C., Ulbrich, K., Wolfert, M. A., and Seymour, L. W. (2000) DNA delivery systems based on complexes of DNA with synthetic polycations and their copolymers. *J Control Release 65*, 149-71.

(41) Subr, V., Kostka, L., Selby-Milic, T., Fisher, K., Ulbrich, K., Seymour, L. W., and Carlisle, R. C. (2009) Coating of adenovirus type 5 with polymers containing quaternary amines prevents binding to blood components. *J Control Release 135*, 152-8.

(42) York, A. W., Zhang, Y., Holley, A. C., Guo, Y., Huang, F., and McCormick, C. L. (2009) Facile synthesis of multivalent folate-block copolymer conjugates via aqueous RAFT polymerization: targeted delivery of siRNA and subsequent gene suppression. *Biomacromolecules 10*, 936-43.

(43) Callahan, J., and Kopecek, J. (2006) Semitelechelic HPMA copolymers functionalized with triphenylphosphonium as drug carriers for membrane transduction and mitochondrial localization. *Biomacromolecules 7*, 2347-56.

(44) Rihova, B., Bilej, M., Vetvicka, V., Ulbrich, K., Strohalm, J., Kopecek, J., and Duncan, R. (1989) Biocompatibility of N-(2-hydroxypropyl) methacrylamide copolymers containing adriamycin. Immunogenicity, and effect on haematopoietic stem cells in bone marrow in vivo and mouse splenocytes and human peripheral blood lymphocytes in vitro. *Biomaterials 10*, 335-42.

(45) Rihova, B., Ulbrich, K., Kopecek, J., and Mancal, P. (1983) Immunogenicity of N-(2-hydroxypropyl)-methacrylamide copolymers--potential hapten or drug carriers. *Folia Microbiol (Praha) 28*, 217-27.

(46) Dintzis, R. Z., Okajima, M., Middleton, M. H., Greene, G., and Dintzis, H. M. (1989) The immunogenicity of soluble haptenated polymers is determined by molecular mass and hapten valence. *J Immunol 143*, 1239-44.

(47) Luten, J., Akeroyd, N., Funhoff, A., Lok, M. C., Talsma, H., and Hennink, W. E. (2006) Methacrylamide polymers with hydrolysis-sensitive cationic side groups as degradable gene carriers. *Bioconjug Chem 17*, 1077-84.

(48) Rihova, B., Kopecek, J., Ulbrich, K., Pospisil, M., and Mancal, P. (1984) Effect of the chemical structure of N-(2-hydroxypropyl)methacrylamide copolymers on their ability to induce antibody formation in inbred strains of mice. *Biomaterials 5*, 143-8.

(49) Liu, J., Bauer, H., Callahan, J., Kopeckova, P., Pan, H., and Kopecek, J. (2010) Endocytic uptake of a large array of HPMA copolymers: Elucidation into the dependence on the physicochemical characteristics. *J Control Release 143*, 71-9.

(50) Dash, P. R., Read, M. L., Barrett, L. B., Wolfert, M. A., and Seymour, L. W. (1999) Factors affecting blood clearance and in vivo distribution of polyelectrolyte complexes for gene delivery. *Gene Ther 6*, 643-50.

(51) Lv, H., Zhang, S., Wang, B., Cui, S., and Yan, J. (2006) Toxicity of cationic lipids and cationic polymers in gene delivery. *J Control Release 114*, 100-9.

(52) Hwang, S. J., and Davis, M. E. (2001) Cationic polymers for gene delivery: designs for overcoming barriers to systemic administration. *Curr Opin Mol Ther 3*, 183-91.

(53) Reschel, T., Konak, C., Oupicky, D., Seymour, L. W., and Ulbrich, K. (2002) Physical properties and in vitro transfection efficiency of gene delivery vectors based on complexes of DNA with synthetic polycations. *J Control Release 81*, 201-17.

(54) Giantsos, K. M., Kopeckova, P., and Dull, R. O. (2009) The use of an endothelium-targeted cationic copolymer to enhance the barrier function of lung capillary endothelial monolayers. *Biomaterials 30*, 5885-91.

(55) Asgeirsdottir, S. A., Talman, E. G., de Graaf, I. A., Kamps, J. A., Satchell, S. C., Mathieson, P. W., Ruiters, M. H., and Molema, G. (2010) Targeted transfection increases siRNA uptake and gene silencing of primary endothelial cells in vitro--a quantitative study. *J Control Release 141*, 241-51.

(56) Adrian, J. E., Morselt, H. W., Suss, R., Barnert, S., Kok, J. W., Asgeirsdottir, S. A., Ruiters, M. H., Molema, G., and Kamps, J. A. (2010) Targeted SAINT-O-Somes for improved intracellular delivery of siRNA and cytotoxic drugs into endothelial cells. *J Control Release 144*, 341-9.

(57) van Kasteren, S. I., Campbell, S. J., Serres, S., Anthony, D. C., Sibson, N. R., and Davis, B. G. (2009) Glyconanoparticles allow pre-symptomatic in vivo imaging of brain disease. *Proc Natl Acad Sci U S A 106*, 18-23.

(58) Minaguchi, J., Oohashi, T., Inagawa, K., Ohtsuka, A., and Ninomiya, Y. (2008) Transvascular accumulation of Sialyl Lewis X conjugated liposome in inflamed joints of collagen antibody-induced arthritic (CAIA) mice. *Arch Histol Cytol 71*, 195-203.

(59) Mulligan, M. S., Lowe, J. B., Larsen, R. D., Paulson, J., Zheng, Z. L., DeFrees, S., Maemura, K., Fukuda, M., and Ward, P. A. (1993) Protective effects of sialylated oligosaccharides in immune complex-induced acute lung injury. *J Exp Med 178*, 623-31.

(60) Barthel, S. R., Gavino, J. D., Descheny, L., and Dimitroff, C. J. (2007) Targeting selectins and selectin ligands in inflammation and cancer. *Expert Opin Ther Targets 11*, 1473-91.

(61) Cummings, R. D., and Smith, D. F. (1992) The selectin family of carbohydrate-binding proteins: structure and importance of carbohydrate ligands for cell adhesion. *Bioessays 14*, 849-56.

(62) Johnston, G. I., Cook, R. G., and McEver, R. P. (1989) Cloning of GMP-140, a granule membrane protein of platelets and endothelium: sequence similarity to proteins involved in cell adhesion and inflammation. *Cell 56*, 1033-44.

(63) Lowe, J. B., Stoolman, L. M., Nair, R. P., Larsen, R. D., Berhend, T. L., and Marks, R. M. (1990) ELAM-1--dependent cell adhesion to vascular endothelium determined by a transfected human fucosyltransferase cDNA. *Cell 63*, 475-84.

(64) Walz, G., Aruffo, A., Kolanus, W., Bevilacqua, M., and Seed, B. (1990) Recognition by ELAM-1 of the sialyl-Lex determinant on myeloid and tumor cells. *Science 250*, 1132-5.

(65) Martens, C. L., Cwirla, S. E., Lee, R. Y., Whitehorn, E., Chen, E. Y., Bakker, A., Martin, E. L., Wagstrom, C., Gopalan, P., Smith, C. W., and et al. (1995) Peptides which bind to E-selectin and block neutrophil adhesion. *J Biol Chem 270*, 21129-36.

(66) Subramaniam, M., Koedam, J. A., and Wagner, D. D. (1993) Divergent fates of P- and E-selectins after their expression on the plasma membrane. *Mol Biol Cell 4*, 791-801.

(67) Bernardes-Silva, M., Anthony, D. C., Issekutz, A. C., and Perry, V. H. (2001) Recruitment of neutrophils across the blood-brain barrier: the role of E- and P-selectins. *J Cereb Blood Flow Metab 21*, 1115-24.

(68) Pohl, U., Herlan, K., Huang, A., and Bassenge, E. (1991) EDRF-mediated shear-induced dilation opposes myogenic vasoconstriction in small rabbit arteries. *Am J Physiol 261*, H2016-23.

(69) Jacob, M., Rehm, M., Loetsch, M., Paul, J. O., Bruegger, D., Welsch, U., Conzen, P., and Becker, B. F. (2007) The endothelial glycocalyx prefers albumin for evoking shear stress-induced, nitric oxide-mediated coronary dilatation. *J Vasc Res 44*, 435-43.

(70) Dull, R. O., Mecham, I., and McJames, S. (2007) Heparan sulfates mediate pressure-induced increase in lung endothelial hydraulic conductivity via nitric oxide/reactive oxygen species. *Am J Physiol Lung Cell Mol Physiol 292*, L1452-8.

(71) Davies, P. F. (1995) Flow-mediated endothelial mechanotransduction. *Physiol Rev 75*, 519-60.

(72) Helmke, B. P., Thakker, D. B., Goldman, R. D., and Davies, P. F. (2001) Spatiotemporal analysis of flow-induced intermediate filament displacement in living endothelial cells. *Biophys J 80*, 184-94.

(73) Wei, Z., Costa, K., Al-Mehdi, A. B., Dodia, C., Muzykantov, V., and Fisher, A. B. (1999) Simulated ischemia in flow-adapted endothelial cells leads to generation of reactive oxygen species and cell signaling. *Circ Res 85*, 682-9.

(74) Fritz, J. S., and Schenk, G. H. (1987) *Quantitative analytical chemistry*, 5th ed., Allyn and Bacon, Boston.

(75) Samejima, K., Dairman, W., Stone, J., and Udenfriend, S. (1971) Condensation of ninhydrin with aldehydes and primary amines to yield highly fluorescent ternary products. II. Application to the detection and assay of peptides, amino acids, amines, and amino sugars. *Anal Biochem 42*, 237-47.

(76) Janczyk, P., Hansen, S., Bahramsoltani, M., and Plendl, J. (2010) The glycocalyx of human, bovine and murine microvascular endothelial cells cultured in vitro. *J Electron Microsc (Tokyo) 59*, 291-8.

(77) Tarbell, J. M. (2010) Shear stress and the endothelial transport barrier. *Cardiovasc Res 87*, 320-30.

(78) Harrison, D. G., Widder, J., Grumbach, I., Chen, W., Weber, M., and Searles, C. (2006) Endothelial mechanotransduction, nitric oxide and vascular inflammation. *J Intern Med 259*, 351-63.

(79) Corson, M. A., James, N. L., Latta, S. E., Nerem, R. M., Berk, B. C., and Harrison, D. G. (1996) Phosphorylation of endothelial nitric oxide synthase in response to fluid shear stress. *Circ Res 79*, 984-91.

(80) Beckman, J. S., and Koppenol, W. H. (1996) Nitric oxide, superoxide, and peroxynitrite: the good, the bad, and ugly. *Am J Physiol 271*, C1424-37.

(81) Chiang, E. T., Camp, S. M., Dudek, S. M., Brown, M. E., Usatyuk, P. V., Zaborina, O., Alverdy, J. C., and Garcia, J. G. (2009) Protective effects of high-molecular weight polyethylene glycol (PEG) in human lung endothelial cell barrier regulation: role of actin cytoskeletal rearrangement. *Microvasc Res 77*, 174-86.

(82) Bertuglia, S., Veronese, F. M., and Pasut, G. (2006) Polyethylene glycol and a novel developed polyethylene glycol-nitric oxide normalize arteriolar response and oxidative stress in ischemia-reperfusion. *Am J Physiol Heart Circ Physiol 291*, H1536-44.

(83) Lopez-Quintero, S. V., Amaya, R., Pahakis, M., and Tarbell, J. M. (2009) The endothelial glycocalyx mediates shear-induced changes in hydraulic conductivity. *Am J Physiol Heart Circ Physiol 296*, H1451-6.

(84) Hubert, C. G., McJames, S. W., Mecham, I., and Dull, R. O. (2006) Digital imaging system and virtual instrument platform for measuring hydraulic conductivity of vascular endothelial monolayers. *Microvasc Res 71*, 135-40.

(85) Rosca, E. V., Gillies, R. J., and Caplan, M. R. (2009) Glioblastoma targeting via integrins is concentration dependent. *Biotechnol Bioeng 104*, 408-17.

(86) Hashida, N., Ohguro, N., Yamazaki, N., Arakawa, Y., Oiki, E., Mashimo, H., Kurokawa, N., and Tano, Y. (2008) High-efficacy site-directed drug delivery system using sialyl-Lewis X conjugated liposome. *Exp Eye Res 86*, 138-49.

(87) Gesner, B. M., and Ginsburg, V. (1964) Effect of Glycosidases on the Fate of Transfused Lymphocytes. *Proc Natl Acad Sci U S A 52*, 750-5.

(88) Foxall, C., Watson, S. R., Dowbenko, D., Fennie, C., Lasky, L. A., Kiso, M., Hasegawa, A., Asa, D., and Brandley, B. K. (1992) The three members of the selectin receptor family recognize a common carbohydrate epitope, the sialyl Lewis(x) oligosaccharide. *J Cell Biol 117*, 895-902.

(89) Moore, K. L., Varki, A., and McEver, R. P. (1991) GMP-140 binds to a glycoprotein receptor on human neutrophils: evidence for a lectin-like interaction. *J Cell Biol 112*, 491-9.

(90) Zhou, Q., Moore, K. L., Smith, D. F., Varki, A., McEver, R. P., and Cummings, R. D. (1991) The selectin GMP-140 binds to sialylated, fucosylated lactosaminoglycans on both myeloid and nonmyeloid cells. *J Cell Biol 115*, 557-64.

(91) Jahnke, W., Kolb, H. C., Blommers, M. J. J., Magnani, J. L., and Ernst, B. (1997) Comparison of the bioactive conformations of sialyl Lewis(X) and a potent sialyl Lewis(X) mimic. *Angewandte Chemie-International Edition 36*, 2603-2607.

(92) Kogan, T. P., Dupre, B., Keller, K. M., Scott, I. L., Bui, H., Market, R. V., Beck, P. J., Voytus, J. A., Revelle, B. M., and Scott, D. (1995) Rational design and synthesis of small molecule, non-oligosaccharide selectin inhibitors: (alpha-D-mannopyranosyloxy)biphenyl-substituted carboxylic acids. *J Med Chem 38*, 4976-84.

(93) Hirai, M., Minematsu, H., Kondo, N., Oie, K., Igarashi, K., and Yamazaki, N. (2007) Accumulation of liposome with Sialyl Lewis X to inflammation and tumor region: application to in vivo bio-imaging. *Biochem Biophys Res Commun 353*, 553-8.

(94) Buerke, M., Weyrich, A. S., Zheng, Z., Gaeta, F. C., Forrest, M. J., and Lefer, A. M. (1994) Sialyl Lewisx-containing oligosaccharide attenuates myocardial reperfusion injury in cats. *J Clin Invest 93*, 1140-8.

(95) Nelson, R. M., Dolich, S., Aruffo, A., Cecconi, O., and Bevilacqua, M. P. (1993) Higher-affinity oligosaccharide ligands for E-selectin. *J Clin Invest 91*, 1157-66.

(96) Ellman, G. L. (1959) Tissue sulfhydryl groups. *Arch Biochem Biophys 82*, 70-7.

(97) Chan, W. C., and White, P. D. (2000) *Fmoc solid phase peptide synthesis : a practical approach*, Oxford University Press, New York.

(98) Gill, S. C., and von Hippel, P. H. (1989) Calculation of protein extinction coefficients from amino acid sequence data. *Anal Biochem 182*, 319-26.

(99) Beauharnois, M. E., Lindquist, K. C., Marathe, D., Vanderslice, P., Xia, J., Matta, K. L., and Neelamegham, S. (2005) Affinity and kinetics of sialyl Lewis-X and core-2 based oligosaccharides binding to L- and P-selectin. *Biochemistry 44*, 9507-19.

(100) Lee, H., Venable, R. M., MacKerell, A. D., and Pastor, R. W. (2008) Molecular dynamics studies of polyethylene oxide and polyethylene glycol: Hydrodynamic radius and shape anisotropy. *Biophysical Journal 95*, 1590-1599.

(101) Kogej, K., Berghmans, H., Reynaers, H., and Paoletti, S. (2004) Unusual behavior of atactic poly(methacrylic acid) in aqueous solutions monitored by wide-angle light scattering. *Journal of Physical Chemistry B 108*, 18164-18173.

(102) KroonBatenburg, L. M. J., Kruiskamp, P. H., Vliegenthart, J. F. G., and Kroon, J. (1997) Estimation of the persistence length of polymers by MD simulations on small fragments in solution. Application to cellulose. *Journal of Physical Chemistry B 101*, 8454-8459.

(103) Sun, M., Graham, J. S., Hegedus, B., Marga, F., Zhang, Y., Forgacs, G., and Grandbois, M. (2005) Multiple membrane tethers probed by atomic force microscopy. *Biophys J 89*, 4320-9.

(104) Kahns, A. H., and Bundgaard, H. (1991) Prodrugs of peptides. 13. Stabilization of peptide amides against alpha-chymotrypsin by the prodrug approach. *Pharm Res 8*, 1533-8.

(105) Veronese, F. M., and Morpurgo, M. (1999) Bioconjugation in pharmaceutical chemistry. *Farmaco 54*, 497-516.

(106) Mitra, G., Mumtaz, S., and Bachhawat, B. K. (1993) Enhanced stability and therapeutic utility of proteins upon conjugation with hydrophilic polymers. *Hindustan Antibiot Bull 35*, 133-56.

(107) Elliott, S., Lorenzini, T., Asher, S., Aoki, K., Brankow, D., Buck, L., Busse, L., Chang, D., Fuller, J., Grant, J., Hernday, N., Hokum, M., Hu, S., Knudten, A., Levin, N., Komorowski, R., Martin, F., Navarro, R., Osslund, T., Rogers, G., Rogers, N., Trail, G., and Egrie, J. (2003) Enhancement of therapeutic protein in vivo activities through glycoengineering. *Nat Biotechnol 21*, 414-21.

(108) Neundorf, I., Rennert, R., Franke, J., Kozle, I., and Bergmann, R. (2008) Detailed analysis concerning the biodistribution and metabolism of human calcitonin-derived cell-penetrating peptides. *Bioconjug Chem 19*, 1596-603.

(109) Rinnbauer, M., Ernst, B., Wagner, B., Magnani, J., Benie, A. J., and Peters, T. (2003) Epitope mapping of sialyl Lewis(x) bound to E-selectin using saturation transfer difference NMR experiments. *Glycobiology 13*, 435-43.

(110) Bak, A., Gudmundsson, O. S., Friis, G. J., Siahaan, T. J., and Borchardt, R. T. (1999) Acyloxyalkoxy-based cyclic prodrugs of opioid peptides: evaluation of the chemical and enzymatic stability as well as their transport properties across Caco-2 cell monolayers. *Pharm Res 16*, 24-9.

(111) Fujita, T., Kawahara, I., Quan, Y., Hattori, K., Takenaka, K., Muranishi, S., and Yamamoto, A. (1998) Permeability characteristics of tetragastrins across intestinal membranes using the Caco-2 monolayer system: comparison between acylation and application of protease inhibitors. *Pharm Res 15*, 1387-92.

(112) Kim, M. K., Brandley, B. K., Anderson, M. B., and Bochner, B. S. (1998) Antagonism of selectin-dependent adhesion of human eosinophils and neutrophils by glycomimetics and oligosaccharide compounds. *Am J Respir Cell Mol Biol 19*, 836-41.

(113) Kurokawa, K., Kumihara, H., and Kondo, H. (2000) A solid-phase synthesis for beta-turn mimetics of sialyl Lewis X. *Bioorg Med Chem Lett 10*, 1827-30.

(114) Seymour, L. W., Duncan, R., Strohalm, J., and Kopecek, J. (1987) Effect of molecular weight (Mw) of N-(2-hydroxypropyl)methacrylamide copolymers on body distribution and rate of excretion after subcutaneous, intraperitoneal, and intravenous administration to rats. *J Biomed Mater Res 21*, 1341-58.

(115) Noronha-Blob, L., Vengris, V. E., Pitha, P. M., and Pitha, J. (1977) Uptake and fate of water-soluble, nondegradable polymers with antiviral activity in cells and animals. *J Med Chem 20*, 356-9.

(116) Yang, J., Jacobsen, M. T., Pan, H., and Kopecek, J. (2010) Synthesis and characterization of enzymatically degradable PEG-based peptide-containing hydrogels. *Macromol Biosci 10*, 445-54.

(117) Dvorak, M., Kopeckova, P., and Kopecek, J. (1999) High-molecular weight HPMA copolymer-adriamycin conjugates. *J Control Release 60*, 321-32.

(118) Ibekwe, V. C., Khela, M. K., Evans, D. F., and Basit, A. W. (2008) A new concept in colonic drug targeting: a combined pH-responsive and bacterially-triggered drug delivery technology. *Aliment Pharmacol Ther 28*, 911-6.

(119) Vaidya, A., Sun, Y., Feng, Y., Emerson, L., Jeong, E. K., and Lu, Z. R. (2008) Contrast-enhanced MRI-guided photodynamic cancer therapy with a pegylated bifunctional polymer conjugate. *Pharm Res 25*, 2002-11.